

Inclusive $Z(\nu\bar{\nu})\gamma$ full Run2 analysis report

Katerina Kazakova^{1, 2}

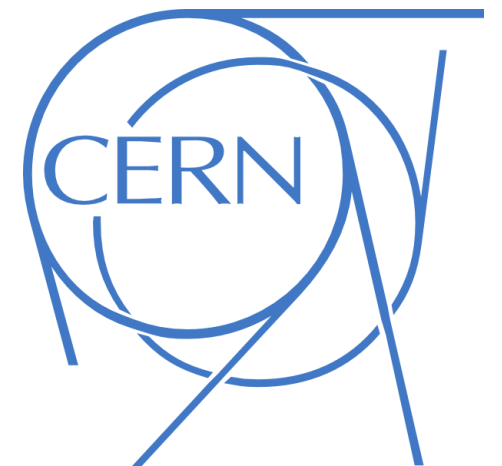
on behalf of the ZnunuGamma group

¹ National Research Nuclear University MEPhI, Moscow

² Joint Institute for Nuclear Research, Dubna



MEPhI@Atlas
meeting
21/06/2024



Motivation

- Standard Model:

⇒ A higher branching ratio of the neutral decay channel in comparison to the charged lepton decays of Z boson and better background control in comparison with the hadronic channel.

⇒ Previous study of this channel — 36.1 fb⁻¹ data. Full Run2 statistics (140 fb⁻¹) → increase of measurement accuracy (expect the experimental sensitivity to increase by a factor of 2).

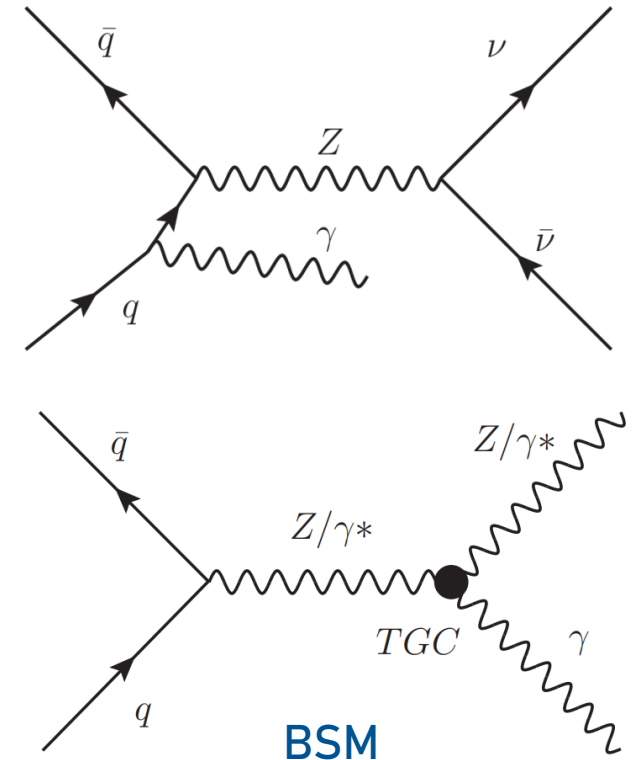
- Goal:

⇒ To obtain integrated and differential cross-sections for 10 observables: E_T^γ , p_T^{miss} , N_{jets} , η_γ , $\Delta\phi(\gamma, p_T^{\text{miss}})$, $\Delta\phi(j_1, j_2)$, $\Delta R(Z, \gamma)$, p_T^{j1} , p_T^{j2} , $m_T^{Z\gamma}$ and compare the results with the theory predictions including NNLO QCD and NLO EWK corrections.

- Beyond SM:

⇒ To obtain the strongest up-to-date limits on anomalous neutral triple gauge-boson couplings (aTGCs) using vertex functions and EFT formalisms.

⇒ Possible combination of the EFT limits between $Z\gamma$ and ZZ .



Glance: [ANA-STDM-2018-54](#)

Selection optimisation

- **Topology:** high-energetic photon and MET.
- Multivariate (MV) method of the selection optimization takes into account the signal significance S as a function of the threshold values of the variables:

$$S = N_{\text{signal}} / \sqrt{N_{\text{signal}} + N_{\text{bkg}}}$$

⇒ The result of the MV optimization process is a set of threshold values for the variables that yield the maximum S .

Selections	Cut Value
E_T^{miss}	$> 130 \text{ GeV}$
E_T^γ	$> 150 \text{ GeV}$
Number of tight isolated photons	$N_\gamma = 1$
Lepton veto	$N_e = 0, N_\mu = 0$
τ veto	$N_\tau = 0$
E_T^{miss} significance	> 11
$ \Delta\phi(\gamma, \vec{p}_T^{\text{miss}}) $	> 0.6
$ \Delta\phi(j_1, \vec{p}_T^{\text{miss}}) $	> 0.3

The significance is increased by 3%

	all cuts	presel. only
Signal		
Z($\nu\nu$) γ QCD	10711 ± 8	13438 ± 9
Z($\nu\nu$) γ EWK	166.3 ± 0.3	300.5 ± 0.4
Total signal	10878 ± 8	13738 ± 9
Background		
W γ QCD	3310 ± 21	6393 ± 28
W γ EWK	109.4 ± 0.6	293.5 ± 1.1
tt, top	177 ± 5	1991 ± 18
W($e\nu$)	3591 ± 487	7934 ± 540
t $\tau\gamma$	178 ± 3	746 ± 6
γ +j	8123 ± 82	63766 ± 211
Zj	415 ± 21	635 ± 25
Z(ll) γ	211 ± 4	399 ± 5
W($\tau\nu$)	640 ± 69	2222 ± 127
Total bkg.	16779 ± 499	84380 ± 595
Stat. signif.	65.4 ± 0.6	43.86 ± 0.14

Beam-induced background suppression: $|\Delta z| < 250 \text{ mm}$

The optimisation procedure is done for three different photon isolation working points FixedCutTight, FixedCutTightCaloOnly and FixedCutLoose.

Background composition

Percentage of
the data

Background composition for $Z(\nu\bar{\nu})\gamma$:

- 35% ● γ + jets – fit to data in additional CR based on MET significance (shape from MC);
- 15% ● $W(\rightarrow l\nu)\gamma$ and $t\bar{t}\gamma$ – fit to data in additional CR based on N leptons (shape from MC);
- 11% ● $e \rightarrow \gamma$ – fake-rate estimation using Z-peak (tag-n-probe) method;
- 8% ● $\text{jet} \rightarrow \gamma$ – ABCD method based on photon ID and isolation (shape from Slice Method);
- 0.9% ● $Z(l^+l^-)\gamma$ – via MC;

$e \rightarrow \gamma$ misID background: Z-peak method

- Background estimation method:

1. Estimating $e \rightarrow \gamma$ fake-rate as $rate_{e \rightarrow \gamma} = \frac{(N_{e\gamma} - N_{bkg})}{(N_{ee} - N_{bkg})}$,

where $N_{e\gamma}$, N_{ee} – number of $e\gamma$ and ee events in Z-peak mass window ($M_Z - 10$ GeV, $M_Z + 10$ GeV), N^{bkg} – background in Z-peak mass window extrapolated from sideband with exponential pol1 or pol2 fit.

Additional W_γ background rejection: $E_T^{miss} < 40$ GeV.

$e\gamma$ pair selection:

signal region **photon with $p_T > 150$ GeV** (probe), selected **Tight electron with $p_T > 25$ GeV** (tag)

ee pair selection:

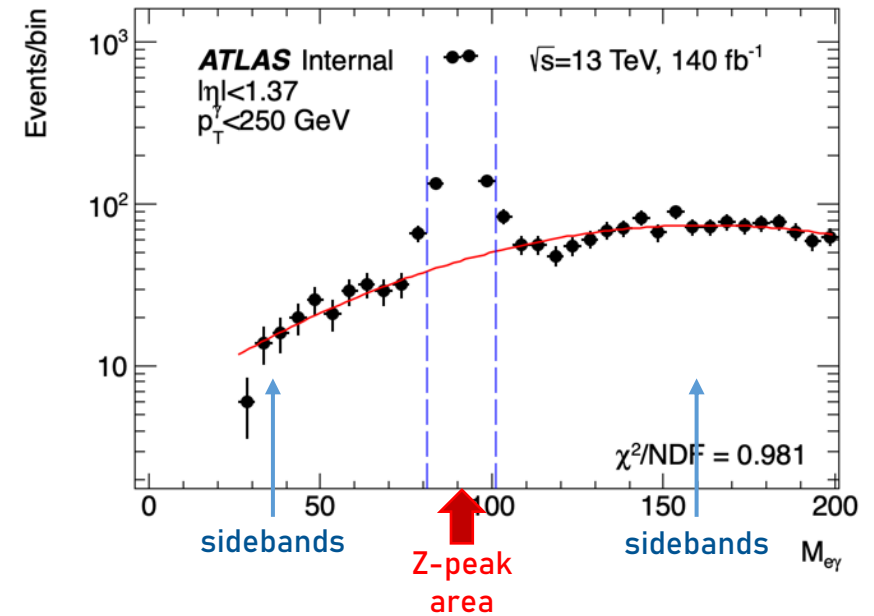
selected **electron with $p_T > 150$ GeV** (probe), selected **opposite sign Tight electron with $p_T > 25$ GeV** (tag)

Since fake rate depends on p_T and η (see backup), three regions are considered:

$|\eta| < 1.37$, $p_T < 250$ GeV and **$|\eta| < 1.37$, $p_T > 250$ GeV** and **$1.52 < |\eta| < 2.37$** (flat distribution on p_T)

2. Building e-probe control region (CR): signal region with selected Tight electron with $p_T > 150$ GeV instead of photon.

3. Scaling data distributions from e-probe CR by fake rate value.



$e \rightarrow \gamma$ misID background: systematics

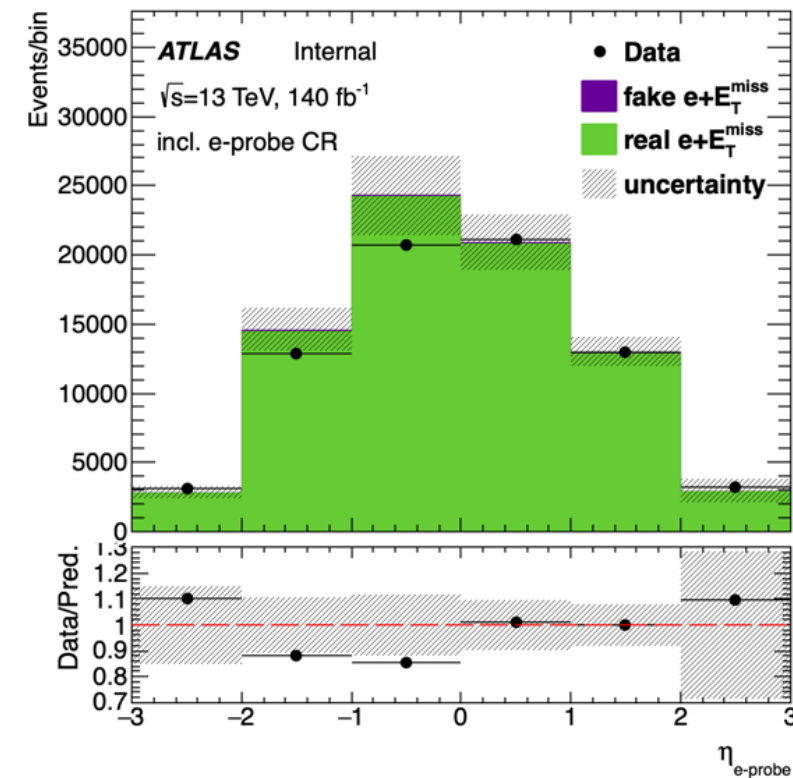
- Systematics on fake-rate estimation (ascending contribution):

- ⇒ Z peak mass window variation (varies from 0.3% to 0.7%).
- ⇒ Background under Z peak evaluation (varies from 3% to 14%).
- ⇒ Difference between "real fake rate" in Z(ee) MC and tag-and-probe method performed on Z(ee) MC (varies from 3% to 15%).

	$150 < E_T^\gamma < 250$ GeV	$E_T^\gamma > 250$ GeV
$0 < \eta < 1.37$	$0.0234 \pm 0.0006 \pm 0.0010$	$0.0193 \pm 0.0013 \pm 0.0038$
$1.52 < \eta < 2.37$	$0.0714 \pm 0.0019 \pm 0.0074$	

First uncertainty is statistical, second is systematical.

Total systematics on fake-rate does not exceed 20%



Background estimation result:

Signal region $2608 \pm 11 \pm 162$

Total syst. on the background yield: 6%

jet $\rightarrow \gamma$ misID background: ABCD-method

- A pair of photons from the decay of neutral mesons (typically a π^0), contained in hadronic jets, can give a signature of EM shower similar to a single isolated photon signature of the electromagnetic (EM) shower.
- Background is estimated from data using 2D-sideband method: photon isolation and identification variables are used to construct the sidebands.
- Correlation is measured in data and MC by $R = \frac{N_A N_D}{N_B N_C}$
- FixedCutLoose isolation working point is used with iso gap of 2 GeV

In ABCD

R factor	loose'2	loose'3	loose'4	loose'5
MC	1.1 ± 0.2	1.1 ± 0.2	1.1 ± 0.2	1.4 ± 0.3

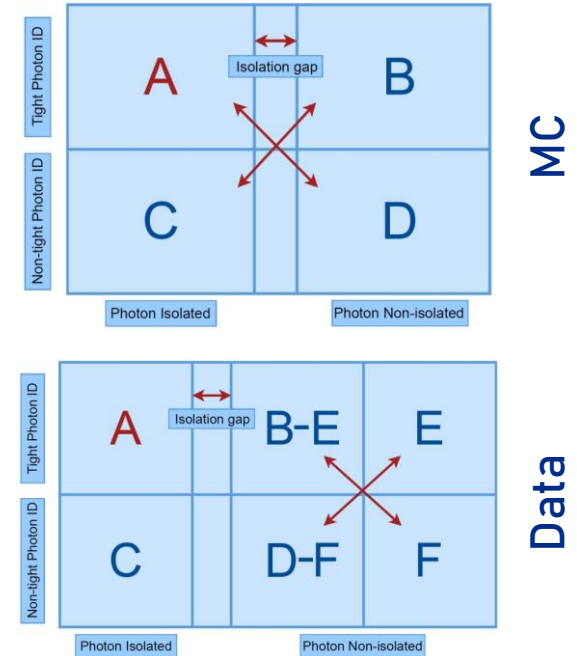
Cut, GeV	loose'2	loose'3	loose'4	loose'5
MC				
4.5	1.18 ± 0.19	1.15 ± 0.16	1.08 ± 0.13	1.11 ± 0.13
7.5	1.12 ± 0.14	1.16 ± 0.13	1.10 ± 0.11	1.11 ± 0.11
10.5	1.15 ± 0.14	1.16 ± 0.13	1.11 ± 0.11	1.12 ± 0.11

Data-driven				
4.5	0.99 ± 0.11	1.05 ± 0.11	1.07 ± 0.09	1.09 ± 0.09
7.5	1.13 ± 0.11	1.09 ± 0.09	1.06 ± 0.08	1.05 ± 0.08
10.5	1.00 ± 0.10	0.99 ± 0.09	0.96 ± 0.07	0.96 ± 0.07

In B-E, E, D-F and F

Isolation should not correlate with non-tight ID!

$$\frac{N_A^{jet \rightarrow \gamma}}{N_B} = \frac{N_C}{N_D}$$



Resulting R for MC and data

R factor	loose'2	loose'3	loose'4	loose'5
MC	0.99 ± 0.15	1.05 ± 0.11	1.07 ± 0.14	1.1 ± 0.3

jet \rightarrow γ misID background: uncertainties

- Statistical uncertainty:

\Rightarrow The event yields of four regions in data and non jet \rightarrow γ background are varied by $\pm 1\sigma$ independently (9%).

\Rightarrow The statistical uncertainty on the signal leakage parameters is negligible.

Total statistics: 9%.

Central value	1765^{+164}_{-160}
Loose'2	+240
Loose'4	+85
Loose'5	-55
Isolation gap +0.3 GeV	-60
Isolation gap -0.3 GeV	+33

- Systematic uncertainty :

\Rightarrow Anti-tight definition and isolation gap choice - variations of ABCD regions determination by $\pm 1\sigma$ changes in data yield (14%).

\Rightarrow The deviations from the nominal value from varying R factor by ± 0.10 (10%).

\Rightarrow Uncertainty coming from the signal leakage parameters is obtained via using different generators and parton shower models (0.7%).

Central value	1765^{+164}_{-160}
$R + \Delta R$	+180
$R - \Delta R$	-178

Signal leakage parameters	MadGraph+Pythia8, Sherpa 2.2	MadGraph+Pythia8, MadGraph+Pythia8	Relative deviation
c_B	$(278 \pm 4) \cdot 10^{-5}$	$(47 \pm 2) \cdot 10^{-4}$	7%
c_C	$(3205 \pm 14) \cdot 10^{-5}$	$(330 \pm 6) \cdot 10^{-4}$	3%
c_D	$(178 \pm 11) \cdot 10^{-6}$	$(39 \pm 5) \cdot 10^{-5}$	120%
jet \rightarrow γ estimation	1765	1752	0.7%

\Rightarrow The iso/ID uncertainty on reconstruction photon efficiency $\delta_{\text{eff}}^{\text{iso/ID}}$ (1.3%). ← This source is chosen

Total systematics: 20%.

\Rightarrow Total number of jet \rightarrow γ events: $1770 \pm 160 \pm 350$. Z($\nu\nu$)+jets, multi-jet and W($\tau\nu$) h.c. MC predicts 2000 ± 1300 (stat.)

jet \rightarrow γ misID background: slice method

- The jet \rightarrow γ background shape cannot be properly modeled with MC. For this reason, the shape of jet \rightarrow γ background is estimated via slice method.
- The proposed slice method splits the phase space into four orthogonal regions based on kinematic cuts and the photon isolation.
- The non-isolated regions are split into a set of successive intervals (slices) based on the photon isolation.

⇒ Four isolation slices are chosen: [0.065, 0.090, 0.115, 0.140, 0.165].

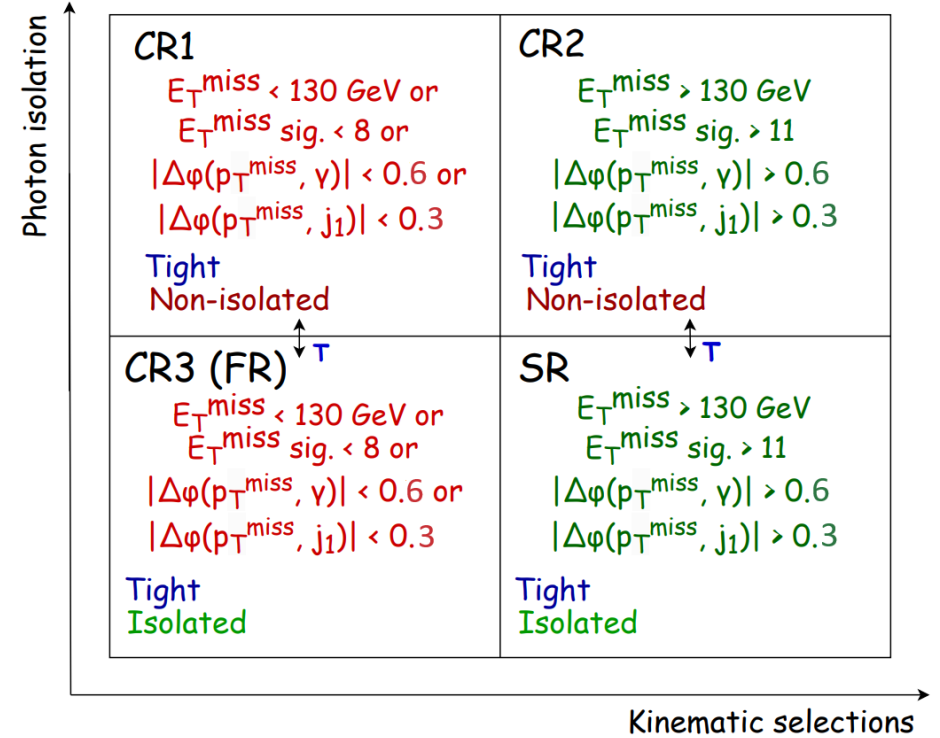
$$N_{CR1(i)}^{jet \rightarrow \gamma} = N_{CR1(i)}^{data} - N_{CR1(i)}^{Z(\nu\bar{\nu})\gamma} - N_{CR1(i)}^{bkg}$$

$$H_{jet \rightarrow \gamma}^{[0.A,0.B]} = H_{data}^{[0.A,0.B]}[X] - H_{sig}^{[0.A,0.B]}[X] - H_{bkg}^{[0.A,0.B]}[X]$$

$$\Delta^{CR2}[X] = \left(\frac{H_{jet \rightarrow \gamma}^{[0.065,0.09]}[X] - H_{jet \rightarrow \gamma}^{[0.115,0.14]}[X]}{2} + \frac{H_{jet \rightarrow \gamma}^{[0.09,0.115]}[X] - H_{jet \rightarrow \gamma}^{[0.14,0.165]}[X]}{2} \right)$$

⇒ The jet \rightarrow γ shape in the SR: $H_{jet \rightarrow \gamma}^{SR} = H_{jet \rightarrow \gamma}^{[0.A_1,0.B_1]}[X] + 2 \cdot \Delta^{CR}[X]$

← The correction term

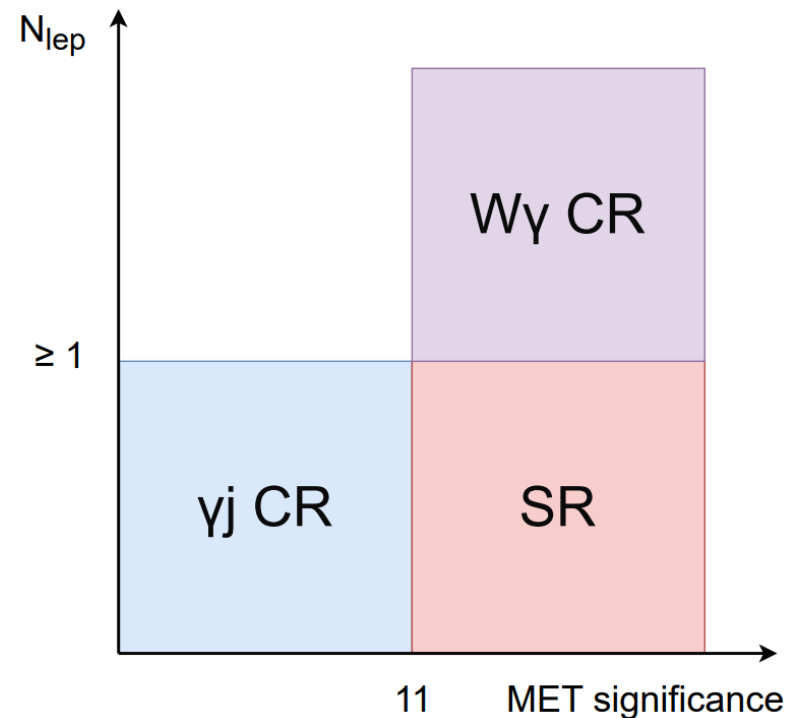
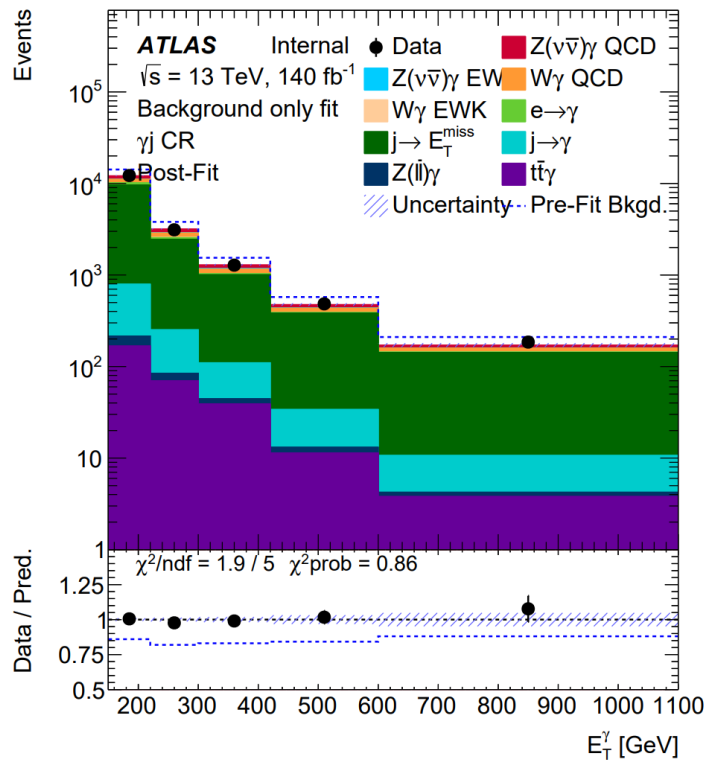
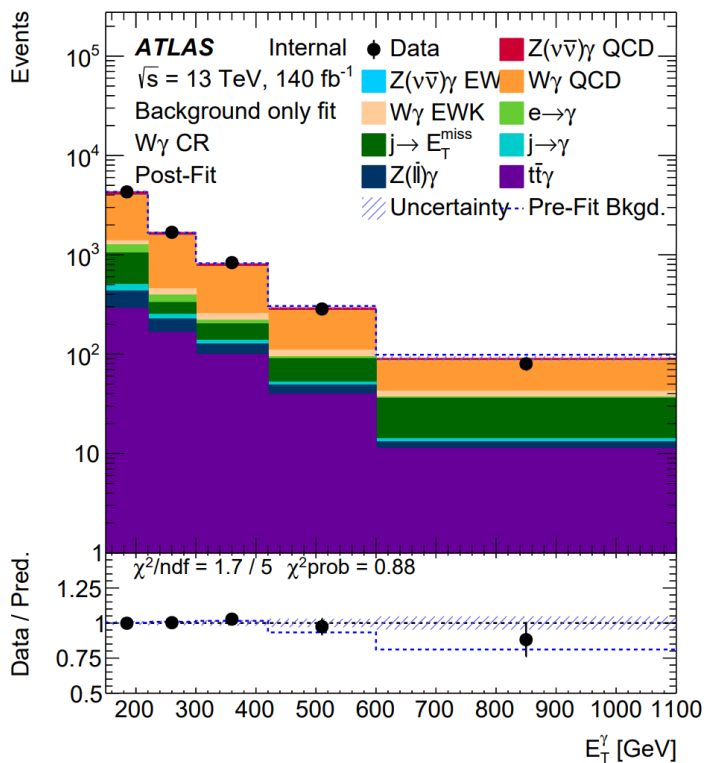


Template fit

- Three free parameters are introduced in the combined fit: a signal strength parameter $\mu(Zg)$ and two normalization factors $\mu(Wg)$ and $\mu(\gamma j)$ used to scale the yields of $W(l\nu)\gamma$ and $t\bar{t}\gamma$ and γ +jets processes.

→ The binned likelihood function used in the analysis is:

$$\mathcal{L}(\mu, \theta) = \prod_r \left[\prod_i^{\text{bins} \in r} \text{Pois}(N_i^{\text{data}} | \mu v_i^s \eta^s(\theta) + v_i^b \eta^b(\theta)) \right] \cdot \prod_i^{\text{nuis. par.}} \mathcal{L}(\theta_i)$$



	SR	$W\gamma$ CR	γj CR
$\mu_{Z\gamma}$	✓		
$\mu_{W\gamma}$	✓	✓	✓
$\mu_{\gamma j}$	✓	✓	✓

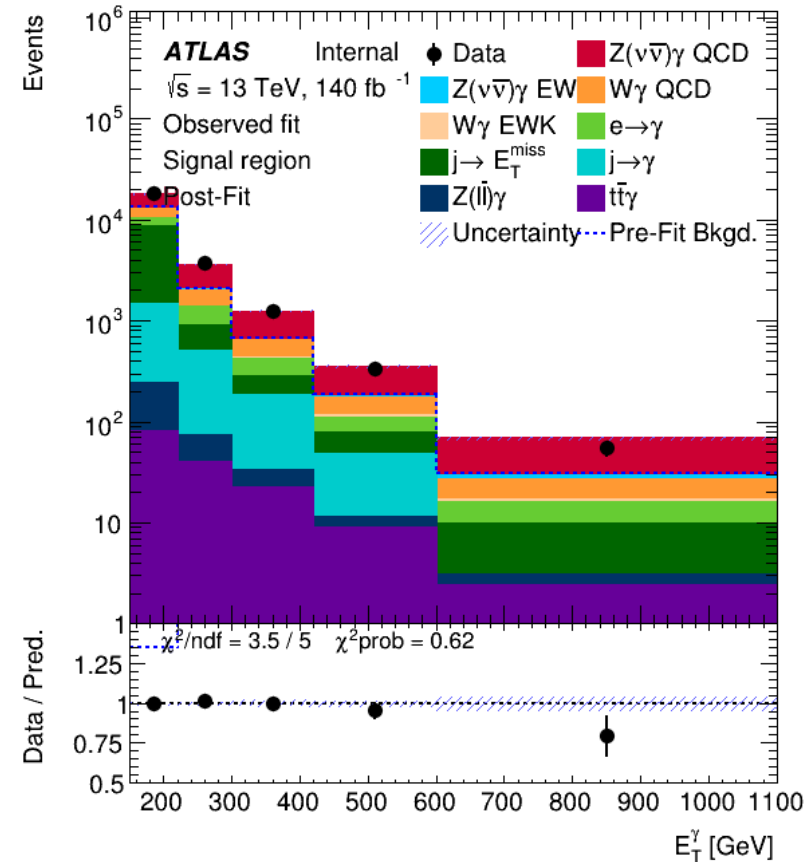
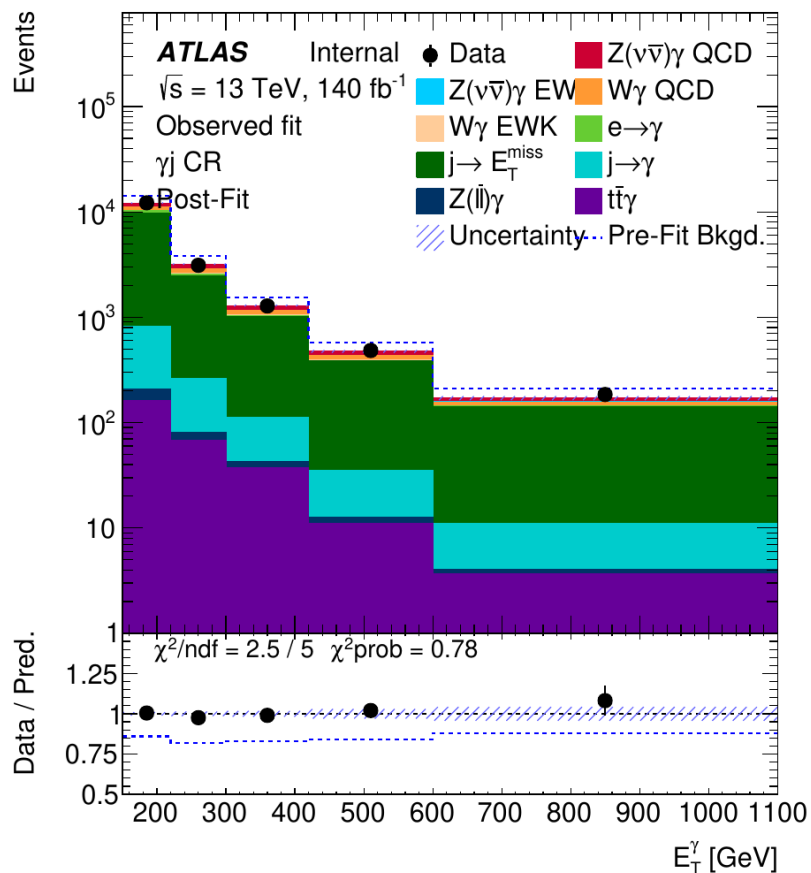
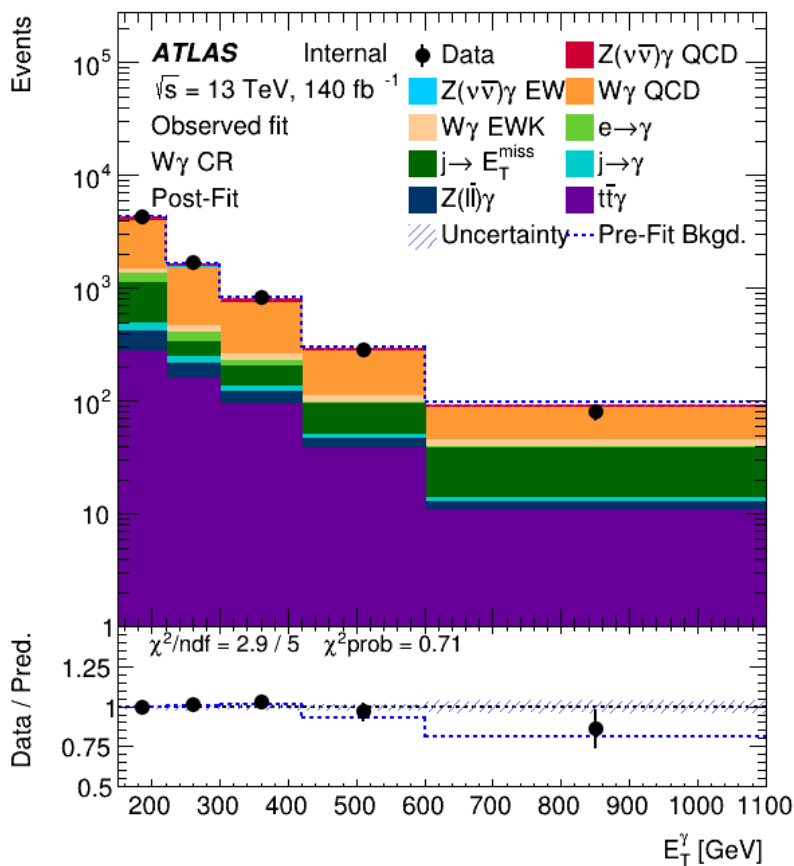
Results of background only fit:

$$\mu(Wg) = 0.93 \pm 0.13$$

$$\mu(\gamma j) = 0.74 \pm 0.12$$

Template fit

- Using the Asimov data: $\mu_{Z\gamma} = 1.00 \pm 0.08$, $\mu_{W\gamma} = 0.93 \pm 0.12$ and $\mu_{j\gamma} = 0.74 \pm 0.10$. Expected signal significance 69σ .
- Fit in the SR and CRs:



$\Rightarrow \mu_{Z\gamma} = 0.70 \pm 0.06$, $\mu_{W\gamma} = 0.92 \pm 0.06$ and $\mu_{j\gamma} = 0.88 \pm 0.08$. Observed signal significance 50σ .

Unfolding and differential measurement

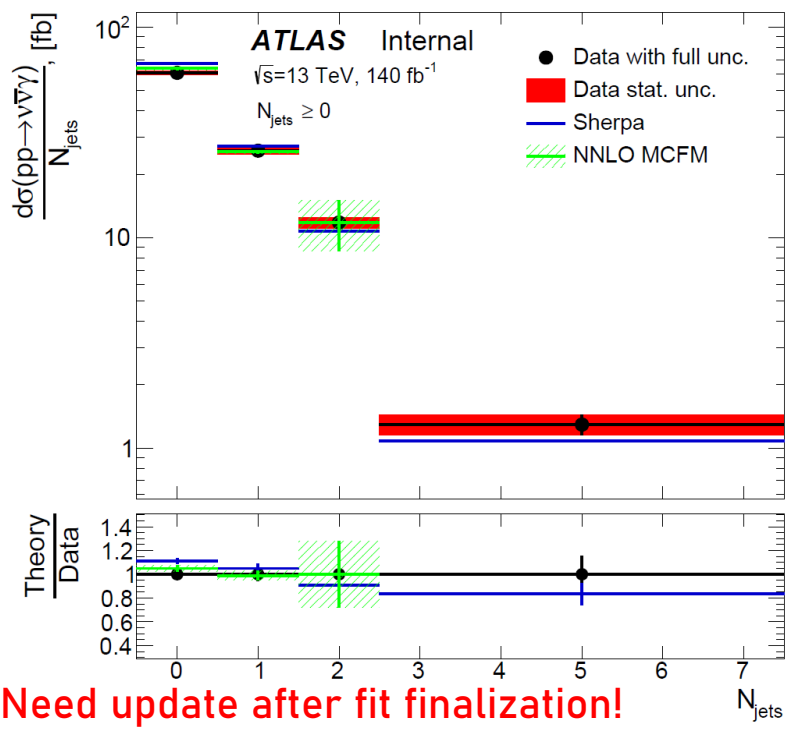
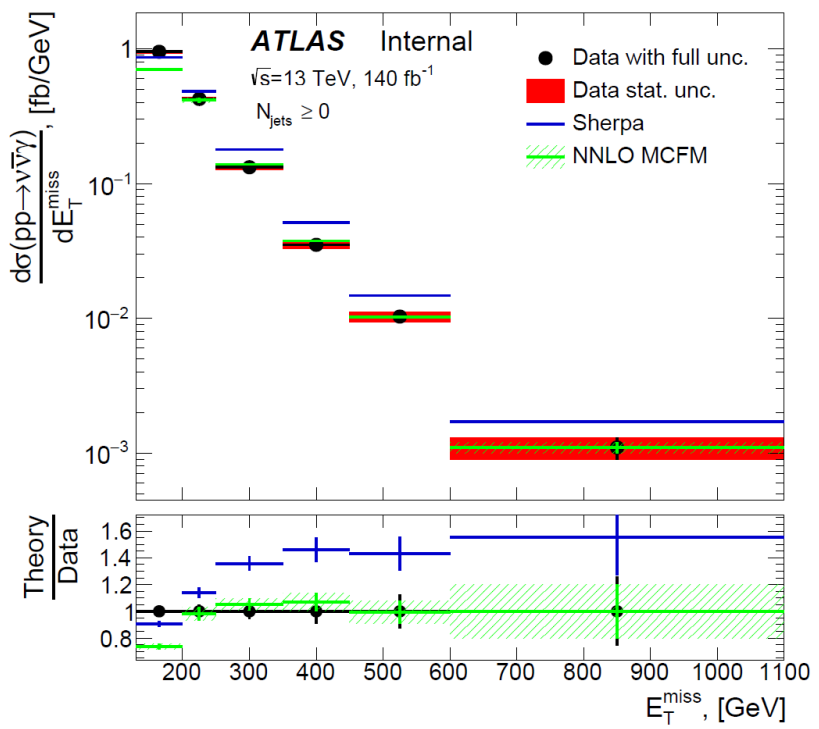
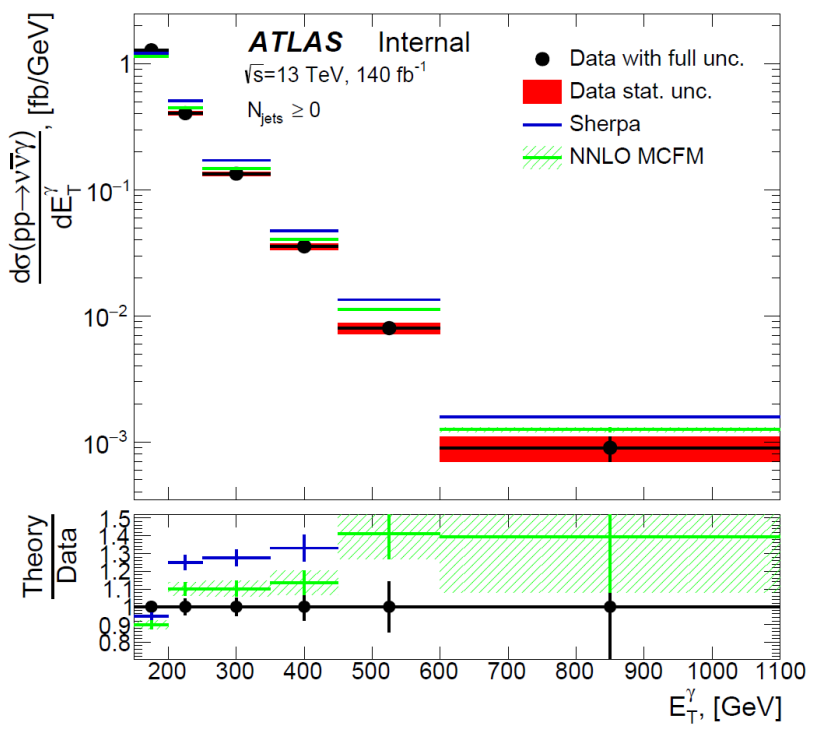
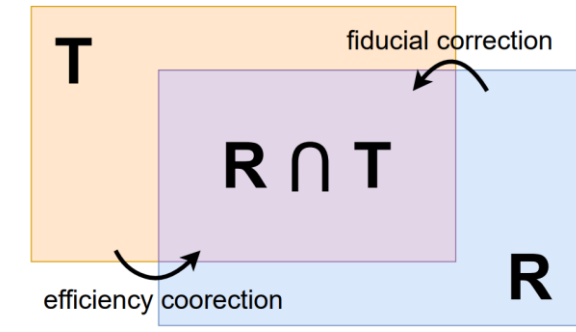
- The goal of unfolding is to take the measured observable and translate it into the true observable.

⇒ The response matrix R relates true vector x and observed vector y : $\hat{R}x = y$

⇒ The response matrix is defined as: $R_{ij} = \frac{1}{\alpha_i} \epsilon_j M_{ij}$ Migration matrix: $M_{ij} = \frac{N_{ij}^{\text{det.} \cap \text{fid.}}}{N_j^{\text{det.} \cap \text{fid.}}}$

⇒ The unfolding procedure is performed according to the maximum likelihood method via **TRExFitter**.

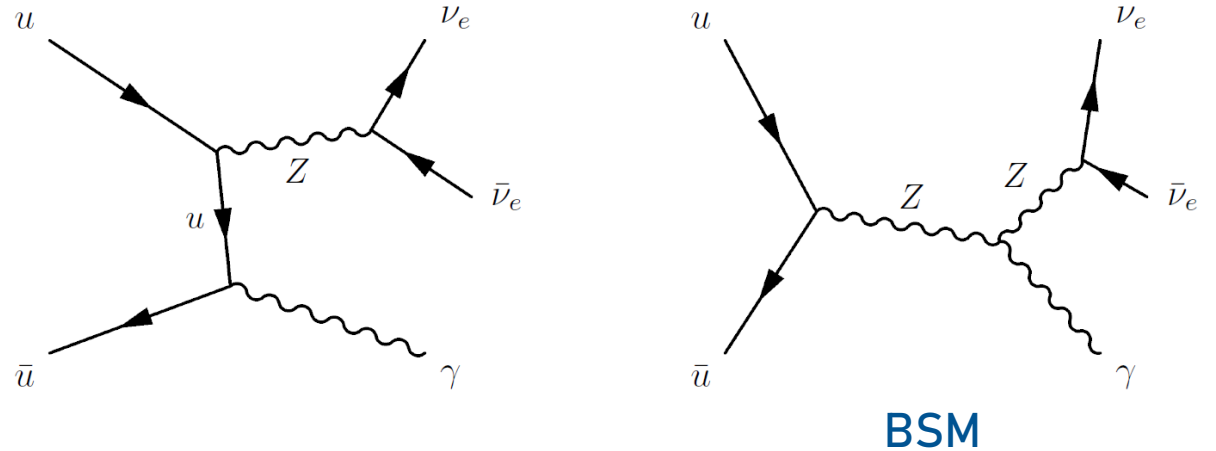
⇒ The differential cross-section is defined by equation: $\sigma_j = \frac{N_j^{\text{unfold}}}{(\int \mathcal{L} dt) \cdot \Delta x_j}$



Need update after fit finalization!

aTGC: introduction

- $Z(\nu\nu)\gamma$ production is very sensitive to the neutral triple gauge couplings (aTGCs). aTGCs are zero in the SM at the tree level.
- Two ways to describe aTGCs: effective field theory and vertex function approach. Both formalisms were improved by theorists and new terms in both formalisms appear.



⇒ State-of-the-art UFO models are needed to generate the events. For both formalisms models with new terms were created.

EFT: model NTGC_all, [JIRA ticket](#). VF: model NTGC_VF, [JIRA ticket](#).

EFT: 6 Wilson coefficients (C_{G^+}/Λ^4 , C_{G^-}/Λ^4 , $C_{\tilde{B}W}/\Lambda^4$, C_{BW}/Λ^4 , C_{BB}/Λ^4 , C_{WW}/Λ^4).

VF: 12 parameters ($h_i^V; i=1..6; V=Z, \gamma$). Only $i=3..5$ are planned to be constrained.

aTGC: current results

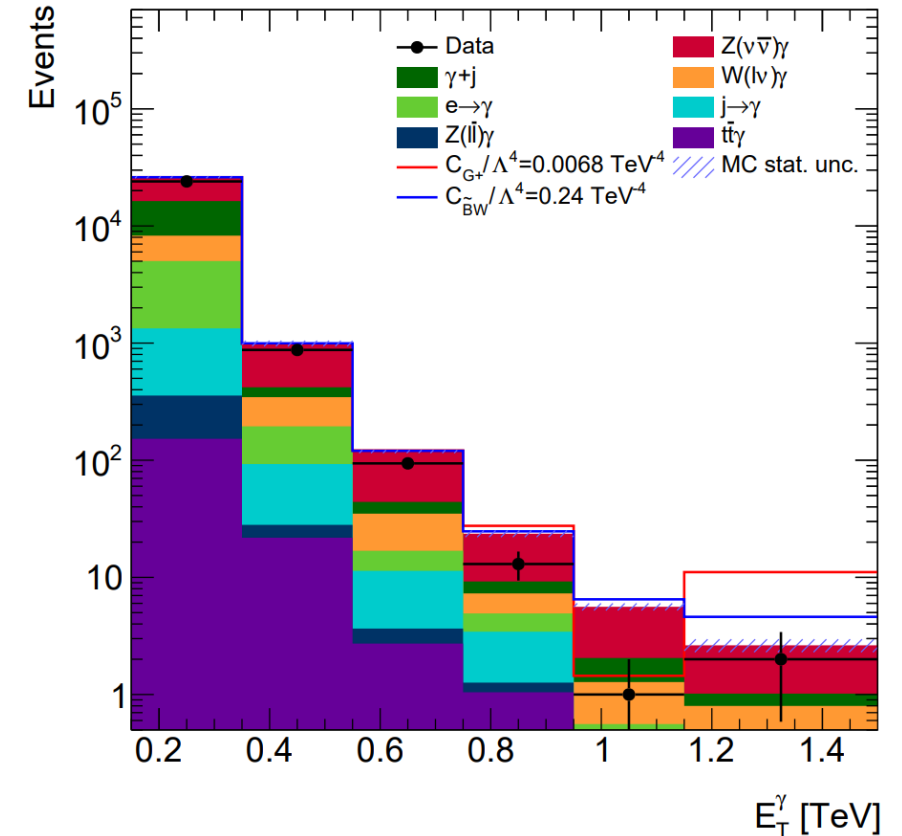
- Plan is to search for CP-conserving effects only. Search for CP-violating effects requires identification of the decay products.
- EFT samples were prepared, VF samples request in progress.
- Strategy: reco-level fit of the E_T^γ distribution. Preliminary results:

EFT

Coef.	Exp. limits [TeV^{-4}]	Obs. limits [TeV^{-4}]	$\sqrt{s_{\text{max}}}$ [TeV]
C_{G+}/Λ^4	[-0.0065; 0.0047]	[-0.0045; 0.0068]	11.2
C_{G-}/Λ^4	[-0.30; 0.34]	[-0.21; 0.27]	22.3
$C_{\tilde{B}W}/\Lambda^4$	[-0.35; 0.34]	[-0.25; 0.24]	15.8
C_{BW}/Λ^4	[-0.63; 0.63]	[-0.45; 0.45]	19.9
C_{BB}/Λ^4	[-0.25; 0.25]	[-0.18; 0.18]	25.5
C_{WW}/Λ^4	[-1.3; 1.3]	[-0.90; 0.90]	16.2

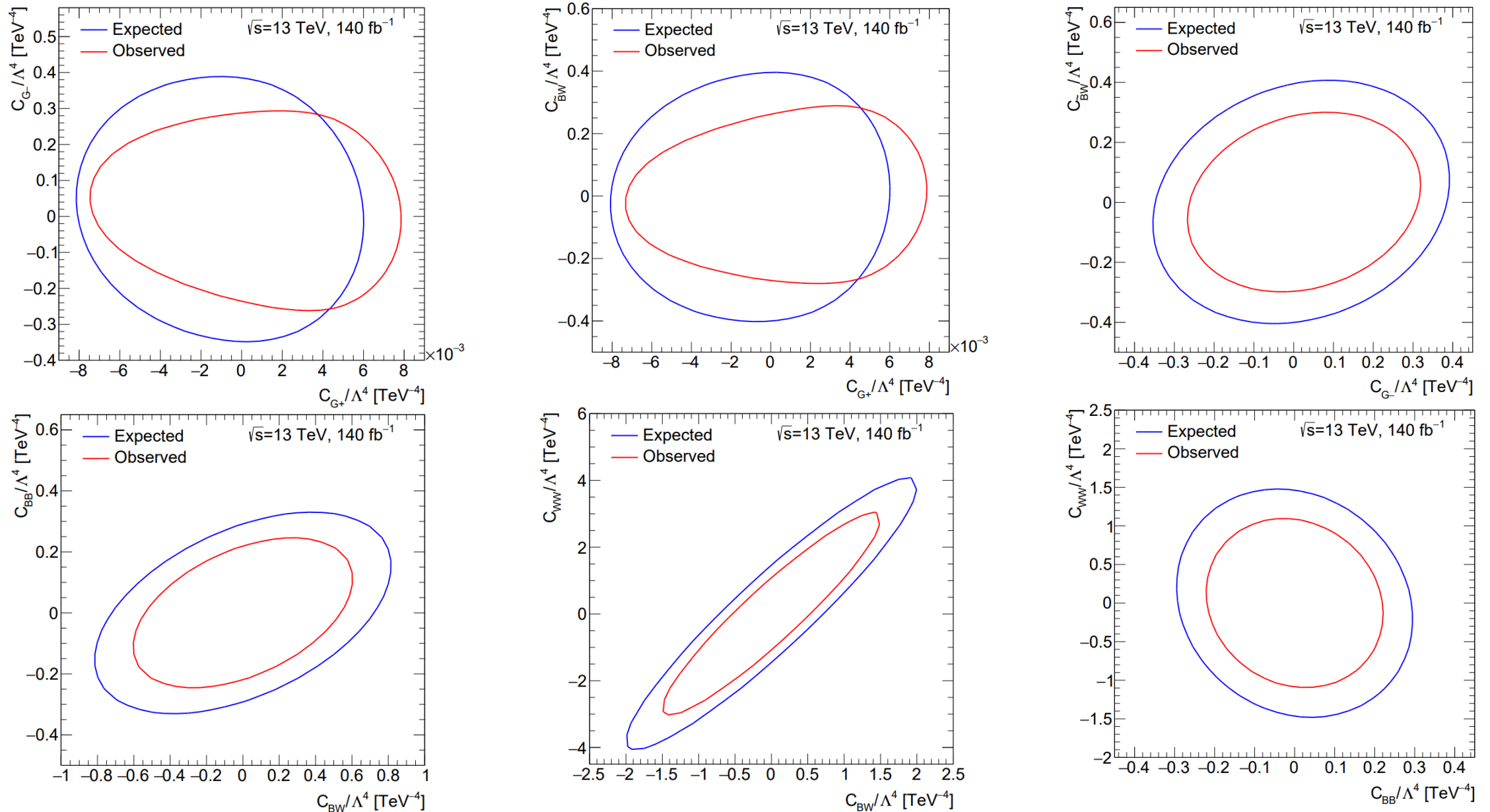
VF

Coef.	Exp. limits	Obs. limits	$\sqrt{s_{\text{max}}}$ [TeV]
h_3^γ	$[-2.2; 2.2] \times 10^{-4}$	$[-1.4; 1.7] \times 10^{-4}$	18
h_3^Z	$[-2.0; 2.1] \times 10^{-4}$	$[-1.4; 1.4] \times 10^{-4}$	17
h_4^γ	$[-2.1; 2.0] \times 10^{-7}$	$[-1.9; 1.8] \times 10^{-7}$	11
h_4^Z	$[-2.0; 2.0] \times 10^{-7}$	$[-1.8; 1.8] \times 10^{-7}$	10
h_5^γ	$[-1.0; 1.0] \times 10^{-7}$	$[-0.9; 0.9] \times 10^{-7}$	11
h_5^Z	$[-0.9; 1.2] \times 10^{-7}$	$[-0.7; 1.2] \times 10^{-7}$	10



Last column is the center-of-mass energy at which unitarity is violated. Values are large, therefore, the unitarity is preserved.

aTGC: 2D limits



Summary

- All steps of inclusive $Z(\nu\bar{\nu})\gamma$ Run2 analysis are already done: selection optimisation, data-driven estimation of $e \rightarrow \gamma$ and $\text{jet} \rightarrow \gamma$, fit procedure, control plots, unfolding, differential cross-sections.

Plans:

- ⇒ To solve problems systematics.
- ⇒ To update and to obtain other observables differential cross-section plots.
- ⇒ To continue work on limits on aTGCs.
- ⇒ Almost all chapters of the internal note are ready, but need update.
- ⇒ EB request ASAP.

Thank you for your attention!

BACK-UP

Questions

1) What is the signal significance for MC16a, d and e?

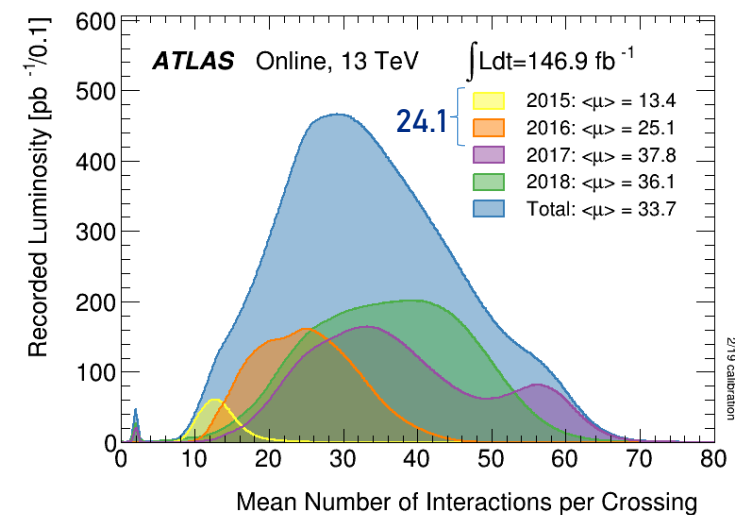
Process	MC16a	MC16d	MC16e
Signal			
Z($\nu\nu$) γ QCD	2915 \pm 4	3345 \pm 5	4452 \pm 5
Z($\nu\nu$) γ EWK	45.57 \pm 16	51.80 \pm 0.19	68.9 \pm 0.2
Total signal	2961 \pm 4	3396 \pm 5	4521 \pm 5
Background			
W γ QCD	884 \pm 11	1026 \pm 13	1400 \pm 13
W γ EWK	29.5 \pm 0.3	34.1 \pm 0.4	45.8 \pm 0.4
tt, top	58 \pm 3	62 \pm 4	81 \pm 4
W($e\nu$)	788 \pm 221	1322 \pm 303	1480 \pm 310
tt γ	48.3 \pm 1.4	55.3 \pm 1.7	74.6 \pm 1.8
γ +j	1829 \pm 35	2746 \pm 53	3549 \pm 51
Zj	134 \pm 11	115 \pm 12	165 \pm 13
Z(l l) γ	56 \pm 2	64 \pm 2	92 \pm 2
W($\tau\nu$)	147 \pm 20	191 \pm 46	302 \pm 48
Total bkg.	3973 \pm 225	5616 \pm 312	7190 \pm 318
Stat. signif.	35.6 \pm 0.6	35.8 \pm 0.6	41.8 \pm 0.6

Process	MC16a	MC16d	MC16e
Signal, fb			
Z($\nu\nu$) γ QCD	79.543 \pm 0.11	74.95 \pm 0.11	75.73 \pm 0.09
Z($\nu\nu$) γ EWK	1.243 \pm 0.04	1.161 \pm 0.04	1.172 \pm 0.03
Total signal	80.78 \pm 0.11	76.09 \pm 0.11	76.89 \pm 0.09
Background, fb			
W γ QCD	24.1 \pm 0.3	23.0 \pm 0.3	23.8 \pm 0.2
W γ EWK	0.805 \pm 0.008	0.764 \pm 0.009	0.779 \pm 0.007
tt, top	1.58 \pm 0.08	1.39 \pm 0.09	1.38 \pm 0.07
W($e\nu$)	22 \pm 6	30 \pm 7	25 \pm 5
tt γ	1.32 \pm 0.04	1.24 \pm 0.04	1.27 \pm 0.03
γ +j	49.9 \pm 1.0	61.5 \pm 1.2	60.4 \pm 0.9
Zj	3.7 \pm 0.3	2.6 \pm 0.3	2.8 \pm 0.2
Z(l l) γ	1.53 \pm 0.05	1.43 \pm 0.04	1.56 \pm 0.03
W($\tau\nu$)	4.0 \pm 0.5	4.3 \pm 1.0	5.1 \pm 0.8
Total bkg.	108 \pm 6	126 \pm 7	122 \pm 5
Stat. signif.	0.426 \pm 0.007	0.377 \pm 0.006	0.386 \pm 0.006

2015-2016: 36.64674 fb⁻¹

2017: 44.6306 fb⁻¹

2018: 58.7916 fb⁻¹ $\mathcal{L} = \frac{\mu n_b f_r}{\sigma_{inel}}$



2) To show the estimates of fake rates from data (e \rightarrow γ estimation) without third systematic

fake rate	$150 < E_T^\gamma < 250 \text{ GeV}$ $0 < \eta < 1.37$	$E_T^\gamma > 250 \text{ GeV}$ $0 < \eta < 1.37$	$1.52 < \eta < 2.37$
Z(ee) MC tag-n-probe	0.0218 \pm 0.0004	0.0197 \pm 0.0005	0.0762 \pm 0.0012
Z(ee) MC mass window variation	0.0217 \pm 0.0004	0.0198 \pm 0.0005	0.0765 \pm 0.0012
Z(ee) MC "real"	0.022 \pm 0.002	0.023 \pm 0.002	0.084 \pm 0.004

	$150 < E_T^\gamma < 250 \text{ GeV}$	$E_T^\gamma > 250 \text{ GeV}$
$0 < \eta < 1.37$	0.0234 \pm 0.0006 \pm 0.0009	0.0193 \pm 0.0013 \pm 0.0027
$1.52 < \eta < 2.37$	0.0714 \pm 0.0019 \pm 0.0021	

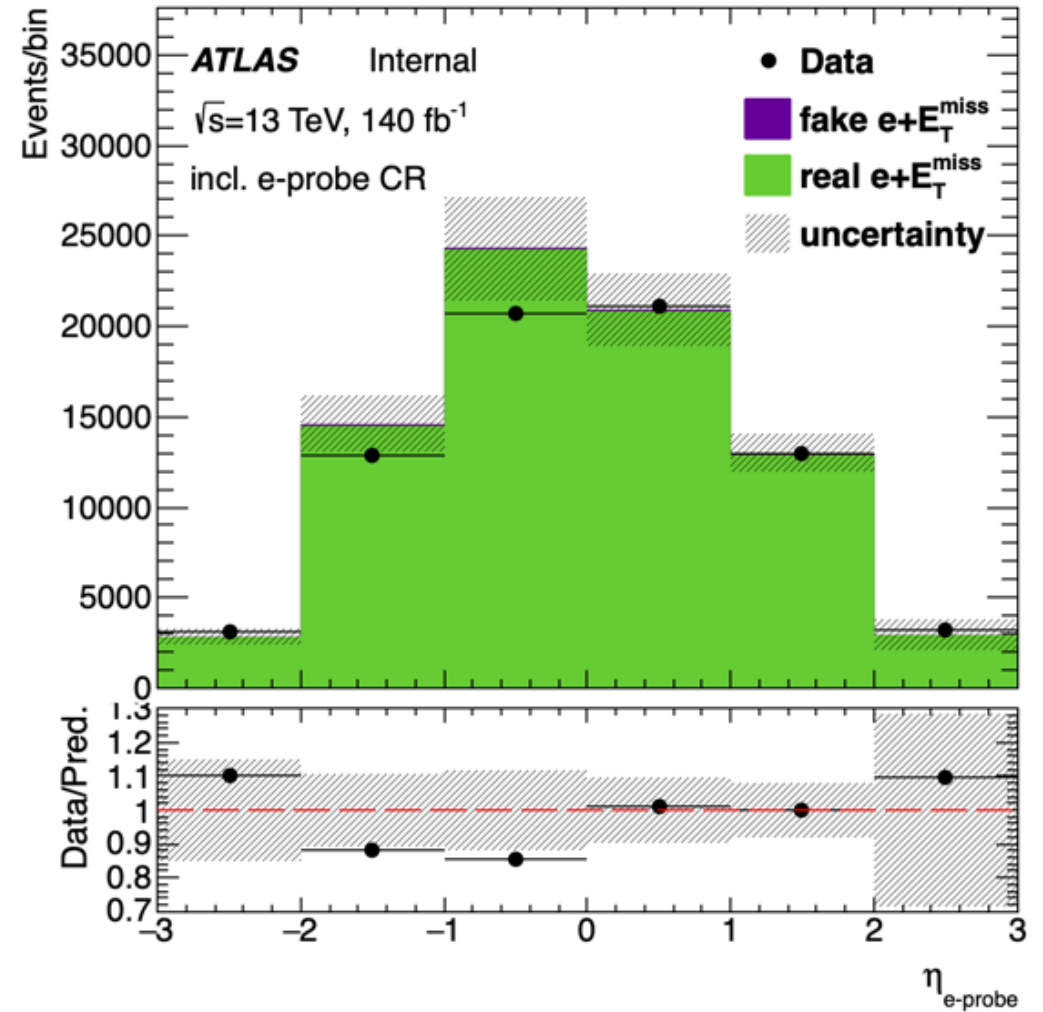
Questions

3) To check if there is really small background “fake e+MET” in the e-probe CR?

Answer: e + MET mostly consists of Zj and multijet processes due to misID of jet as electron. This background was estimated in VBS analysis and results from MC coincide with data within uncertainty. The estimate from MC is 26 ± 14 , the estimate from data (using ABCD method) is $32 \pm 26 \pm 8$ (VBS analysis).

3) Are you sure that in Mee production there are backgrounds? Check the possible background from jets.

Answer: Work on this issue is in progress. We sent samples to the grid to add the required branch to the tree. It took quite a long time



Questions

1) What is the signal significance for MC16a, d and e? \Rightarrow

Process	MC16a	MC16d	MC16e	Run2	Run2 (before opt.)
Signal					
Z($\nu\nu$) γ QCD	2915 \pm 4	3345 \pm 5	4452 \pm 5	10711 \pm 8	13438 \pm 9
Z($\nu\nu$) γ EWK	45.57 \pm 16	51.80 \pm 0.19	68.9 \pm 0.2	166.3 \pm 0.3	300.5 \pm 0.4
Total signal	2961 \pm 4	3396 \pm 5	4521 \pm 5	10878 \pm 8	13738 \pm 9
Background					
W γ QCD	884 \pm 11	1026 \pm 13	1400 \pm 13	3310 \pm 21	6393 \pm 28
W γ EWK	29.5 \pm 0.3	34.1 \pm 0.4	45.8 \pm 0.4	109.4 \pm 0.6	293.5 \pm 1.1
tt, top	58 \pm 3	62 \pm 4	81 \pm 4	177 \pm 5	1991 \pm 18
W($e\nu$)	788 \pm 221	1322 \pm 303	1480 \pm 310	3591 \pm 487	7934 \pm 540
tt γ	48.3 \pm 1.4	55.3 \pm 1.7	74.6 \pm 1.8	178 \pm 3	746 \pm 6
γ +j	1829 \pm 35	2746 \pm 53	3549 \pm 51	8123 \pm 82	63766 \pm 211
Zj	134 \pm 11	115 \pm 12	165 \pm 13	415 \pm 21	635 \pm 25
Z(ll) γ	56 \pm 2	64 \pm 2	92 \pm 2	211 \pm 4	399 \pm 5
W($\tau\nu$)	147 \pm 20	191 \pm 46	302 \pm 48	640 \pm 69	2222 \pm 127
Total bkg.	3973 \pm 225	5616 \pm 312	7190 \pm 318	16779 \pm 499	84380 \pm 595
Stat. signif.	35.6 \pm 0.6	35.8 \pm 0.6	41.8 \pm 0.6	65.4 \pm 0.6	43.86 \pm 0.14

2) Should the third source of systematic (difference between "real fake rate" in Z(ee) MC and tag-and-probe method) be considered for the data-driven background estimation of $e \rightarrow \gamma$?

Answer: This systematic can be disregarded because it is a deviation in MC, meaning this systematic is not mandatory. However, taking it into account makes the estimation more conservative.

3) To show the estimates of fake rates from MC and data ($e \rightarrow \gamma$ estimation)

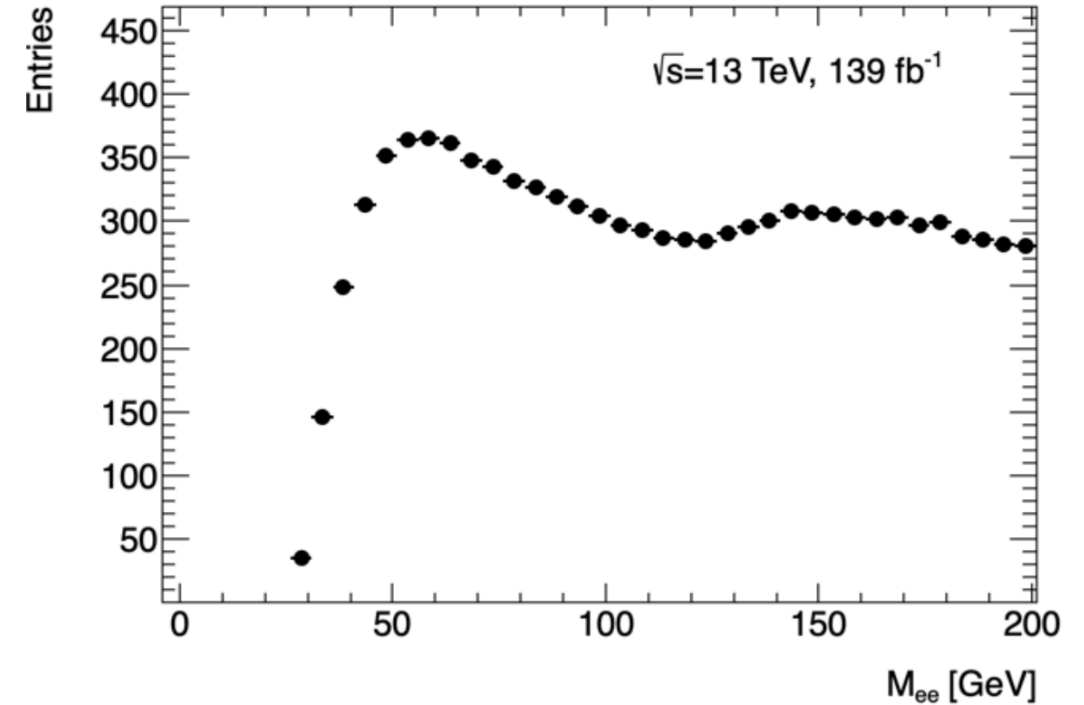
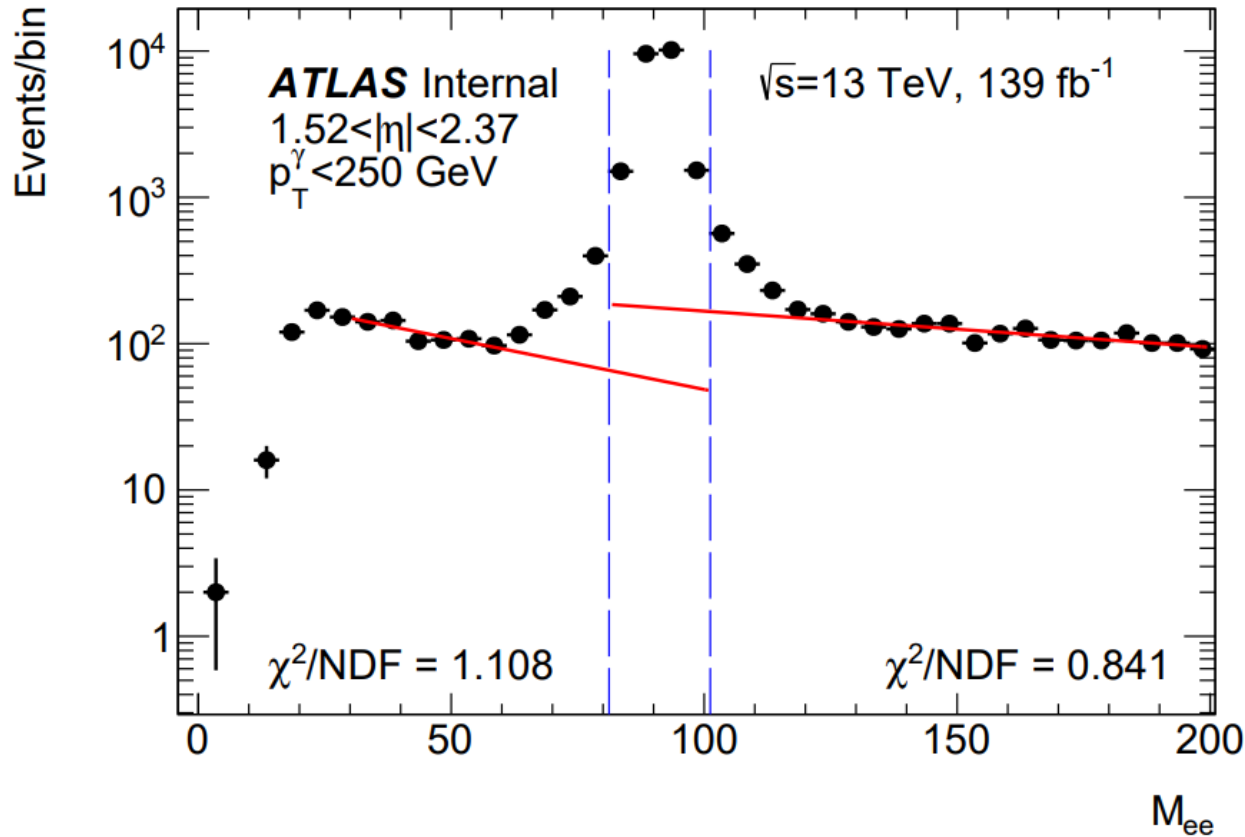
fake rate	$150 < E_T^\gamma < 250 \text{ GeV}$ $0 < \eta < 1.37$	$E_T^\gamma > 250 \text{ GeV}$ $0 < \eta < 1.37$	$1.52 < \eta < 2.37$
Z(ee) MC tag-n-probe	0.0218 \pm 0.0004	0.0197 \pm 0.0005	0.0762 \pm 0.0012
Z(ee) MC mass window variation	0.0217 \pm 0.0004	0.0198 \pm 0.0005	0.0765 \pm 0.0012
Z(ee) MC "real"	0.022 \pm 0.002	0.023 \pm 0.002	0.084 \pm 0.004

	$150 < E_T^\gamma < 250 \text{ GeV}$	$E_T^\gamma > 250 \text{ GeV}$
$0 < \eta < 1.37$	0.0234 \pm 0.0006 \pm 0.0010	0.0193 \pm 0.0013 \pm 0.0038
$1.52 < \eta < 2.37$	0.0714 \pm 0.0019 \pm 0.0074	

4) To show the difference between "real fake rate" in Z(ee) MC and tag-and-probe method (3rd question)

Questions

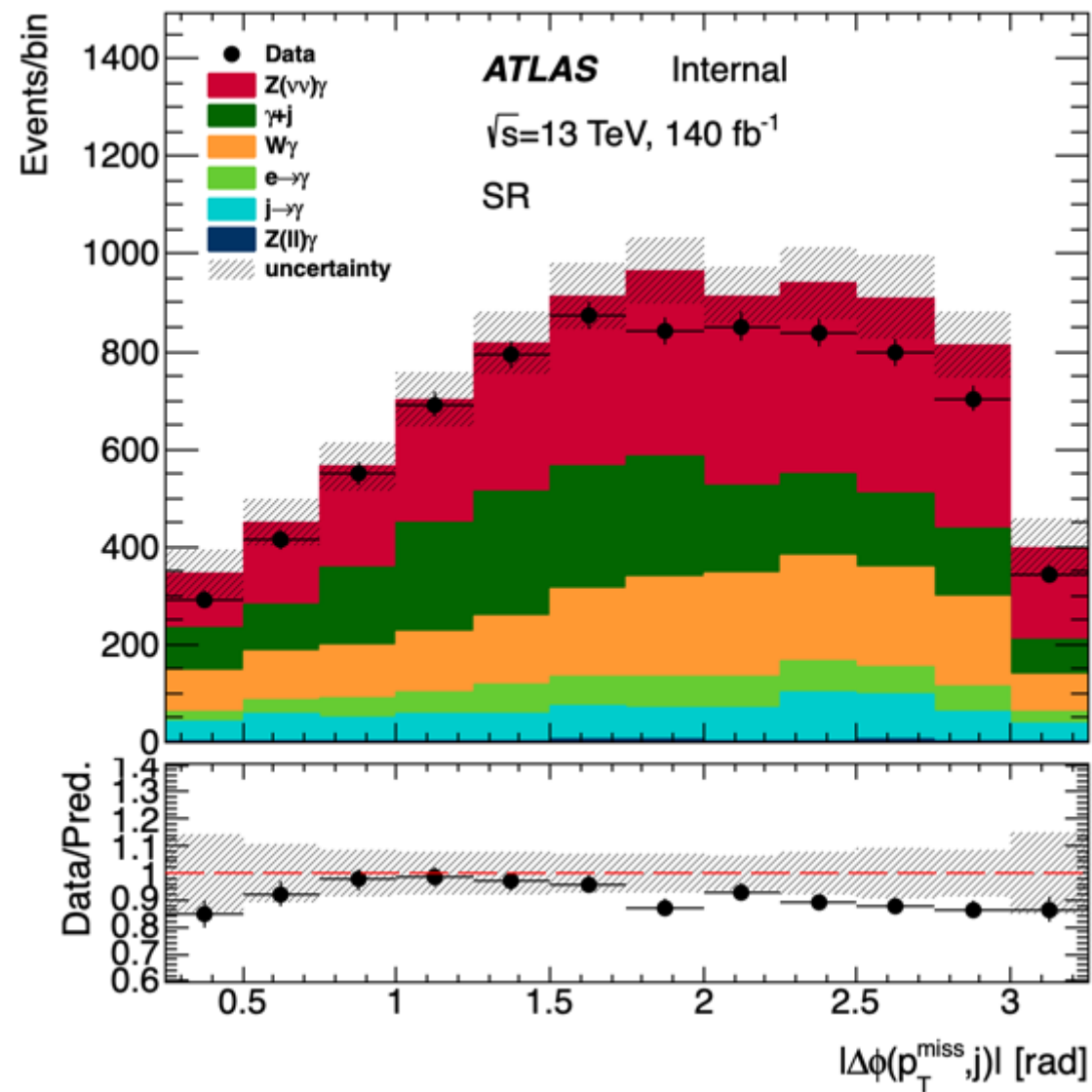
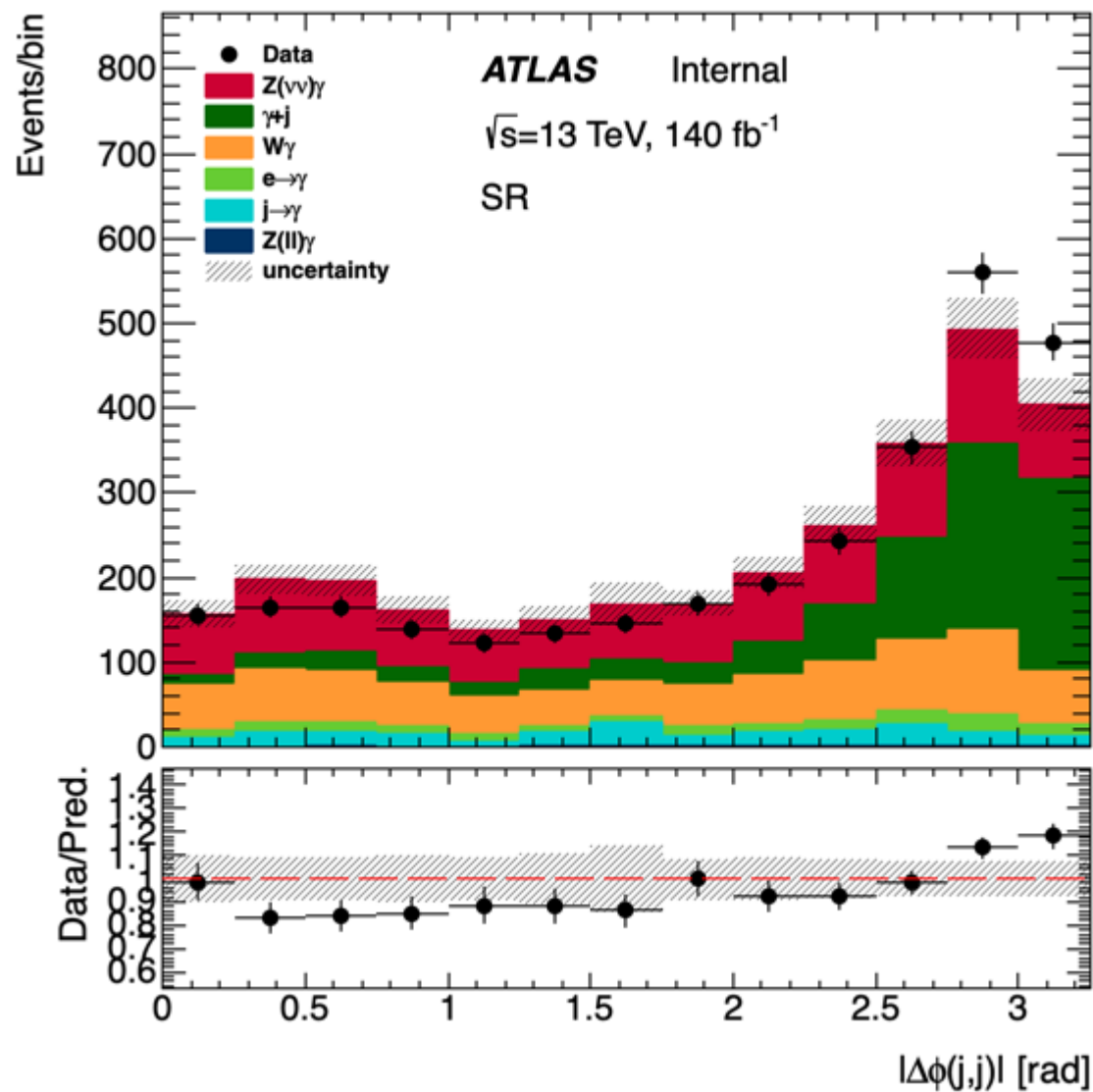
5) Anomaly on the M_{ee} plot in the region < 50 GeV



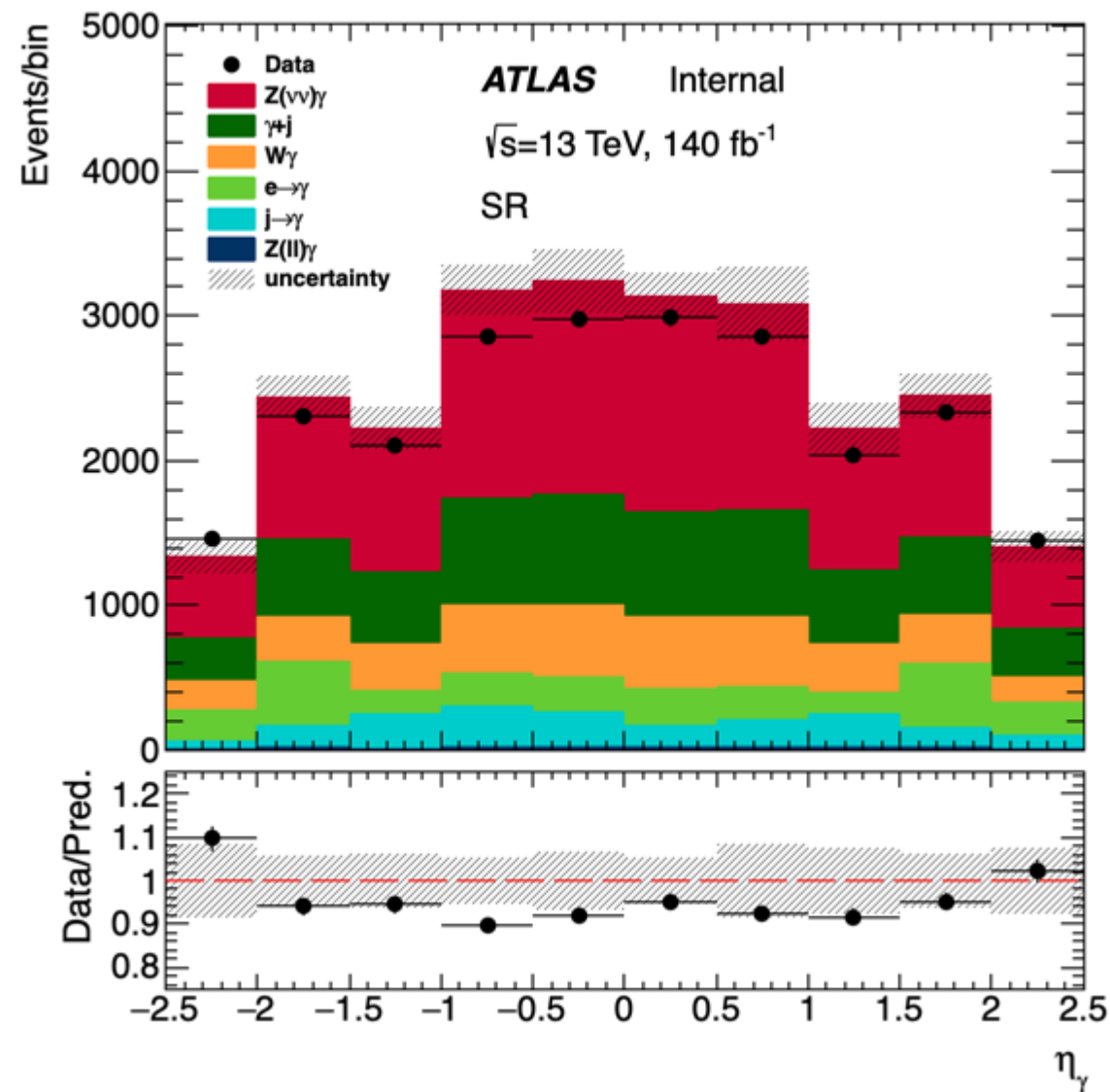
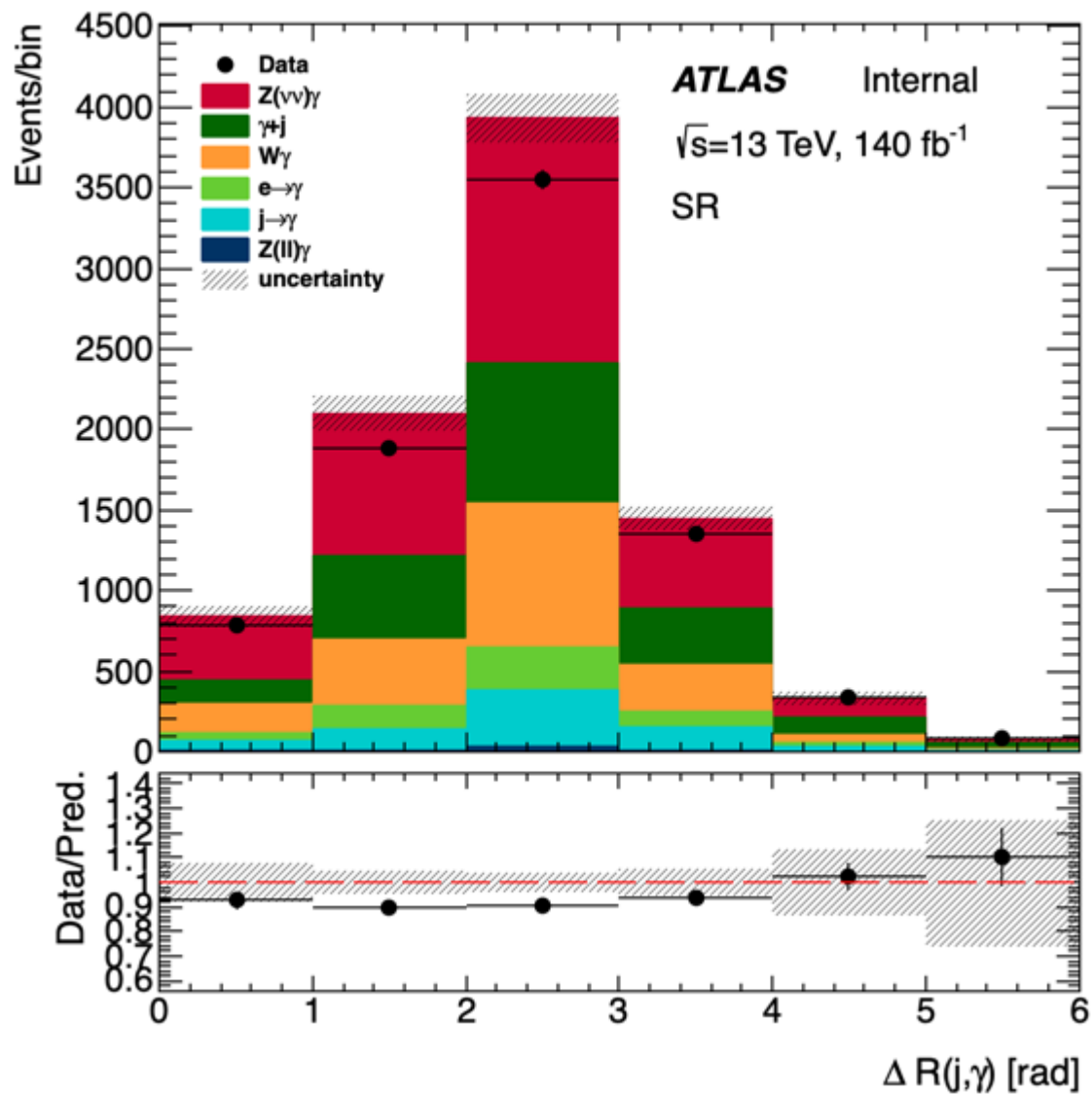
Distribution on the invariant mass of the Drell-Yan ee production in the modelling.

Preliminary answer: This may be related to the distribution on the invariant mass of the Drell-Yan ee production. This shape is caused by the combination of reconstruction and identification efficiencies overlapped with the kinematic distribution on electron p_T .

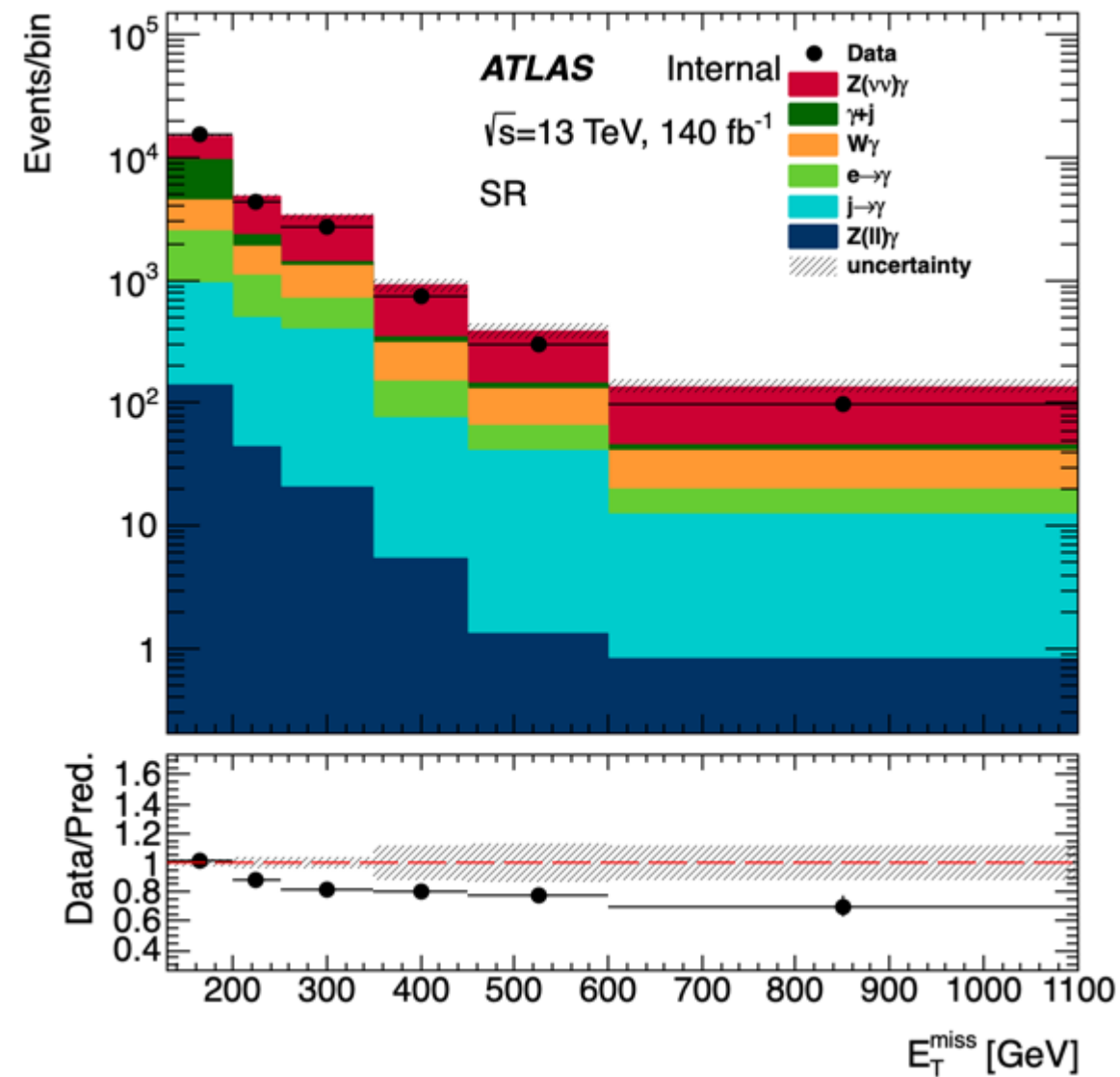
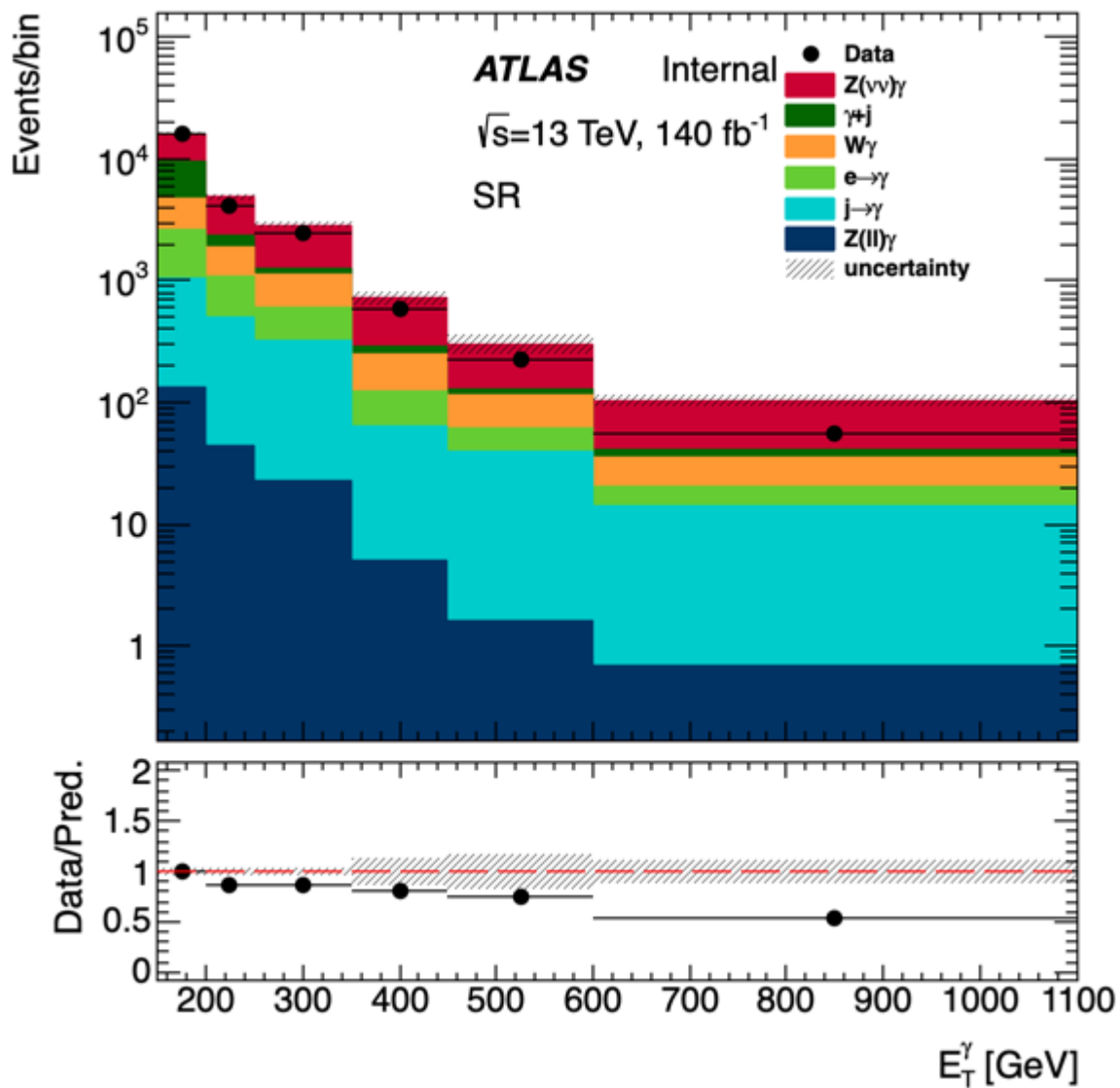
Control plots



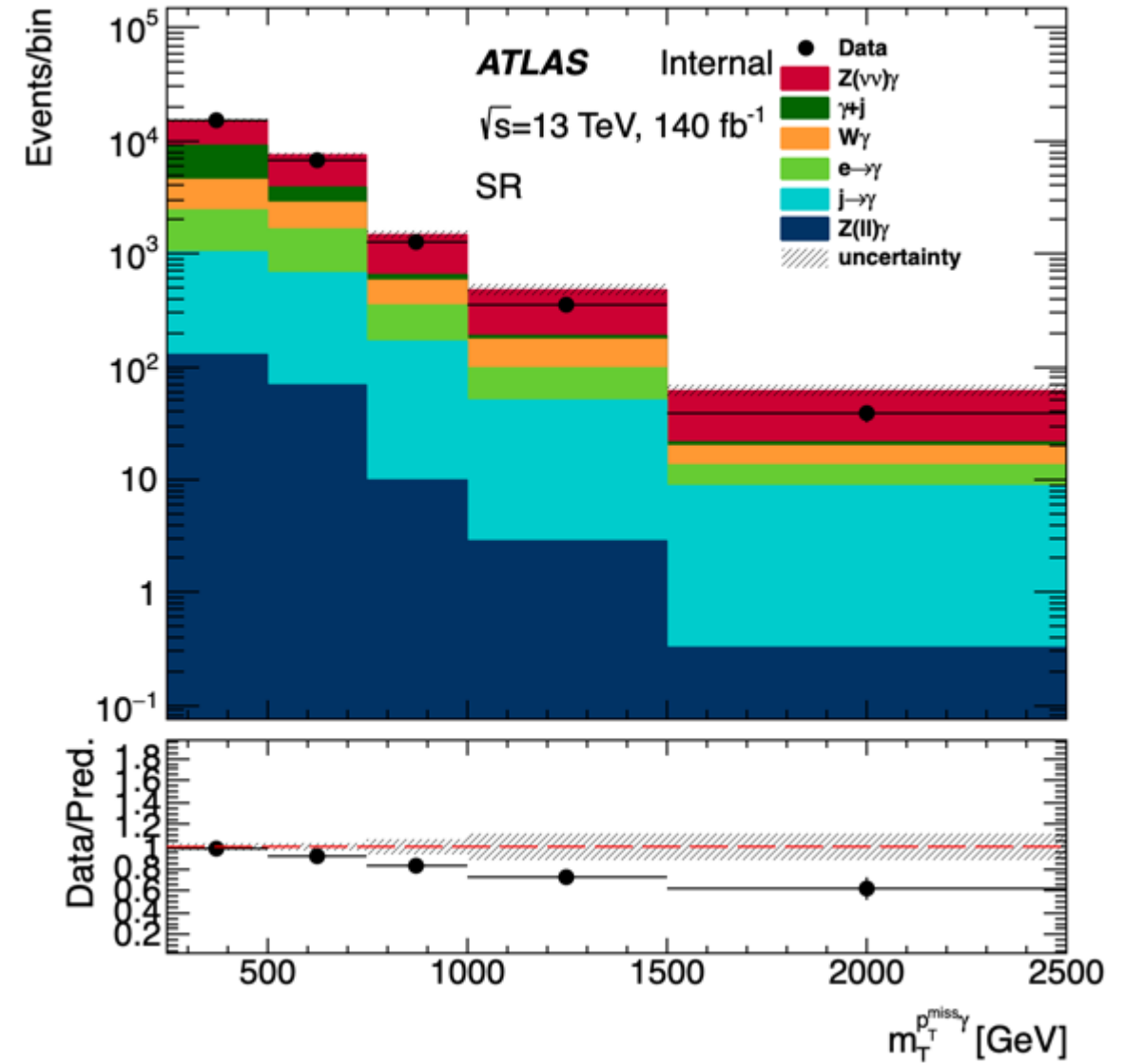
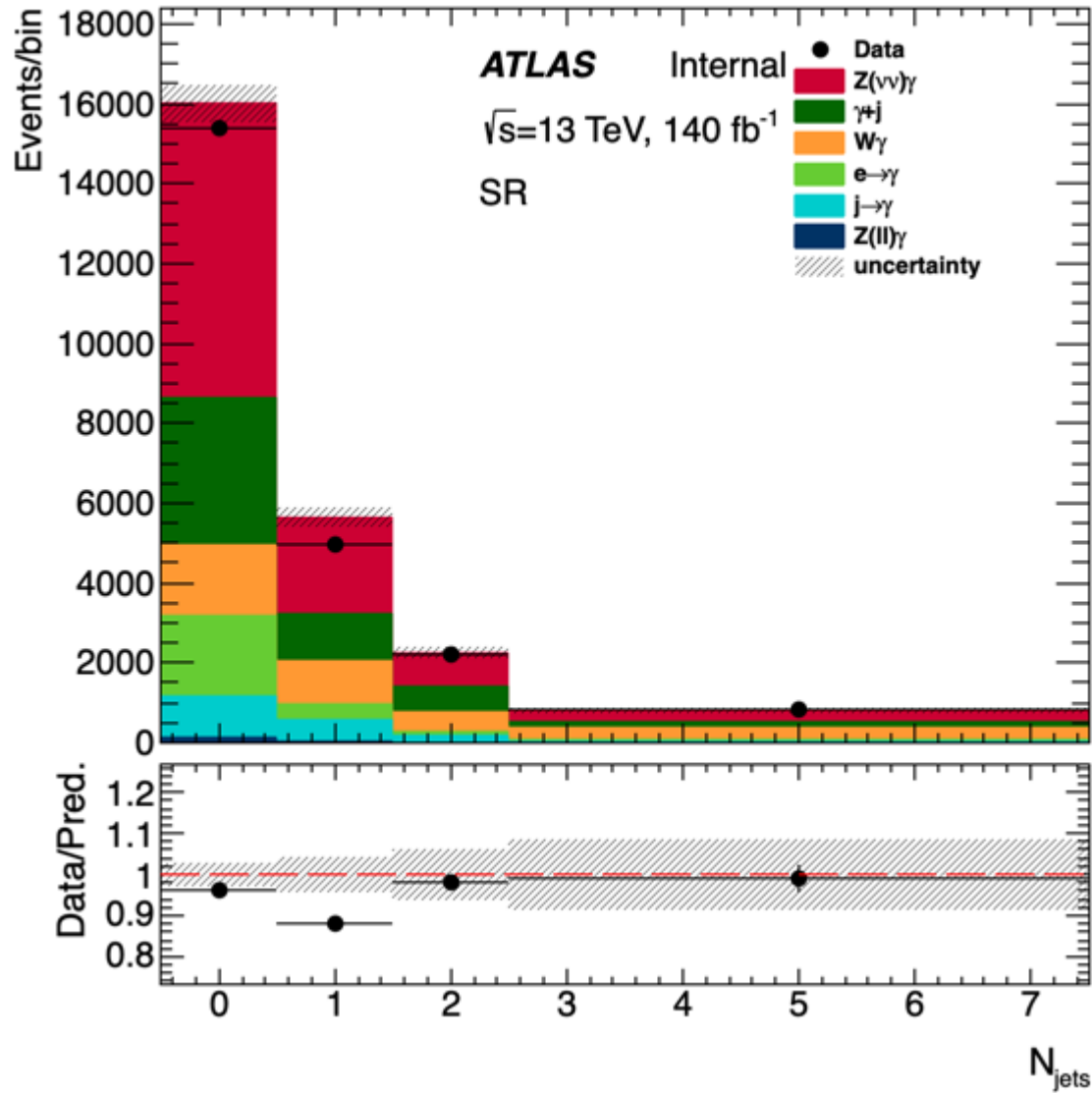
Control plots



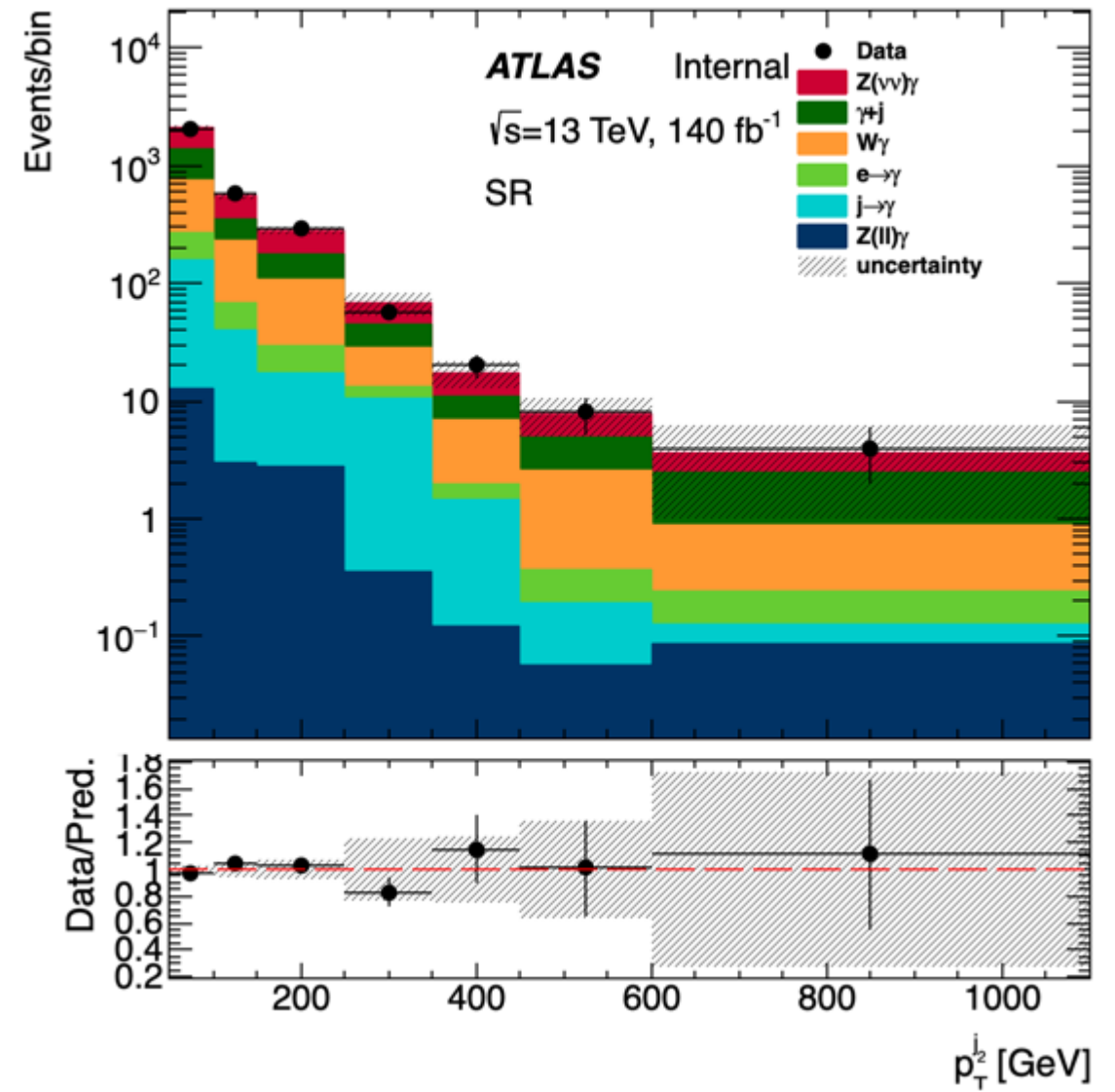
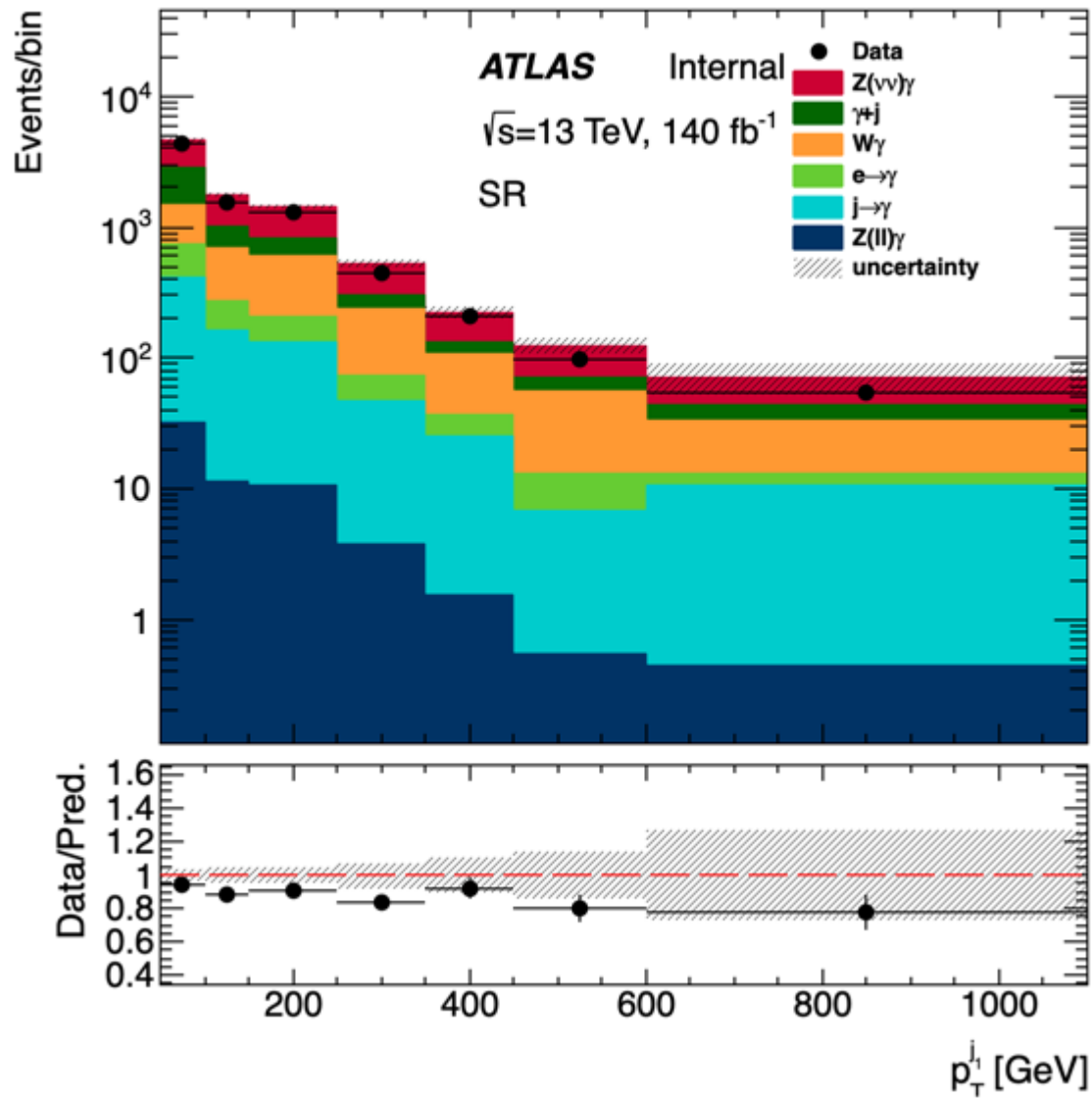
Control plots



Control plots



Control plots

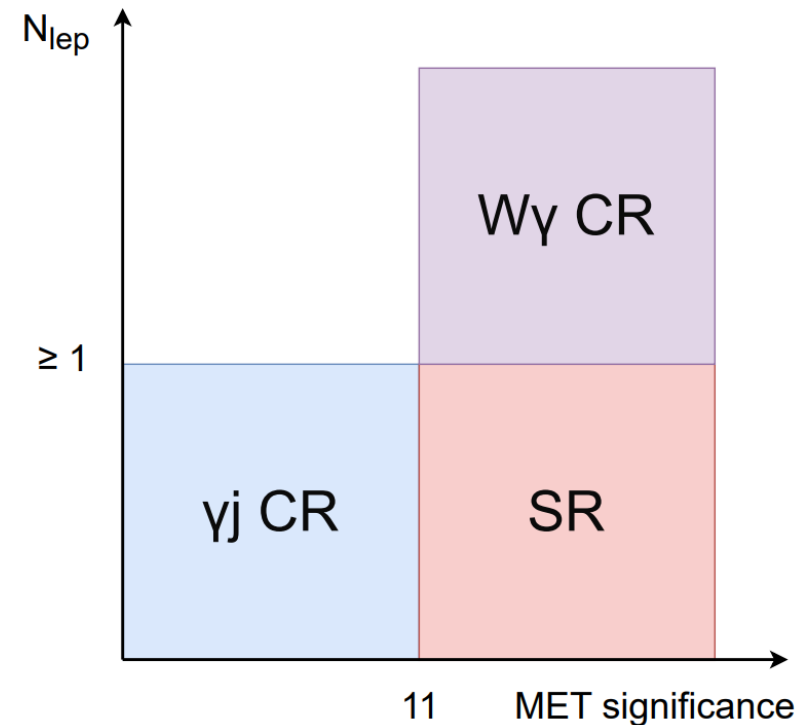
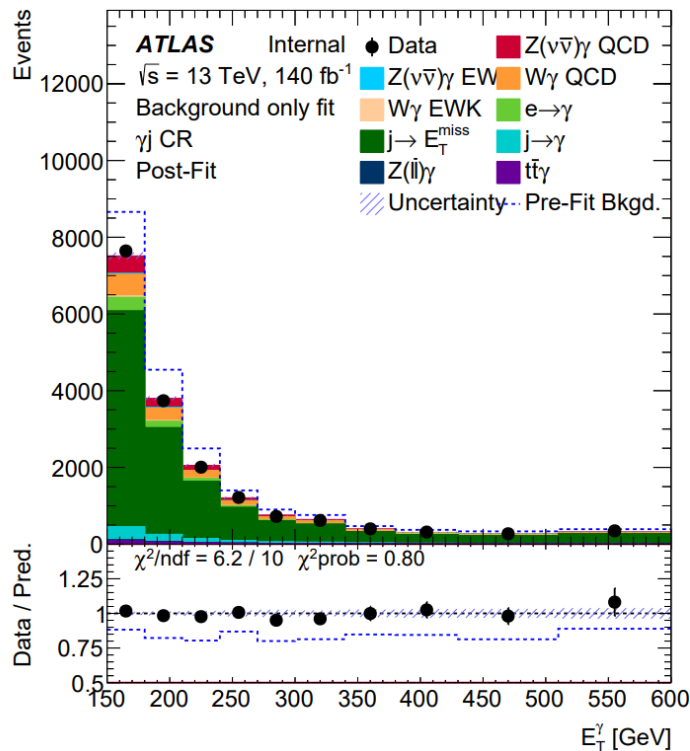
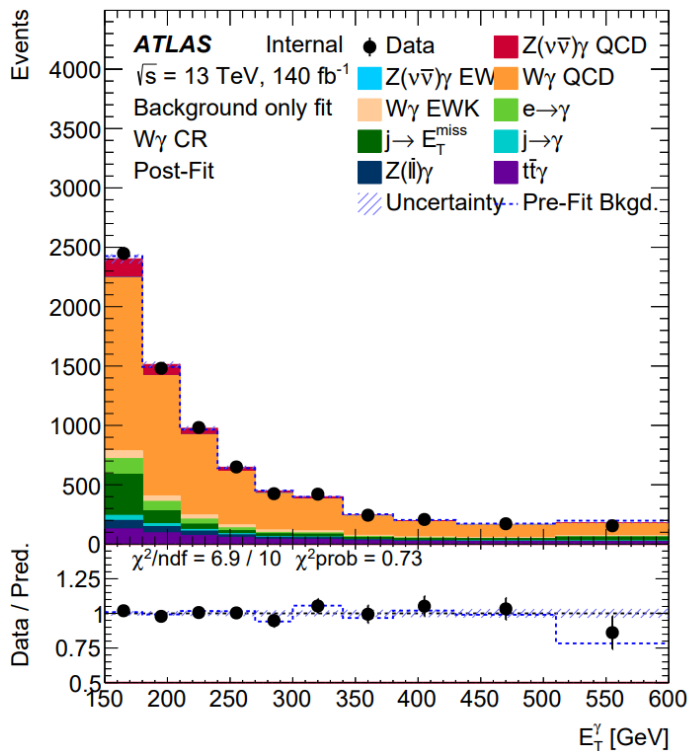


Template fit

- Three free parameters are introduced in the combined fit: a signal strength parameter $\mu(Zg)$ and two normalization factors $\mu(Wg)$ and $\mu(\gamma j)$ used to scale the yields of $W(l\nu)\gamma$ and $t\bar{t}\gamma$ and γ +jets processes.

⇒ The binned likelihood function used in the analysis is:

$$\mathcal{L}(\mu, \theta) = \prod_r \left[\prod_i^{\text{bins} \in r} \text{Pois}(N_i^{\text{data}} | \mu \nu_i^s \eta^s(\theta) + \nu_i^b \eta^b(\theta)) \right] \cdot \prod_i^{\text{nuis. par.}} \mathcal{L}(\theta_i)$$



	SR	$W\gamma$ CR	γj CR
$\mu Z\gamma$	✓		
$\mu W\gamma$	✓	✓	✓
$\mu \gamma j$	✓	✓	✓

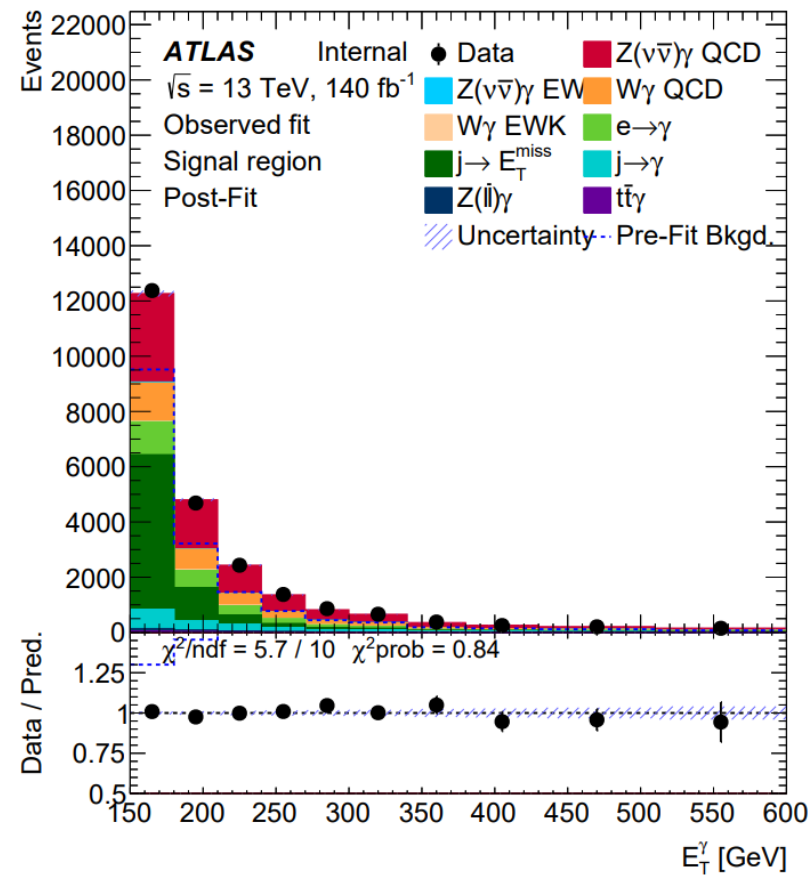
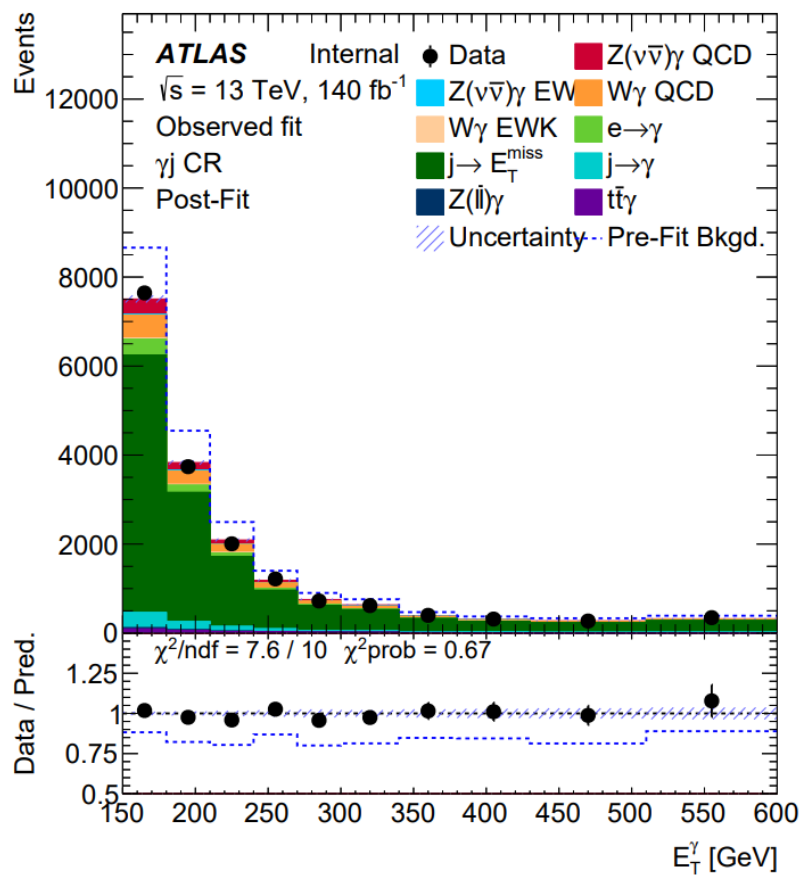
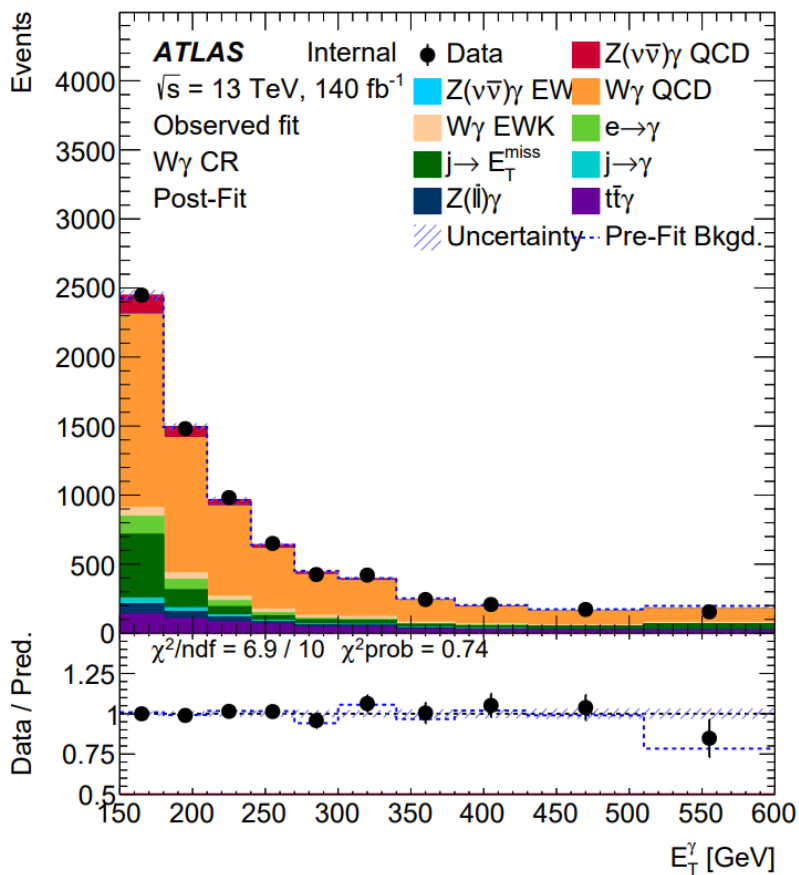
Results of background only fit:

$$\mu(Wg) = 0.93 \pm 0.13$$

$$\mu(\gamma j) = 0.74 \pm 0.12$$

Template fit

- Using the Asimov data: $\mu_{Z\gamma} = 1.00 \pm 0.08$, $\mu_{W\gamma} = 0.93 \pm 0.12$ and $\mu_{j\gamma} = 0.74 \pm 0.10$. Expected signal significance 69σ .
- Fit in the SR and CRs:



$\Rightarrow \mu_{Z\gamma} = 0.70 \pm 0.06$, $\mu_{W\gamma} = 0.92 \pm 0.06$ and $\mu_{j\gamma} = 0.88 \pm 0.08$. Observed signal significance 50σ .

There are some problems with jet systematics!

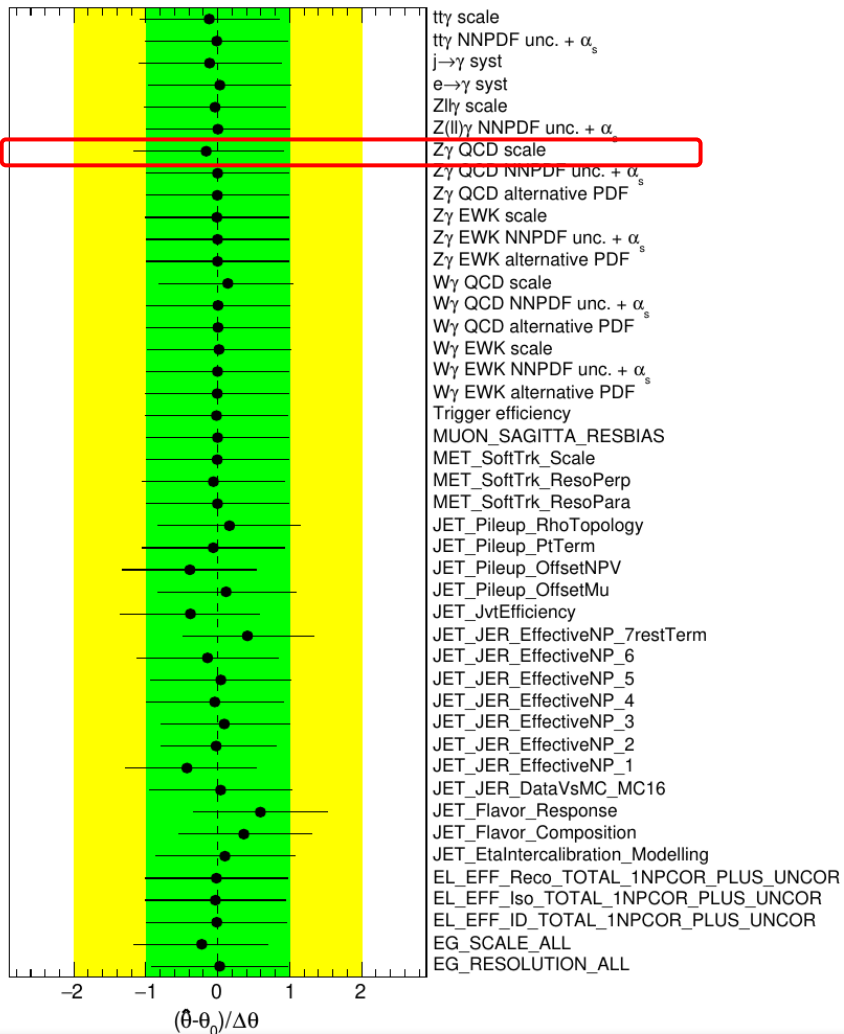
Template fit

Background only + max. symm.

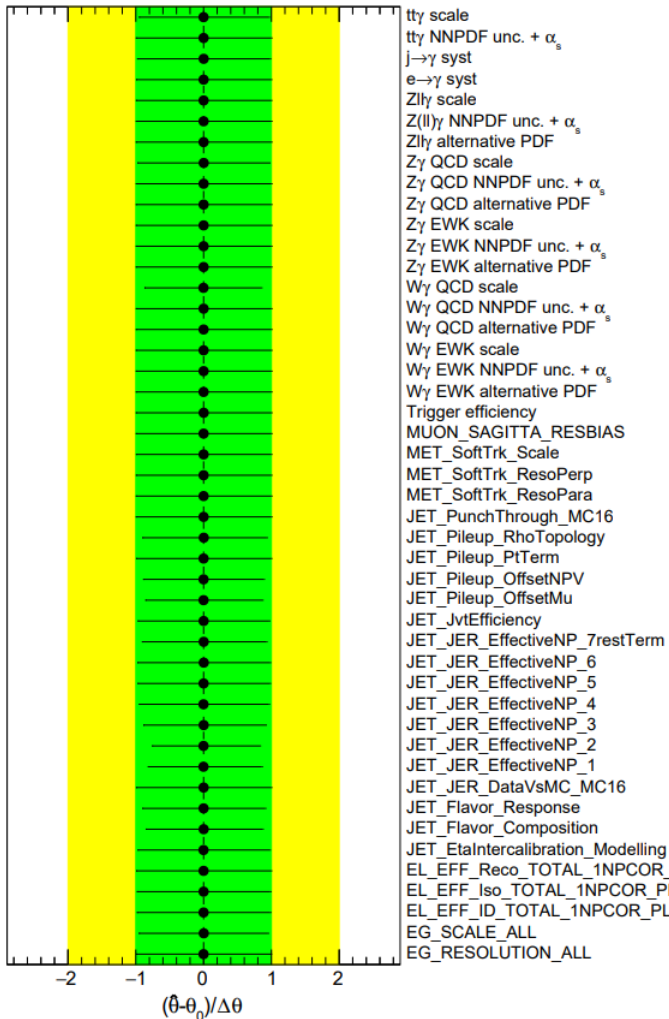
Asimov

Observed

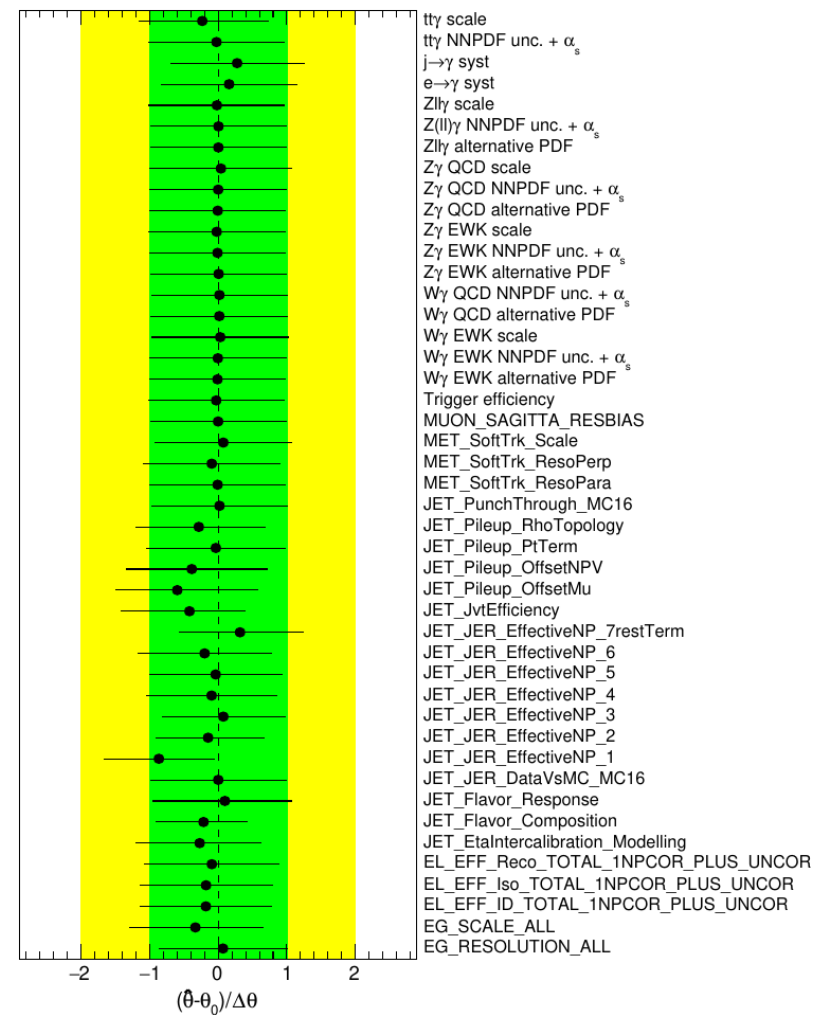
ATLAS Internal



ATLAS Internal

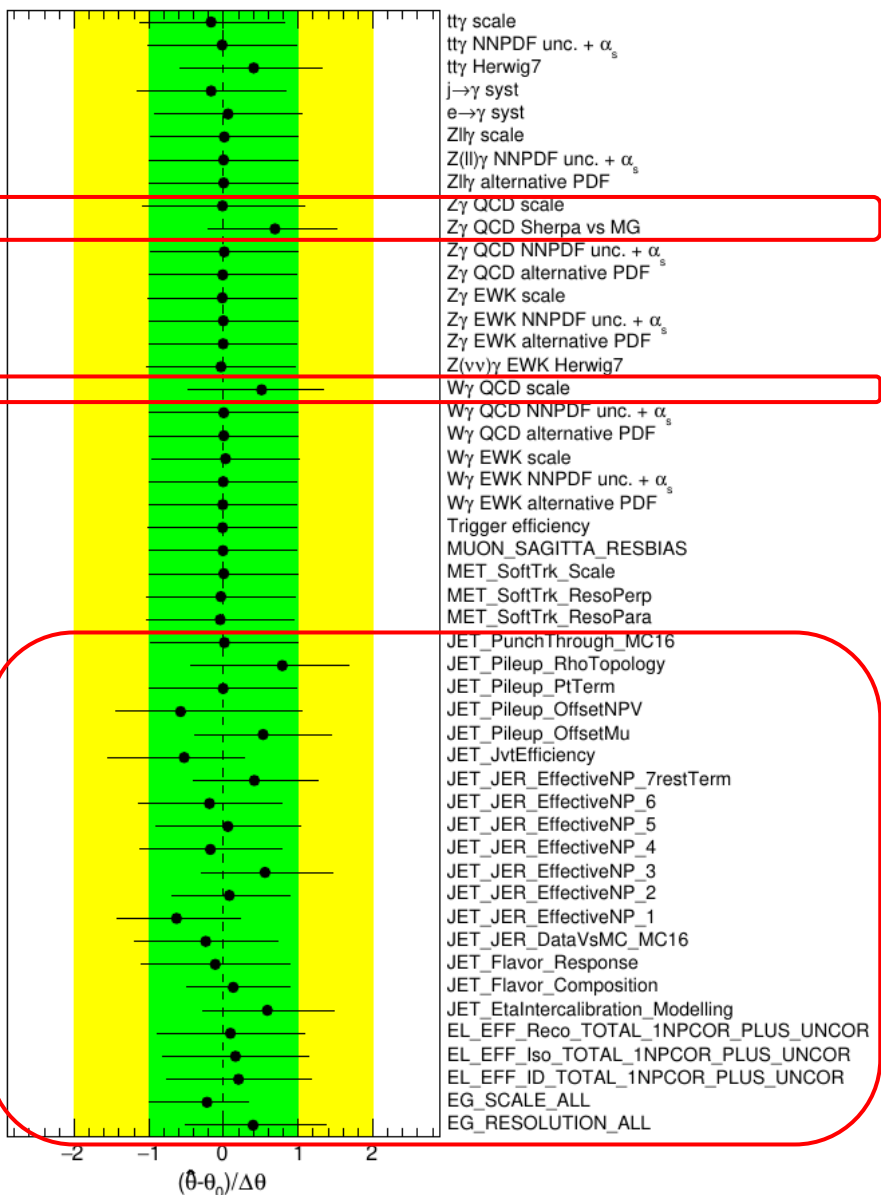


ATLAS Internal



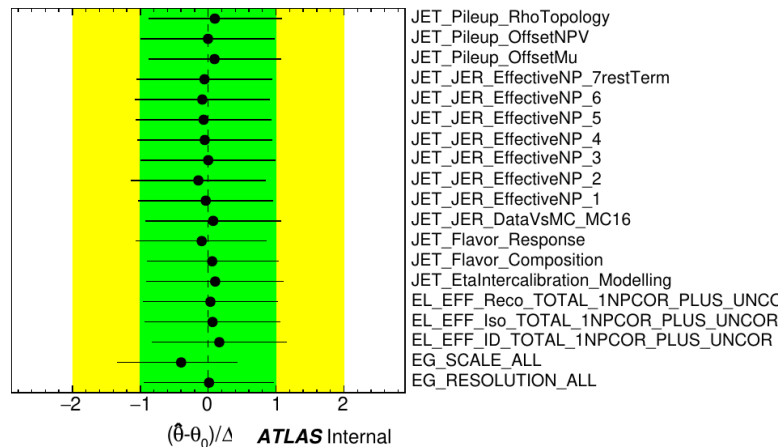
Problems with template fit

ATLAS Internal



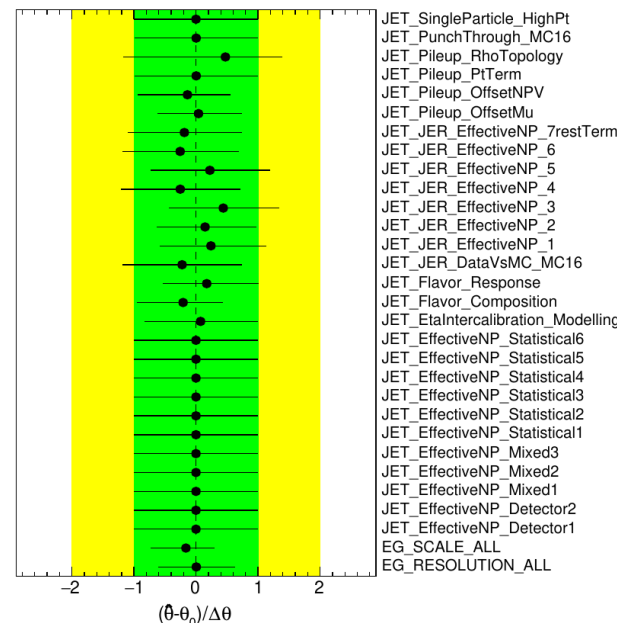
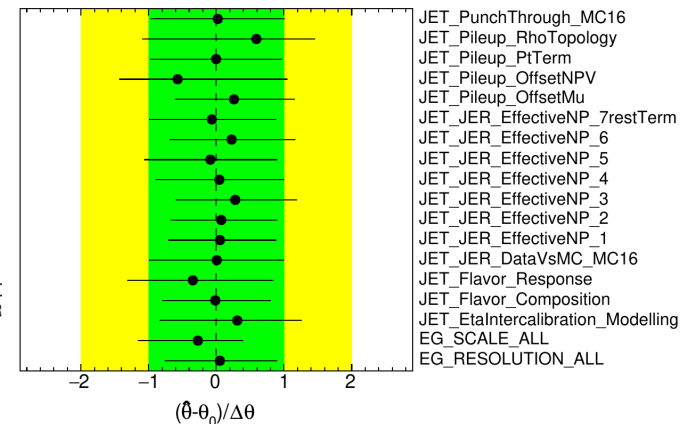
Fit in all CRs w/o gj sample (syst):

ATLAS Internal



Fit in all CRs with cut on MET
 signif < 9 in gj CR:

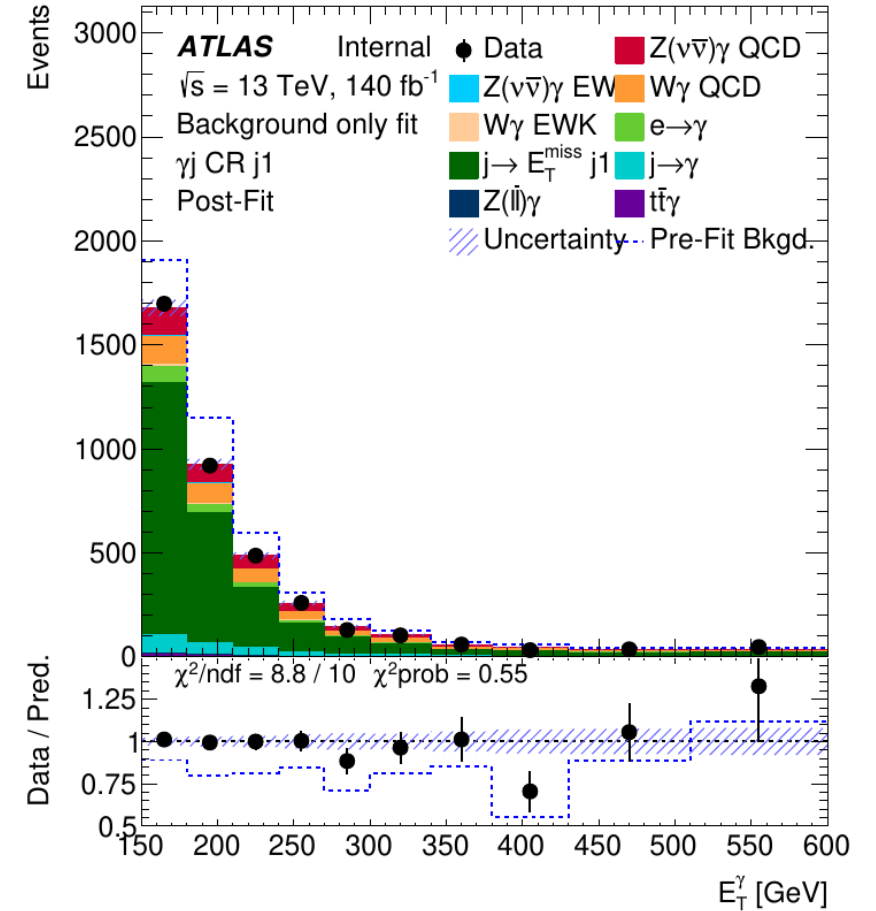
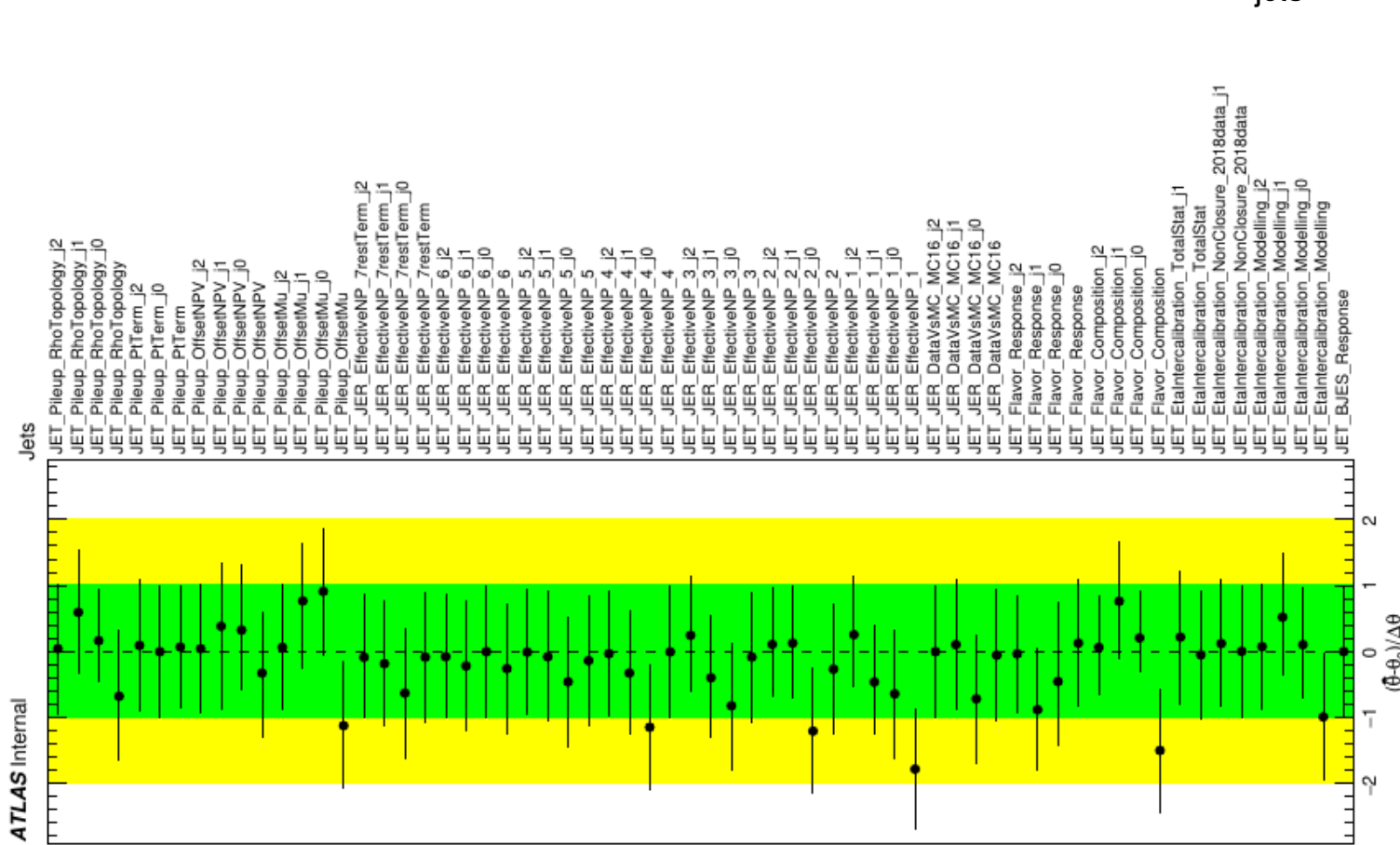
ATLAS Internal



Fit in all CRs with gj
 sample with cut on
 pT soft term:

Problems with template fit: categorisation

- There was an attempt to categorise the events based on N_{jets} in the $g\gamma$ CR (background only fit)

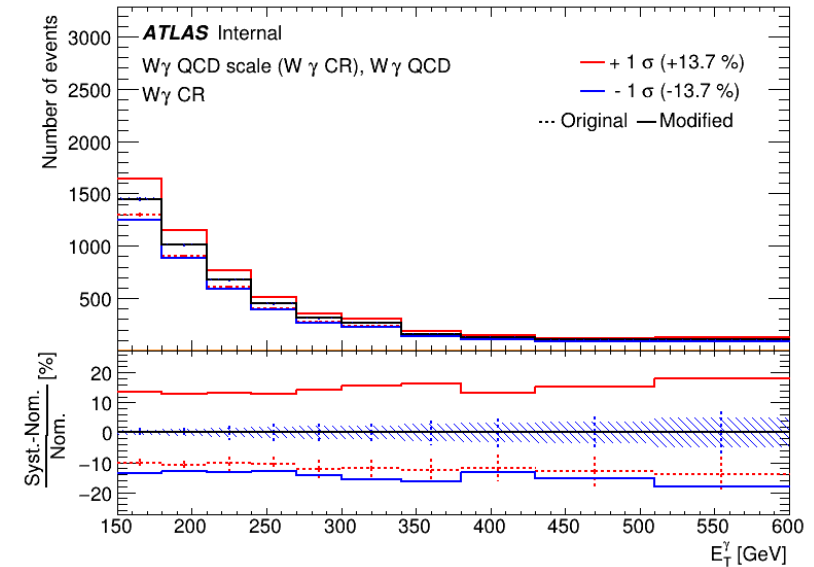
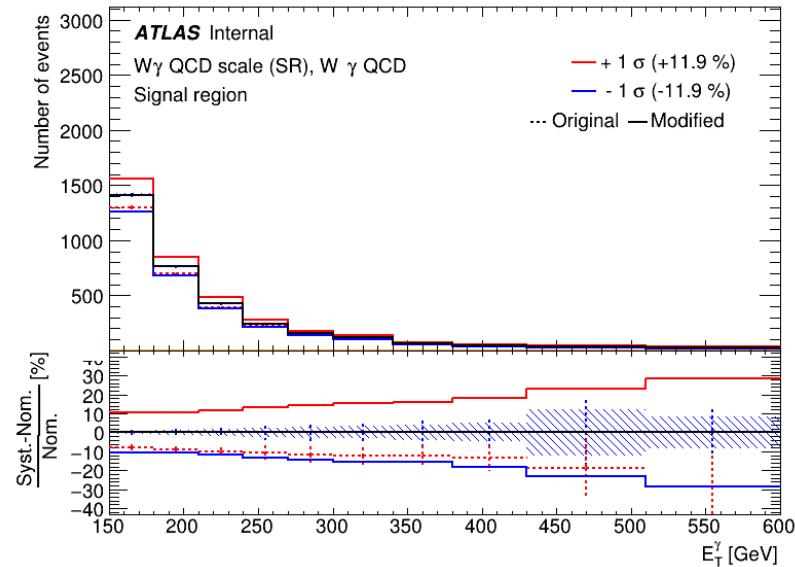
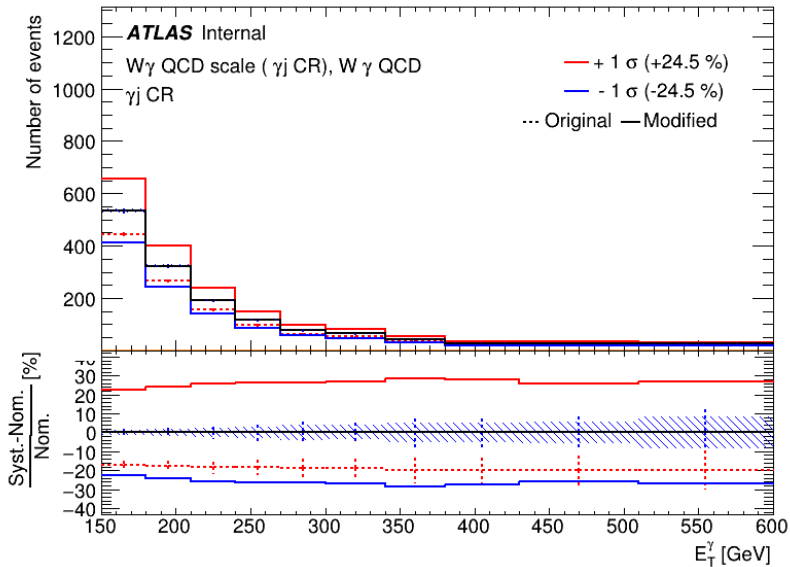
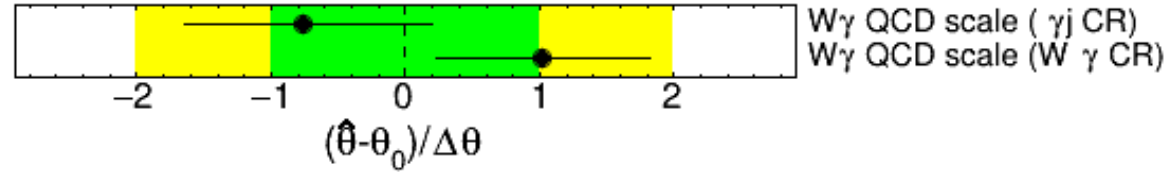


$\Rightarrow \mu_{W\gamma} = 1.06 \pm 0.04, \mu_{\gamma j(0)} = 0.78 \pm 0.09, \mu_{\gamma j(1)} = 0.72 \pm 0.09$ and $\mu_{\gamma j(2)} = 0.73 \pm 0.14.$

more information in back-up

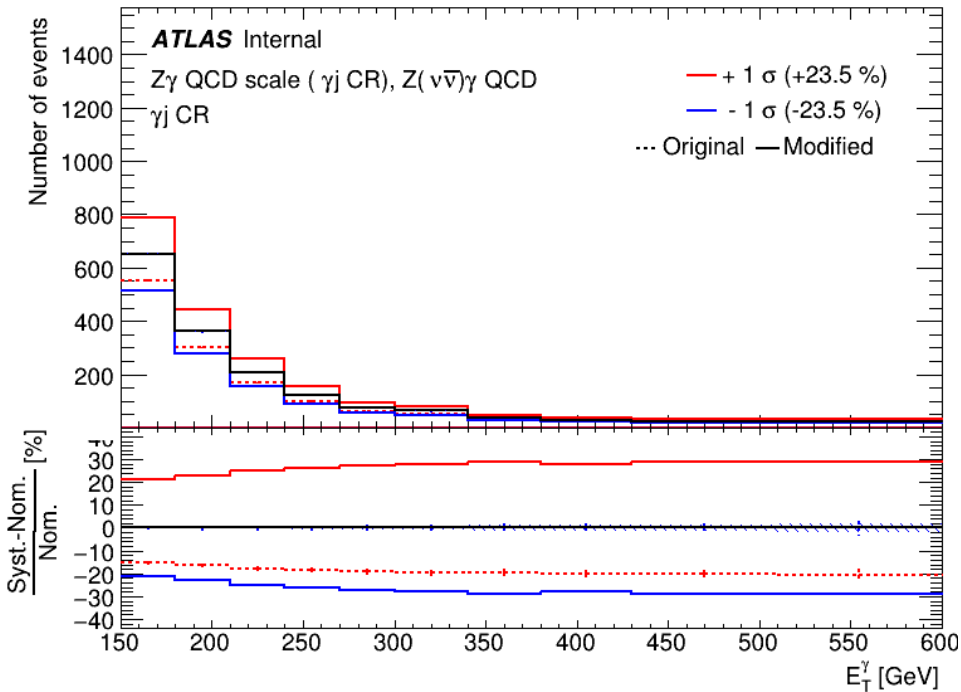
W γ QCD scale: decorrelation

ATLAS Internal

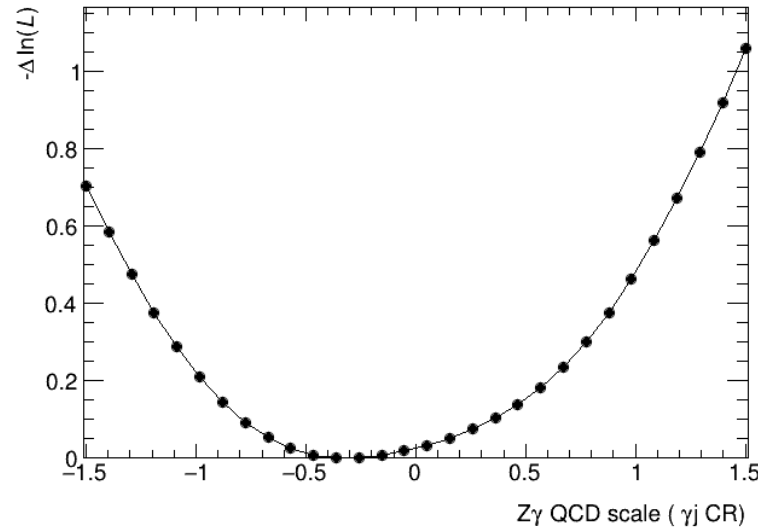
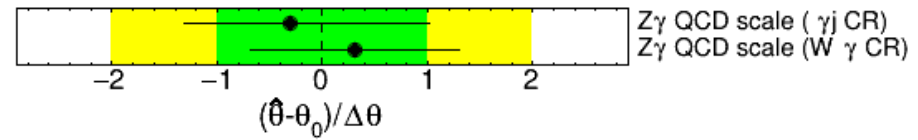


W γ CR causes the shift
The central value is ~ 0.5 with all systematics adding \rightarrow no problem?

Z γ QCD scale: decorrelation



ATLAS Internal



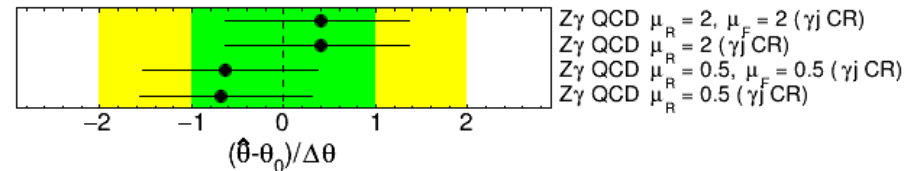
γ_j CR causes the problem:
 flat systematics,
 smooth LH curve,
 asymmetric behaviour:
 -0.313866 +1.3354 -1.00375

ATLAS Internal



Still problematic

ATLAS Internal



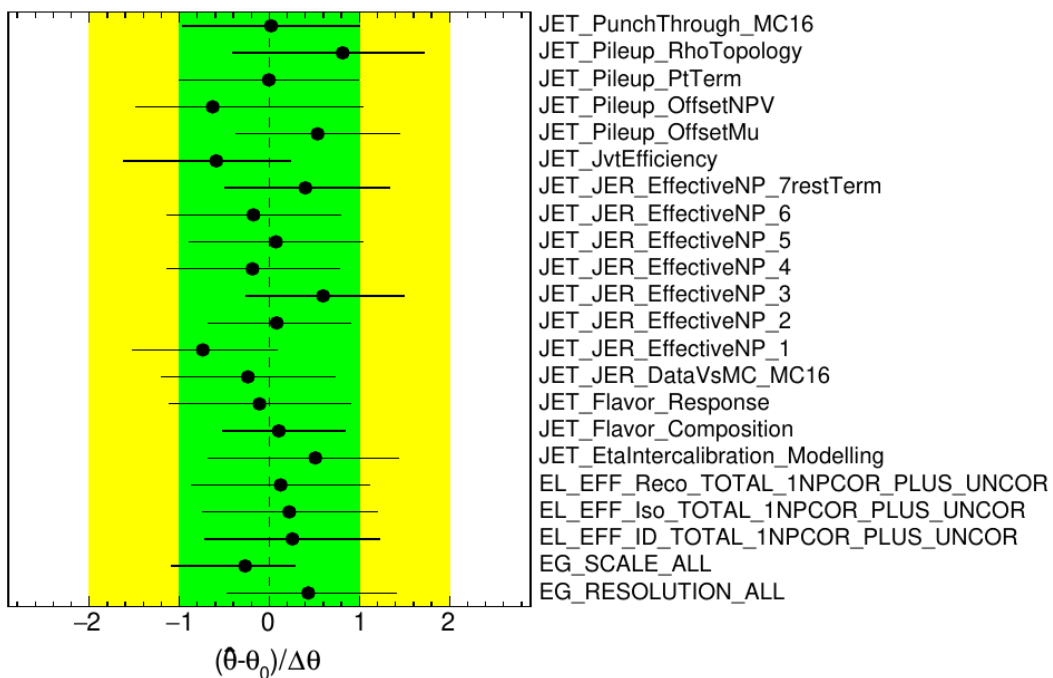
All variations:

Not clear what's going wrong

Fit procedure

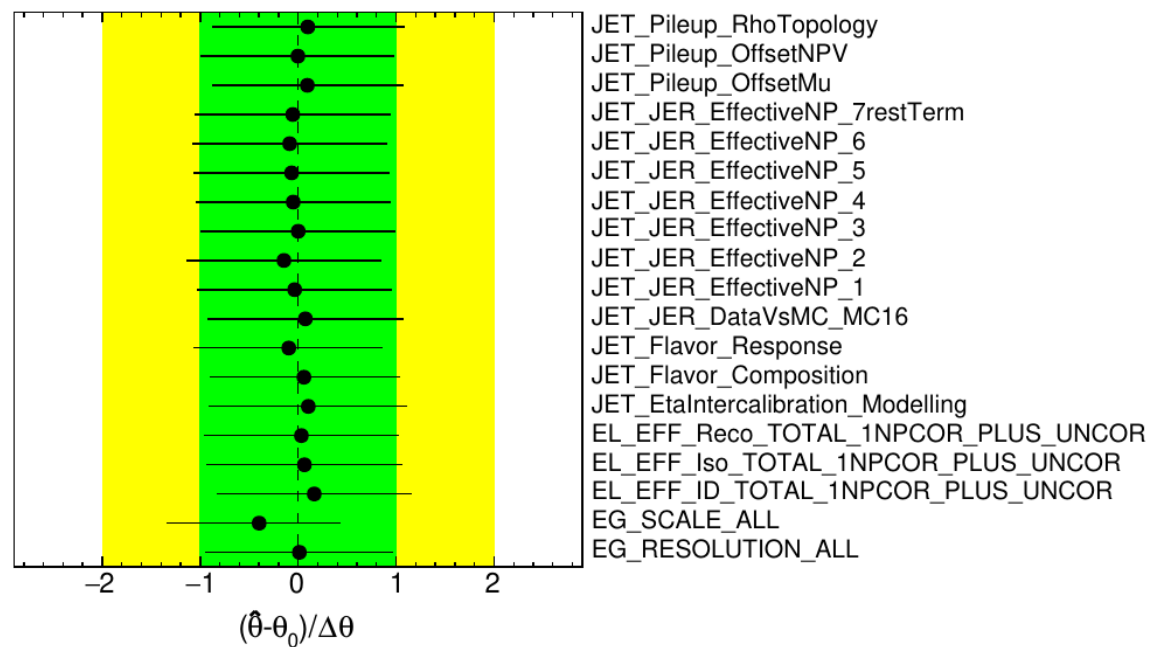
Fit in all CRs with gj sample

ATLAS Internal



Fit in all CRs w/o gj sample

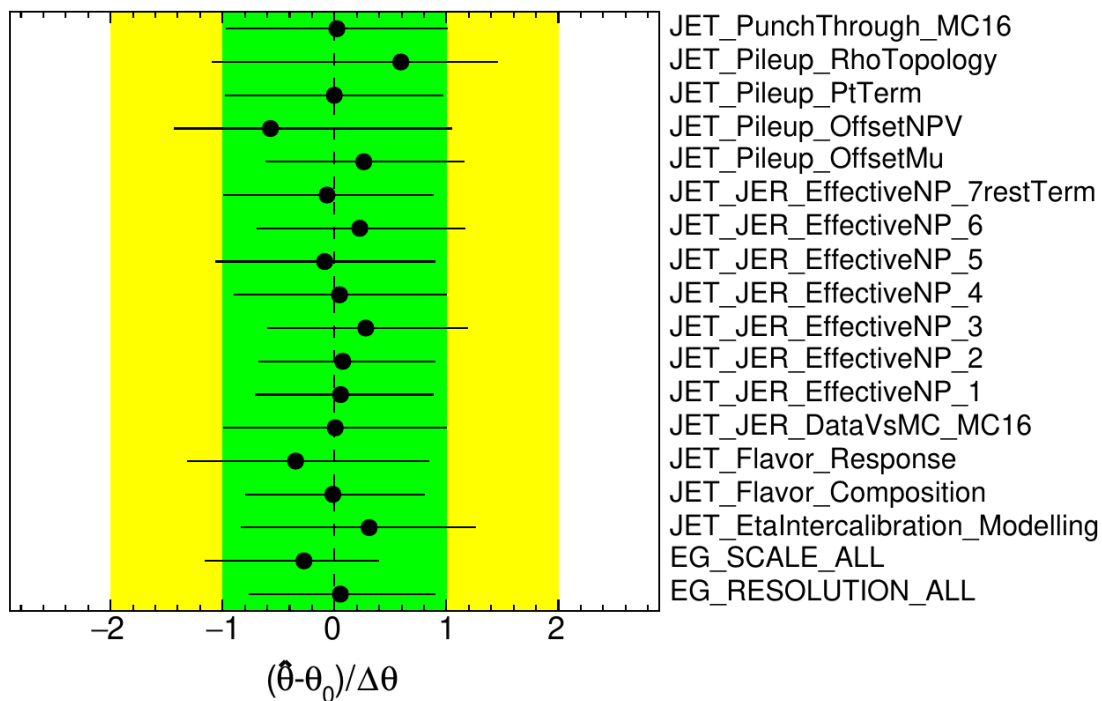
ATLAS Internal



Fit procedure

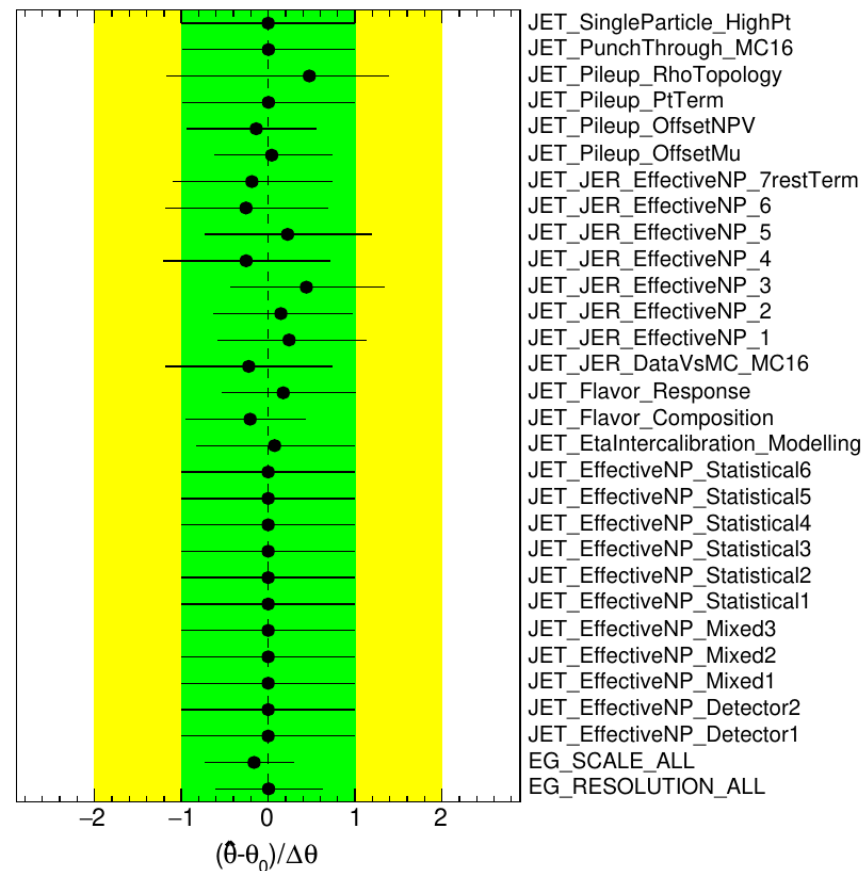
Fit in all CRs with gj sample with
cut on MET signif < 9 in gj CR

ATLAS Internal



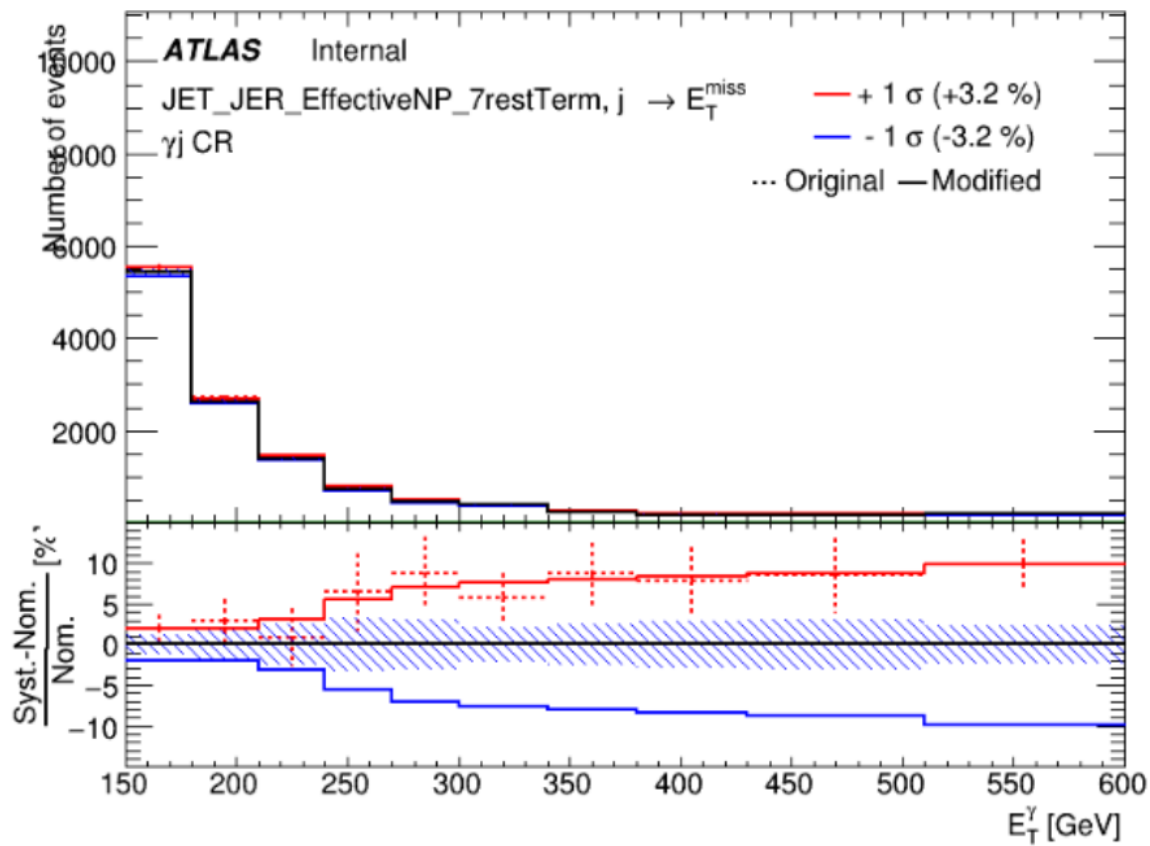
Fit in all CRs with gj sample
with cut on pT soft term

ATLAS Internal

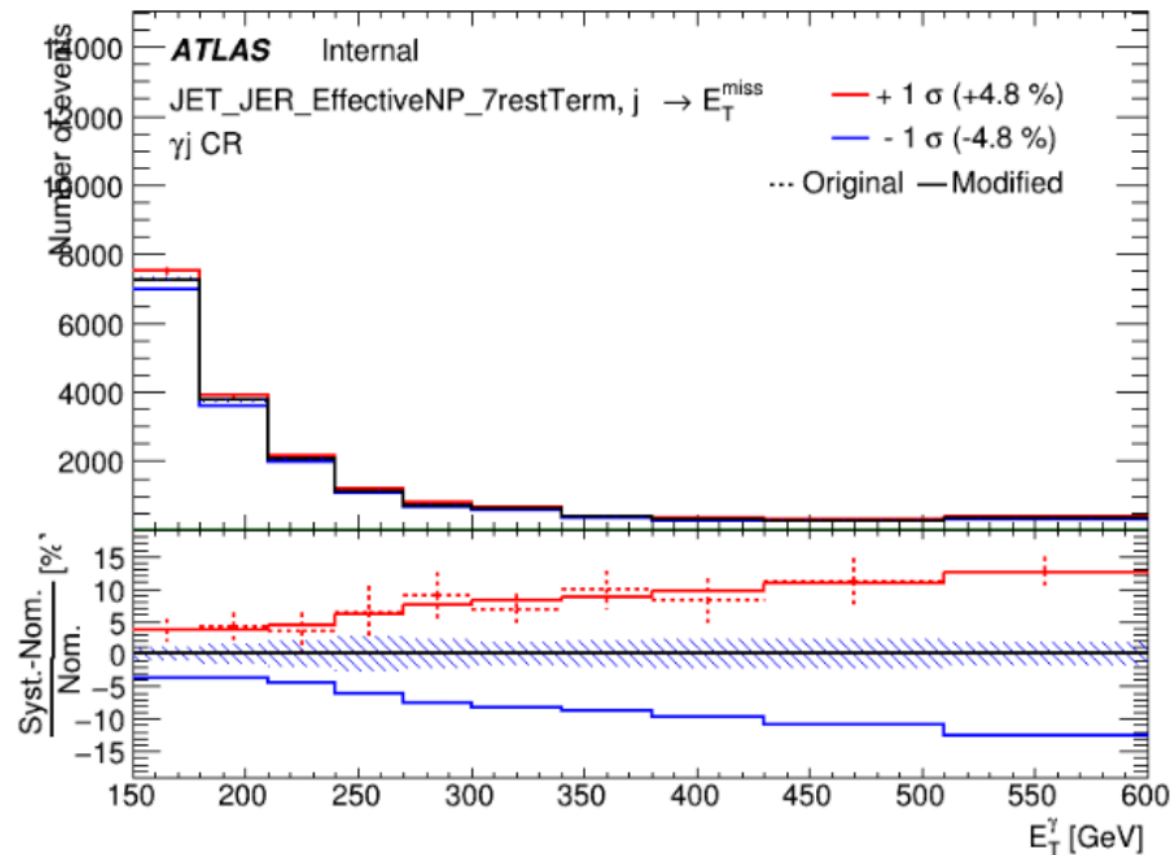


Fit procedure

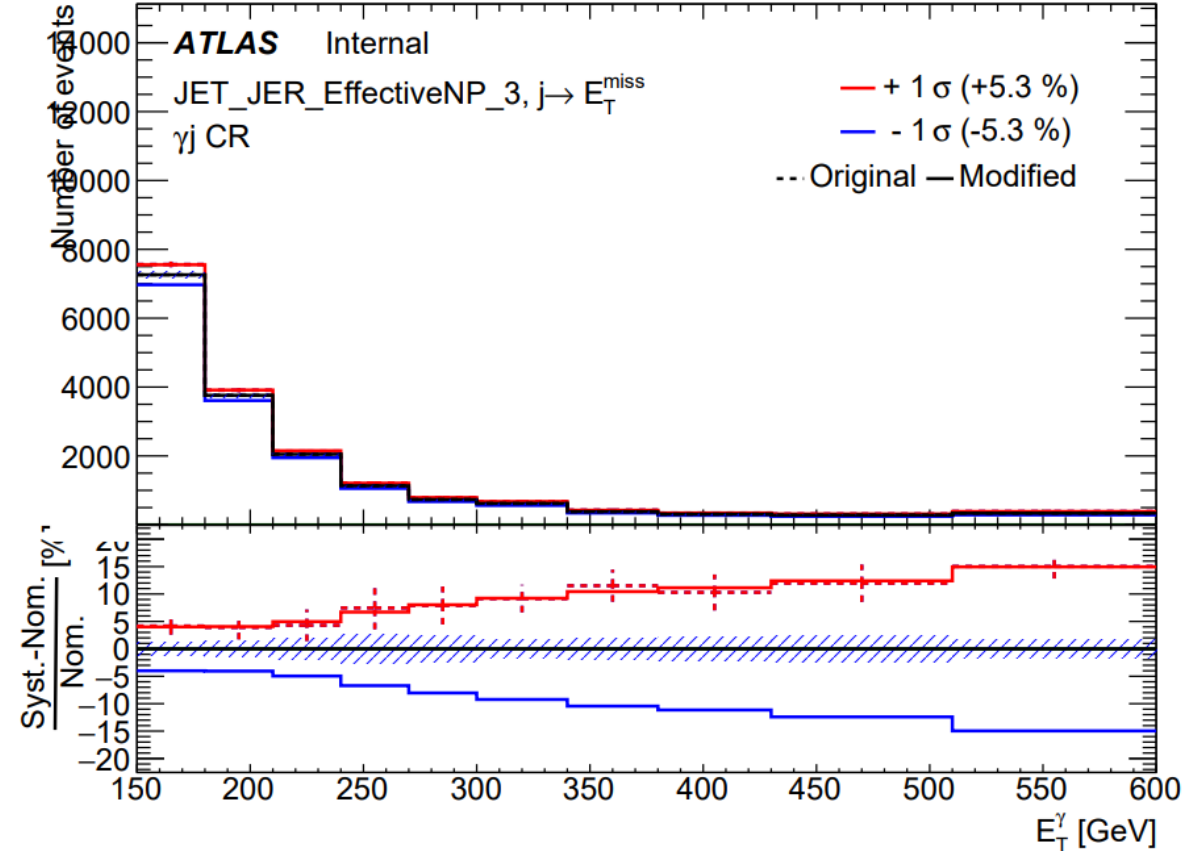
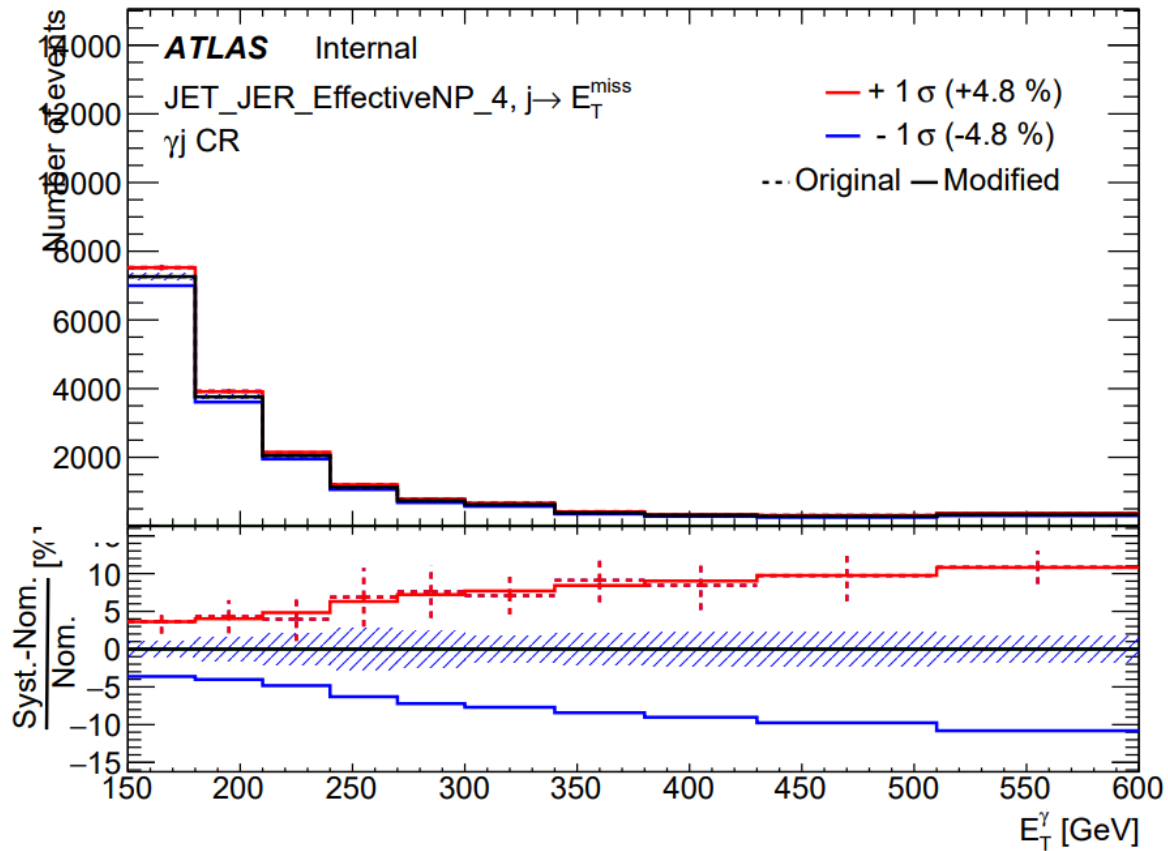
Reproc 21-02-23 with softterm



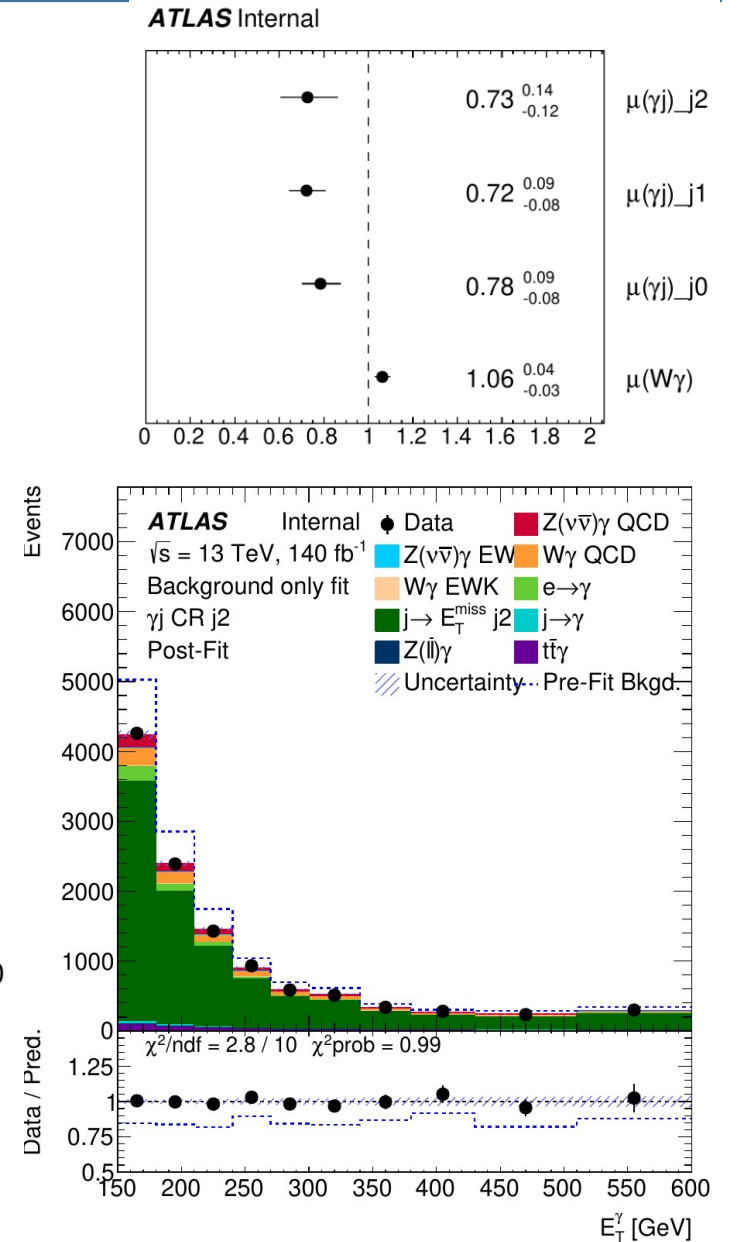
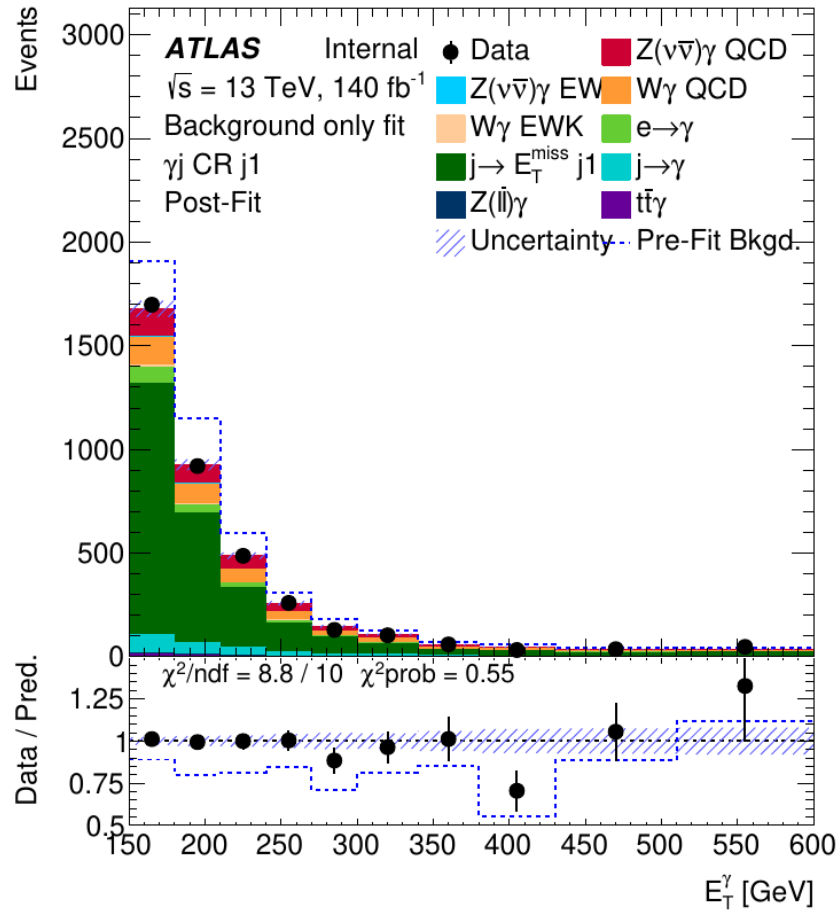
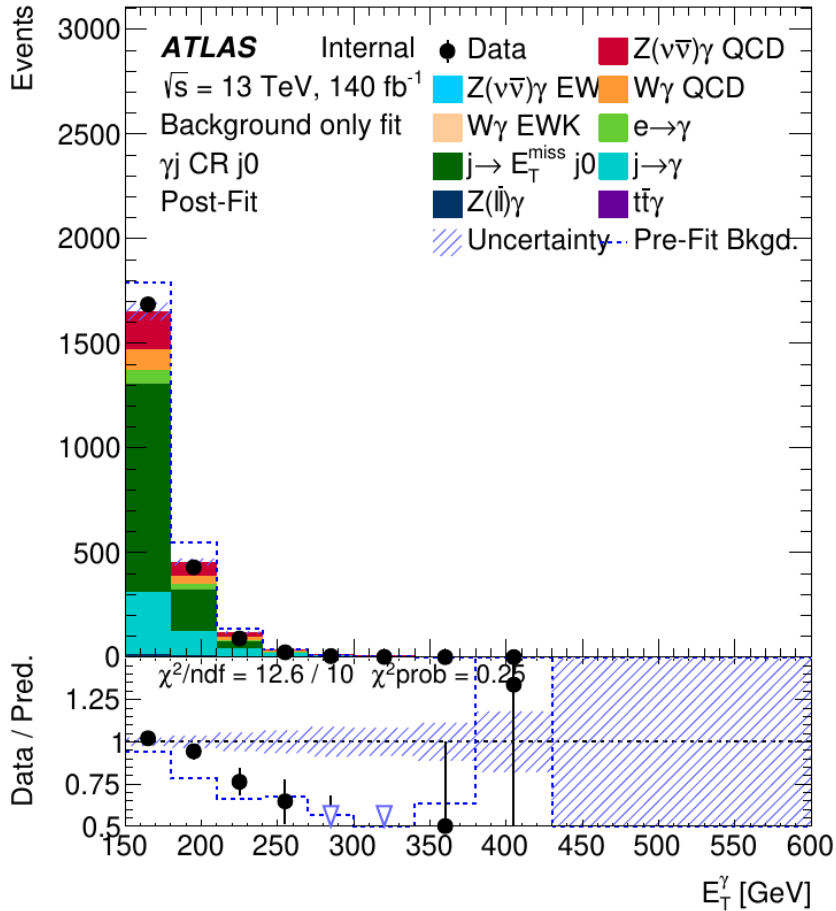
Reproc 03-11-23 w/o softterm



Fit procedure

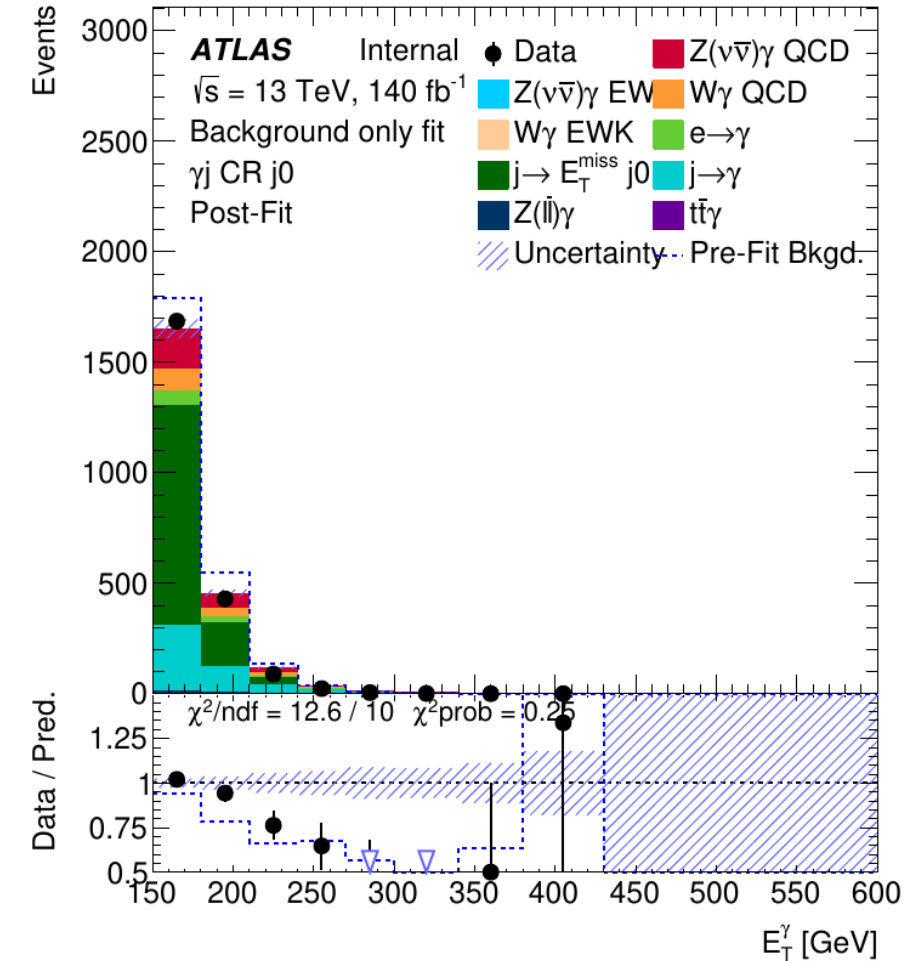
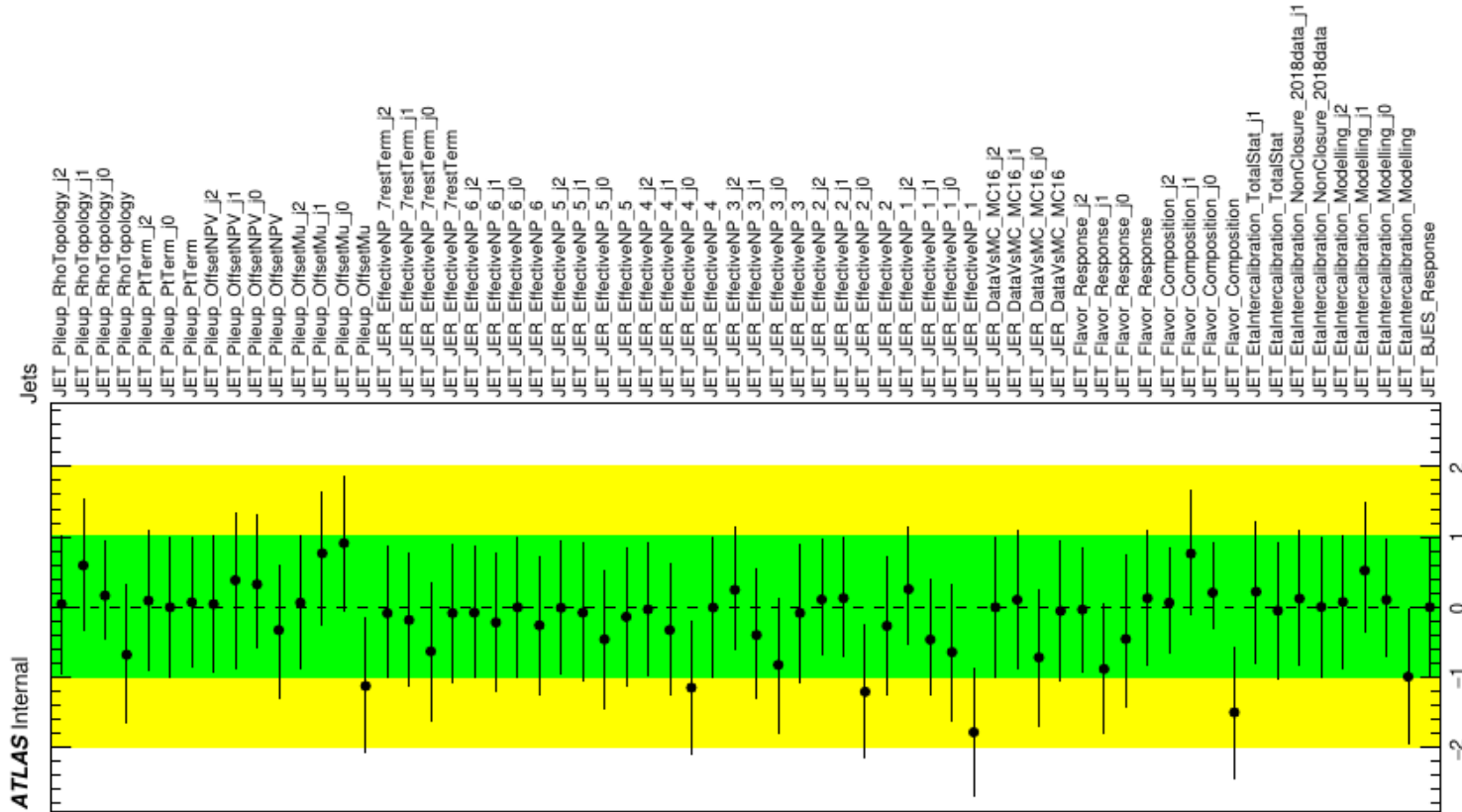


Fit procedure



Problems with template fit: categorisation

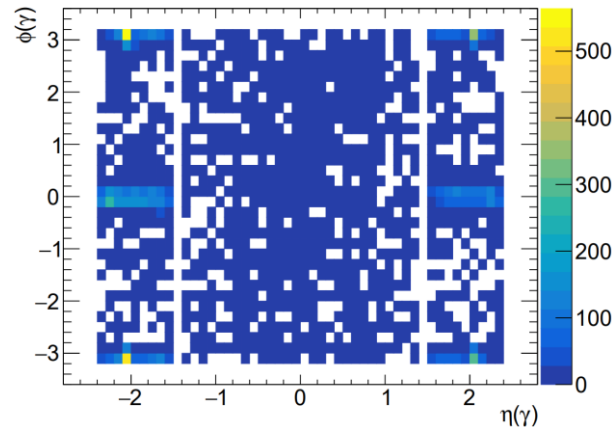
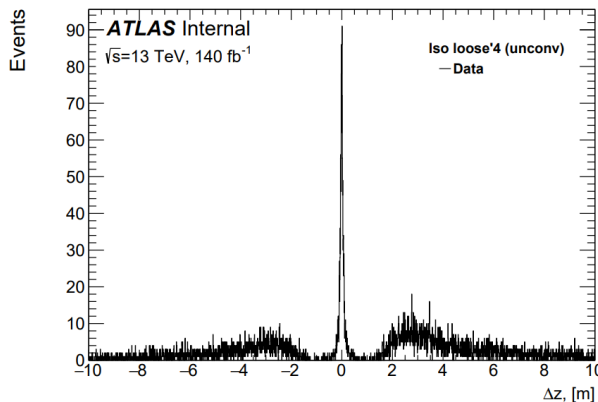
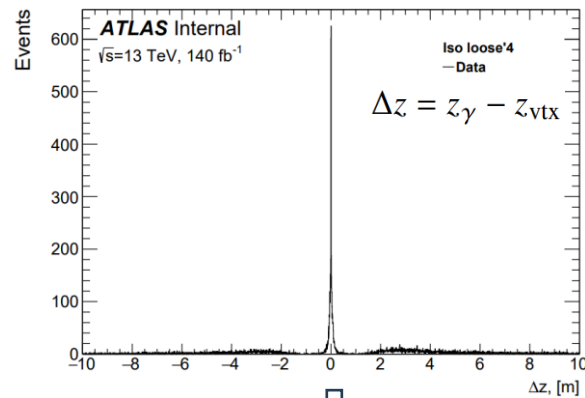
- There was an attempt to categorise the events based on N_{jets} in the $g\bar{j}$ CR (background only fit)



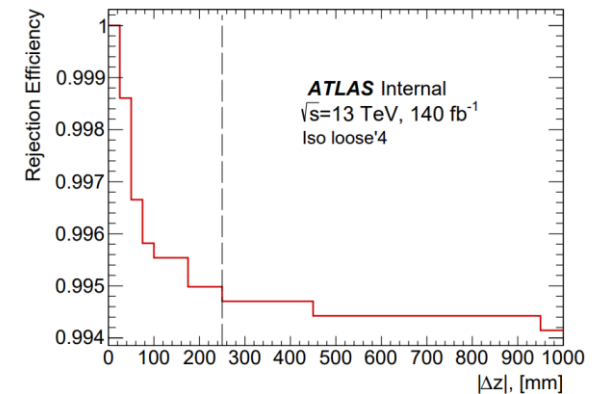
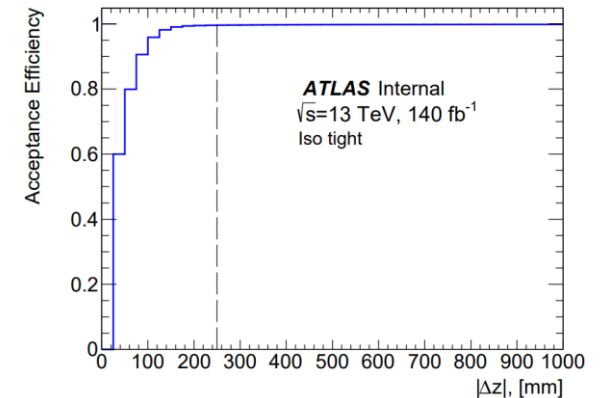
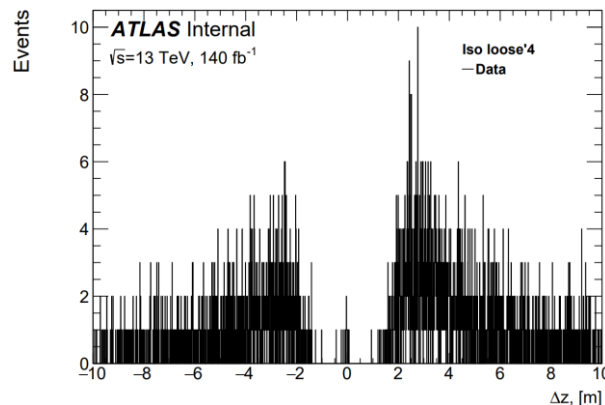
$\Rightarrow \mu_{W\gamma} = 1.06 \pm 0.04, \mu_{\gamma j(0)} = 0.78 \pm 0.09, \mu_{\gamma j(1)} = 0.72 \pm 0.09$ and $\mu_{\gamma j(2)} = 0.73 \pm 0.14.$

Beam-induced background (BIB)

- Muons from pion and kaon decays in hadronic showers, induced by beam losses in non-elastic collisions with gas and detector material, deposit large amount of energy in calorimeters through radiative processes (= fake jets).
- The characteristic peaks of the fake jets due to BIB concentrate at $\pm \pi$ and 0 (mainly due to the bending in the horizontal plane that occurs in the D1 and D2 dipoles and the LHC arc).



Cuts: $|\phi| < 0.2$, $|\phi| \in [2.8; 3.2]$ and $|\eta| > 1.6$



$|\Delta z| < 250$ mm

Rejection efficiency: $(100 \pm 2)\%$

Acceptance efficiency: $(99.6 \pm 0.9)\%$

Selection optimisation

Variable	1	2	3	4
$E_T^{miss} \text{ signif.}$		> 11		—
$\Delta\phi(E_T^{miss}, \gamma)$		> 0.6		—
$\Delta\phi(E_T^{miss}, j_1)$		> 0.3		—
$E_T^{miss}, \text{ GeV}$		>130		—
Signal				
Z($\nu\nu$) γ QCD	9928 \pm 8	10021 \pm 8	10711 \pm 8	13934 \pm 9
Z($\nu\nu$) γ EWK	151.6 \pm 0.3	153.6 \pm 0.3	166.3 \pm 0.3	312.3 \pm 0.4
Total signal	10080 \pm 8	10175 \pm 8	10878 \pm 8	14247 \pm 9
Background				
W γ QCD	3022 \pm 20	3061 \pm 20	3310 \pm 21	6795 \pm 29
W γ EWK	99.9 \pm 0.6	101.3 \pm 0.6	109.4 \pm 0.6	309.8 \pm 1.1
tt, top	156 \pm 5	176 \pm 5	201 \pm 6	2800 \pm 22
W($e\nu$)	3091 \pm 453	3409 \pm 521	3591 \pm 487	8540 \pm 663
tty	161 \pm 3	163 \pm 3	178 \pm 3	787 \pm 6
γ +j	7642 \pm 79	7757 \pm 80	8123 \pm 82	67517 \pm 217
Zj	221 \pm 16	328 \pm 20	415 \pm 21	2583 \pm 50
Z(l)l γ	197 \pm 4	200 \pm 4	211 \pm 4	426 \pm 5
W($\tau\nu$)	412 \pm 65	575 \pm 72	640 \pm 69	4615 \pm 138
Total bkg.	15002 \pm 465	15770 \pm 533	16779 \pm 499	94373 \pm 714
Stat. signif.	63.6 \pm 0.6	63.2 \pm 0.6	65.4 \pm 0.6	43.23 \pm 0.14

Table 33: The results of selection optimisation at three different working points *FixedCutTight*, *FixedCutTightCaloOnly*, *FixedCutLoose*.

Selection optimisation

	E_T^{miss} signif. E_T^{miss} , GeV $\Delta\phi(E_T^{miss}, \gamma)$ $\Delta\phi(E_T^{miss}, j_1)$	E_T^{miss} signif. E_T^{miss} , GeV $\Delta\phi(E_T^{miss}, \gamma)$ $\Delta\phi(E_T^{miss}, j_1)$	E_T^{miss} signif. E_T^{miss} , GeV $\Delta\phi(E_T^{miss}, \gamma)$ $\Delta\phi(E_T^{miss}, j_1)$	E_T^{miss} signif. E_T^{miss} , GeV $\Delta\phi(E_T^{miss}, \gamma)$ $\Delta\phi(E_T^{miss}, j_1)$	E_T^{miss} signif. E_T^{miss} , GeV $\Delta\phi(E_T^{miss}, \gamma)$ $\Delta\phi(E_T^{miss}, j_1)$
Signal					
Z($\nu\nu$) γ QCD	10711 \pm 8	12307 \pm 9	10819 \pm 8	10728 \pm 8	10849 \pm 8
Z($\nu\nu$) γ EWK	166.3 \pm 0.3	251.5 \pm 0.4	167.6 \pm 0.3	168.3 \pm 0.3	171.0 \pm 0.3
Total signal	10878 \pm 8	12559 \pm 9	10987 \pm 8	10897 \pm 8	11020 \pm 8
Background					
W γ QCD	3310 \pm 21	4741 \pm 24	3385 \pm 21	3389 \pm 21	3440 \pm 22
W γ EWK	109.4 \pm 0.6	210.4 \pm 0.9	111.2 \pm 0.6	112.8 \pm 0.7	115.3 \pm 0.7
tt, top	177 \pm 5	631 \pm 10	204 \pm 6	267 \pm 7	209 \pm 6
W($e\nu$)	3591 \pm 487	4372 \pm 517	3827 \pm 506	3883 \pm 487	3627 \pm 487
t $\bar{t}\gamma$	178 \pm 3	508 \pm 5	179 \pm 3	183 \pm 3	192 \pm 3
γ +j	8123 \pm 82	24991 \pm 139	8552 \pm 84	8156 \pm 82	9668 \pm 86
Zj	415 \pm 21	546 \pm 24	419 \pm 21	417 \pm 21	428 \pm 21
Z(l l) γ	211 \pm 4	284 \pm 4	216 \pm 4	212 \pm 4	231 \pm 4
W($\tau\nu$)	640 \pm 69	945 \pm 100	651 \pm 69	821 \pm 70	655 \pm 69
Total bkg.	16779 \pm 499	37229 \pm 546	17544 \pm 518	17440 \pm 499	18566 \pm 500
Stat. signif.	65.4 \pm 0.6	56.3 \pm 0.3	65.0 \pm 0.6	64.7 \pm 0.6	64.1 \pm 0.5

Table 34: Comparison of statistical significance and event returns when each of the optimised variables is excluded. The excluded variable is highlighted in red.

$e \rightarrow \gamma$ misID background: Z-peak method

Selections	Cut Value
E_T^{miss}	$> 130 \text{ GeV}$
$E_T^{e\text{-probe}}$	$> 150 \text{ GeV}$
Number of loose non-isolated photons	$N_\gamma = 0$
Number of tight probe electrons	$N_{e\text{-probe}} = 1$
Lepton veto	$N_\mu + N_\tau = 0$
E_T^{miss} significance	> 11
$ \Delta\phi(e - \text{probe}, \vec{p}_T^{\text{miss}}) $	> 0.6
$ \Delta\phi(j_1, \vec{p}_T^{\text{miss}}) $	> 0.3

Table 5: Event selection criteria for e-probe CR events.

Event yield	real $e + E_T^{\text{miss}}$ (MC)	fake $e + E_T^{\text{miss}}$ (MC)	data
e-probe CR	78079 ± 4078	465 ± 34	74076

Table 6: Event yields for real $e + E_T^{\text{miss}}$ and fake $e + E_T^{\text{miss}}$ prediction and observed data in probe-electron control regions. Indicated uncertainties are statistical.

$e \rightarrow \gamma$ misID background: Z-peak method

fake rate	$150 < E_T^\gamma < 250 \text{ GeV}$ $0 < \eta < 1.37$	$E_T^\gamma > 250 \text{ GeV}$ $0 < \eta < 1.37$	$1.52 < \eta < 2.37$	Total
syst. on fake-rate estimation.	4%	20%	10%	
syst. from stat. unc. on fake-rate	3%	7%	3%	
syst. from impurity of CR	0.16%	0.16%	0.16%	
Total rel. syst.	5%	21%	10%	
Event yield in (incl.) e-probe CR	49673	11492	20855	
Fake-rate	0.0234	0.0193	0.0714	
$e \rightarrow \gamma$ event yield in SR	1062	200	1345	2608
Total abs. syst.	58	42	134	162

Table 35: Systematics breakdown for $e \rightarrow \gamma$ background for SR.

Missing transverse momentum is calculated as the sum of the following terms:

$$E_{x(y)}^{\text{miss}} = E_{x(y)}^{\text{miss,e}} + E_{x(y)}^{\text{miss,\mu}} + E_{x(y)}^{\text{miss,\tau}_{\text{had}}} + E_{x(y)}^{\text{miss,\gamma}} + E_{x(y)}^{\text{miss,jets}} + E_{x(y)}^{\text{miss,SoftTerm}},$$

$e \rightarrow \gamma$ misID background: Z-peak method

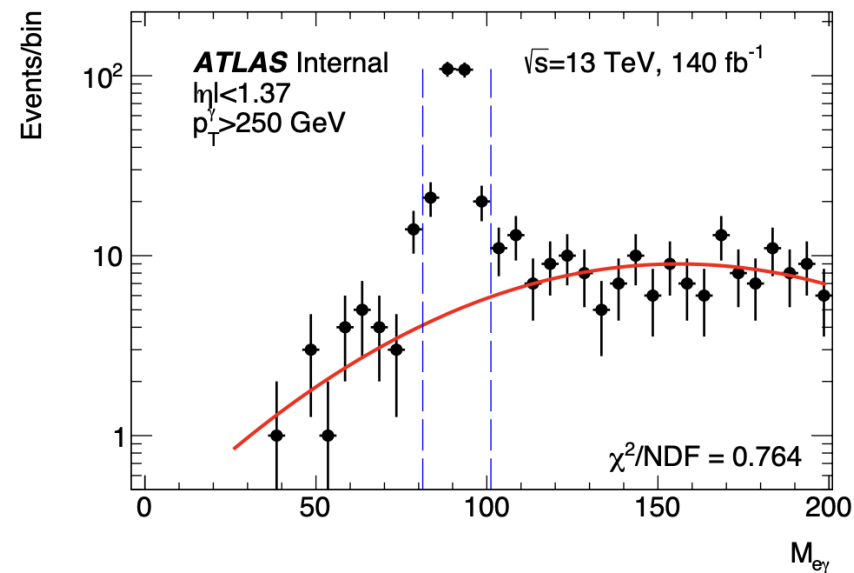
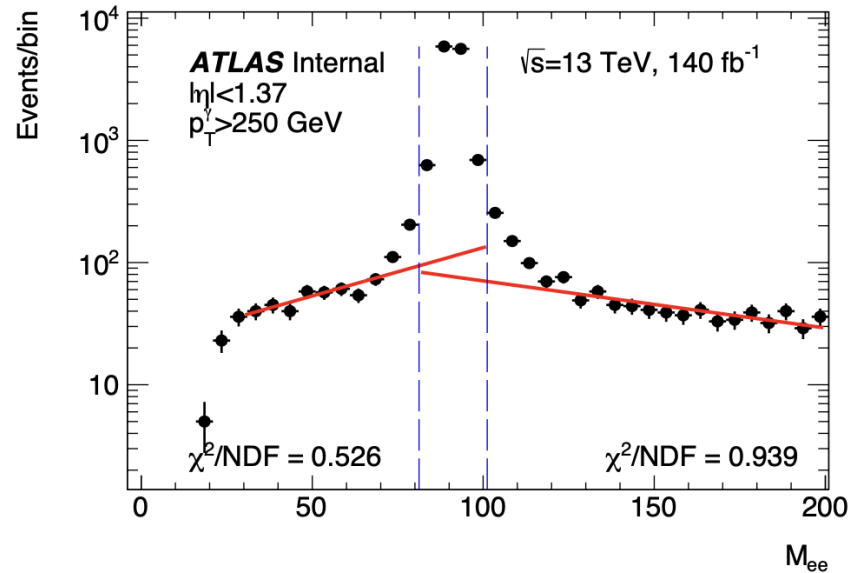
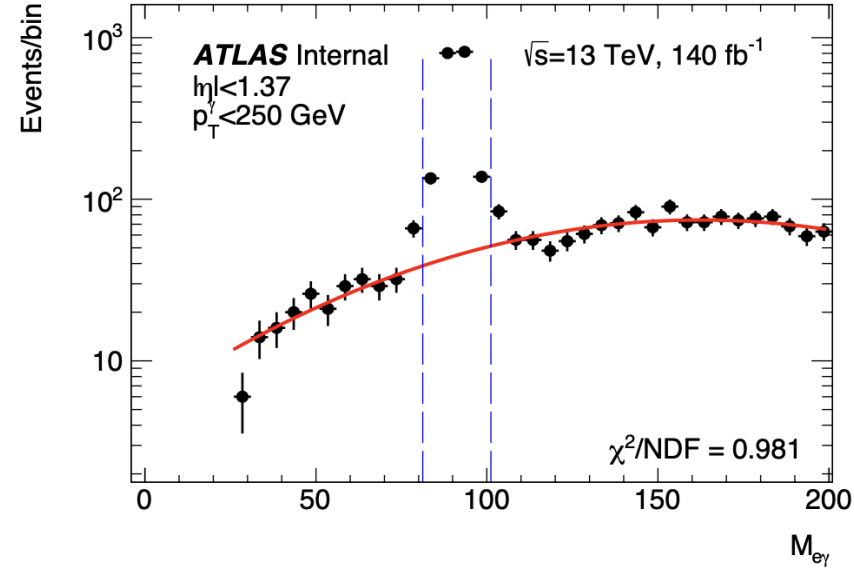
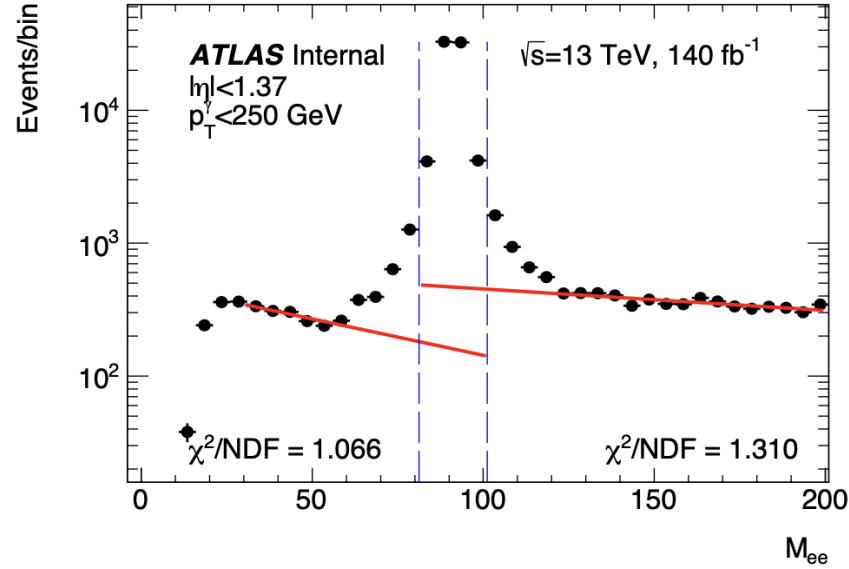
fake rate	$150 < E_T^\gamma < 250 \text{ GeV}$ $0 < \eta < 1.37$	$E_T^\gamma > 250 \text{ GeV}$ $0 < \eta < 1.37$	$1.52 < \eta < 2.37$
Z(ee) MC tag-n-probe	0.0218 ± 0.0004	0.0197 ± 0.0005	0.0762 ± 0.0012
Z(ee) MC mass window variation	0.0217 ± 0.0004	0.0198 ± 0.0005	0.0765 ± 0.0012
Z(ee) MC "real"	0.022 ± 0.002	0.023 ± 0.002	0.084 ± 0.004

Table 33: Electron-to-photon fake rates estimated in MC.

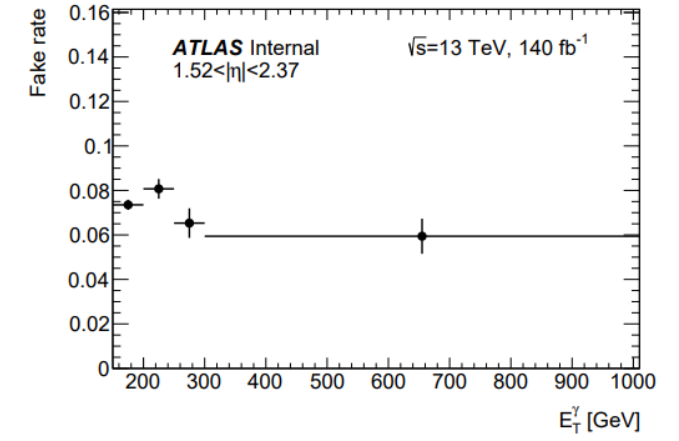
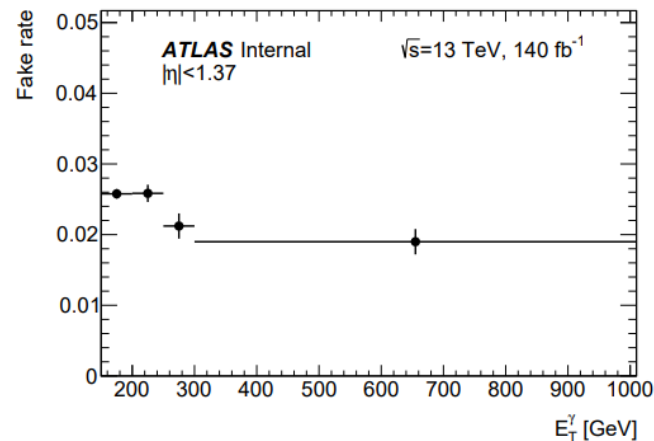
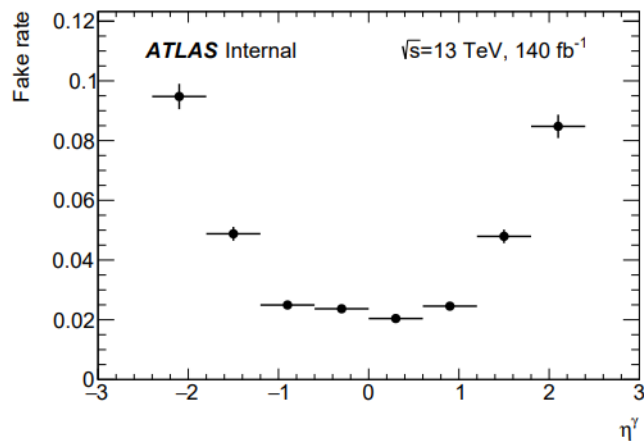
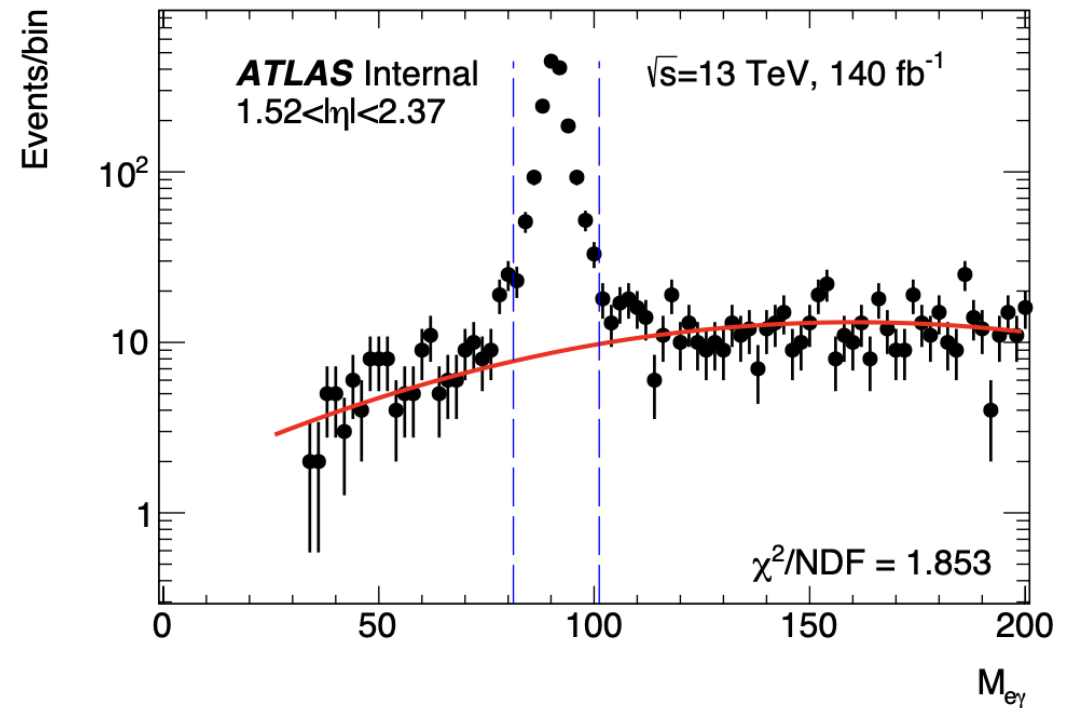
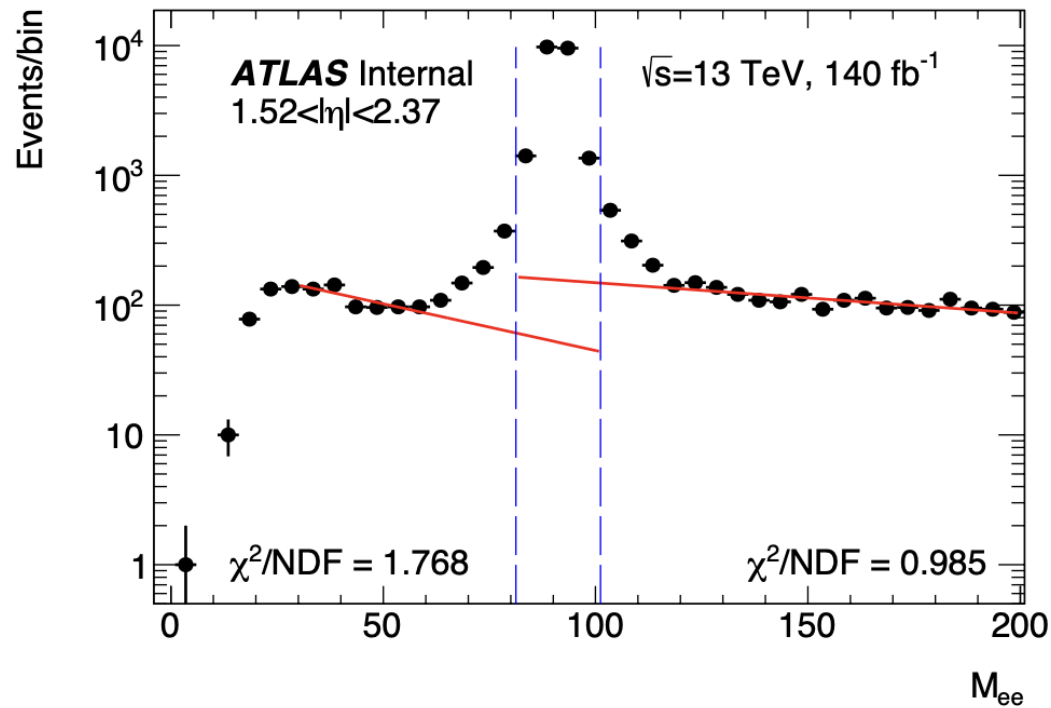
fake rate	$150 < E_T^\gamma < 250 \text{ GeV}$ $0 < \eta < 1.37$	$E_T^\gamma > 250 \text{ GeV}$ $0 < \eta < 1.37$	$1.52 < \eta < 2.37$
syst. from mass window var.:	0.3%	0.7%	0.4%
syst. from tag-n-probe and real f.r.:	3%	15%	10%
Background fit variation	4%	14%	3%
Total syst.:	4%	20%	10%

Table 34: Electron-to-photon fake rate systematics components.

$e \rightarrow \gamma$ misID background: Z-peak method



$e \rightarrow \gamma$ misID background: Z-peak method



jet \rightarrow γ misID background: ABCD method

- Tight and isolated region (region A – equivalent to $Z\gamma$ signal region described in Sec. 4.7): events have a leading photon candidate that is isolated ($E_T^{\text{cone}20} - 0.065p_T^\gamma < 0$ GeV) and passes the *tight* selection.
- Tight but not isolated region (control region B): events have a leading photon candidate that is not isolated ($E_T^{\text{cone}20} - 0.065p_T^\gamma > \text{iso gap}$) and passes the *tight* selection.
- Non-tight and isolated region (control region C): events have a leading photon candidate that is isolated ($E_T^{\text{cone}20} - 0.065p_T^\gamma < 0$ GeV) and passes the *non-tight* selection.
- Non-tight and not isolated region (control region D): events have a leading photon candidate that is not isolated ($E_T^{\text{cone}20} - 0.065p_T^\gamma > \text{iso gap}$) and passes the *non-tight* selection.

- *loose'2*: w_{s3}, F_{side}
- *loose'3*: $w_{s3}, F_{\text{side}}, \Delta E$
- *loose'4*: $w_{s3}, F_{\text{side}}, \Delta E, E_{\text{ratio}}$
- *loose'5*: $w_{s3}, F_{\text{side}}, \Delta E, E_{\text{ratio}}, w_{\text{tot}}$

$$N_A = N_A^{Z(\nu\bar{\nu})\gamma} + N_A^{\text{bkg}} + N_A^{\text{jet}\rightarrow\gamma};$$

$$N_B = c_B N_A^{Z(\nu\bar{\nu})\gamma} + N_B^{\text{bkg}} + N_B^{\text{jet}\rightarrow\gamma};$$

$$N_C = c_C N_A^{Z(\nu\bar{\nu})\gamma} + N_C^{\text{bkg}} + N_C^{\text{jet}\rightarrow\gamma};$$

$$N_D = c_D N_A^{Z(\nu\bar{\nu})\gamma} + N_D^{\text{bkg}} + N_D^{\text{jet}\rightarrow\gamma};$$

$$c_B = \frac{N_B^{Z(\nu\bar{\nu})\gamma}}{N_A^{Z(\nu\bar{\nu})\gamma}};$$

$$c_C = \frac{N_C^{Z(\nu\bar{\nu})\gamma}}{N_A^{Z(\nu\bar{\nu})\gamma}};$$

$$c_D = \frac{N_D^{Z(\nu\bar{\nu})\gamma}}{N_A^{Z(\nu\bar{\nu})\gamma}}.$$

$$N_A^{Z(\nu\bar{\nu})\gamma} = \tilde{N}_A - R(\tilde{N}_B - c_B N_A^{Z(\nu\bar{\nu})\gamma}) \frac{\tilde{N}_C - c_C N_A^{Z(\nu\bar{\nu})\gamma}}{\tilde{N}_D - c_D N_A^{Z(\nu\bar{\nu})\gamma}}.$$

$$a = c_D - R c_B c_C;$$

$$b = \tilde{N}_D + c_D \tilde{N}_A - R(c_B \tilde{N}_C + c_C \tilde{N}_B);$$

$$c = \tilde{N}_D \tilde{N}_A - R \tilde{N}_C \tilde{N}_B.$$

$$N_A^{Z(\nu\bar{\nu})\gamma} = \frac{b - \sqrt{b^2 - 4ac}}{2a},$$

	Data	$W\gamma$	$e \rightarrow \gamma$	$t\bar{t}\gamma$	γ +jet	$Z(l\bar{l})\gamma$
A	23375 ± 153	3420 ± 21	2608 ± 11	178 ± 3	8123 ± 82	211 ± 4
B	270 ± 16	17.7 ± 1.3	4.269 ± 0.016	0.46 ± 0.14	7 ± 3	0.6 ± 0.2
C	4393 ± 66	108 ± 3	92.8 ± 0.3	6.1 ± 0.5	259 ± 13	7.1 ± 0.6
D	497 ± 22	0.6 ± 0.2	0 ± 0	0.07 ± 0.05	0.06 ± 0.06	0 ± 0

jet \rightarrow γ misID background: slice method

To take into account the dependence of the estimate on the photon isolation, the non-isolated regions are split into a set of successive intervals (slices) based on the photon isolation. In this way, the number of $jet \rightarrow \gamma$ background events in each non-isolated slice i of the CR1 $N_{CR1(i)}^{jet \rightarrow \gamma}$ is derived as follows:

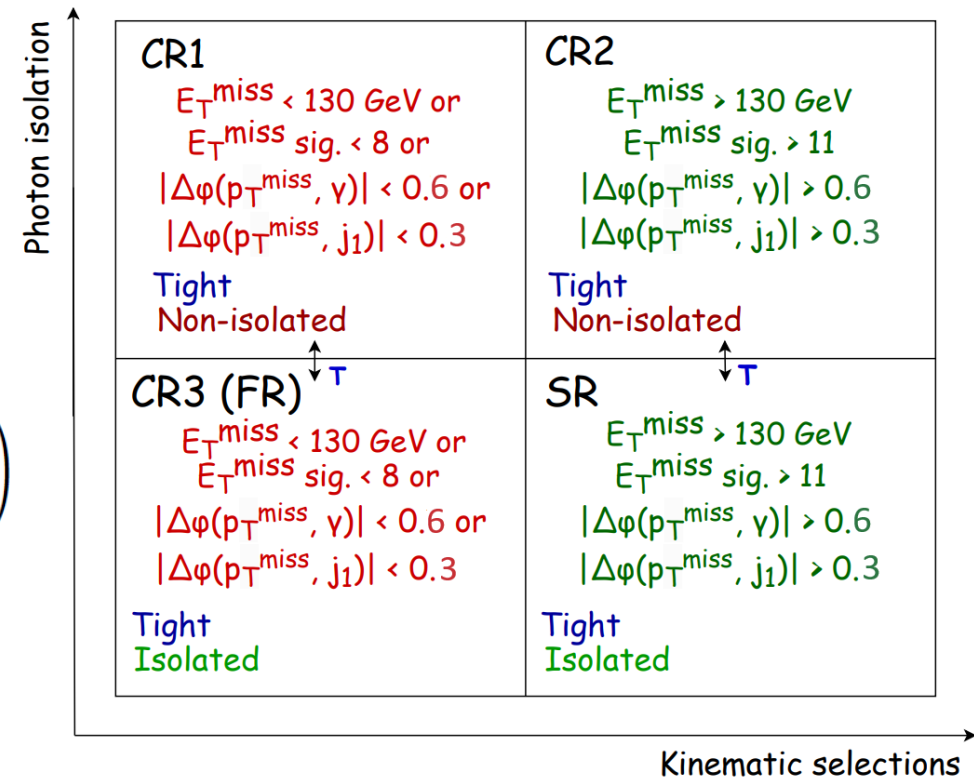
$$N_{CR1(i)}^{jet \rightarrow \gamma} = N_{CR1(i)}^{data} - N_{CR1(i)}^{Z(\nu\bar{\nu})\gamma} - N_{CR1(i)}^{bkg},$$

Four isolation slices are chosen: [0.065, 0.090, 0.115, 0.140, 0.165].

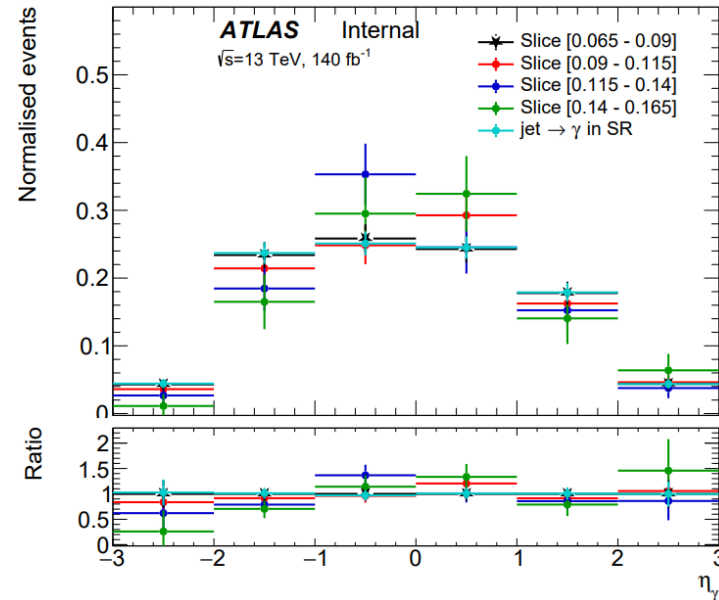
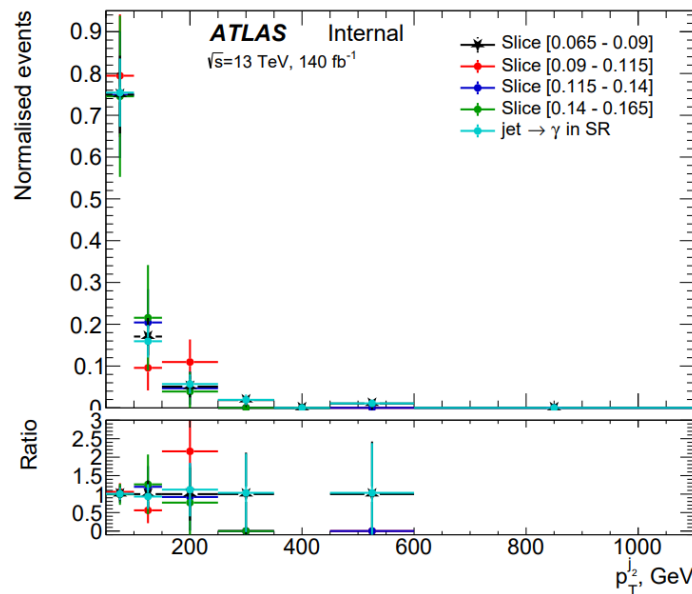
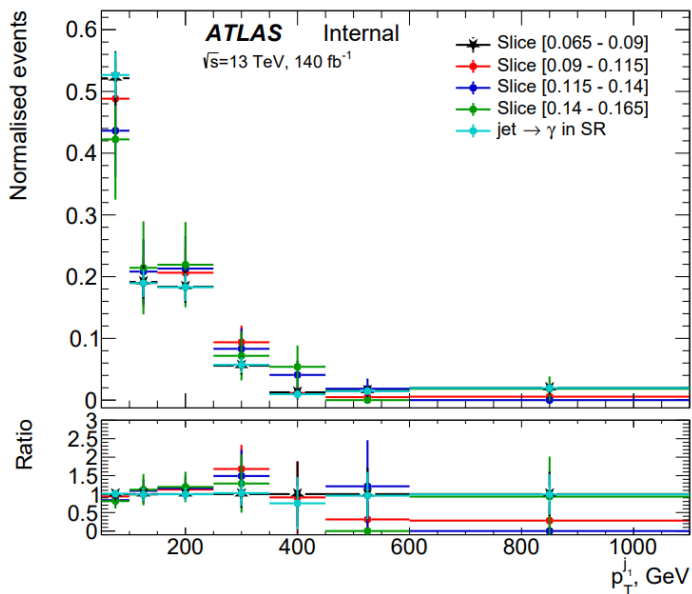
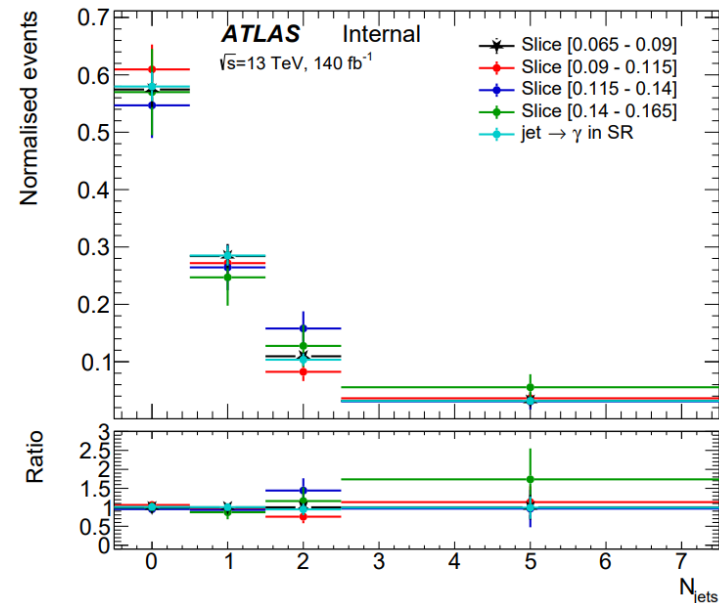
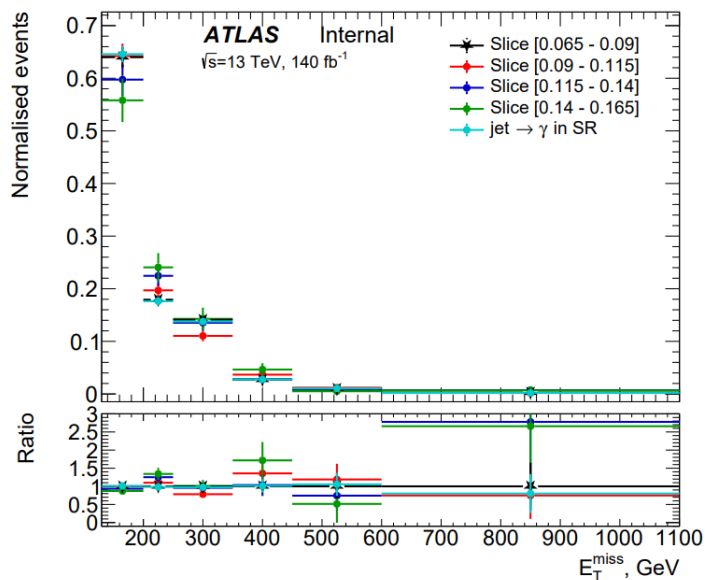
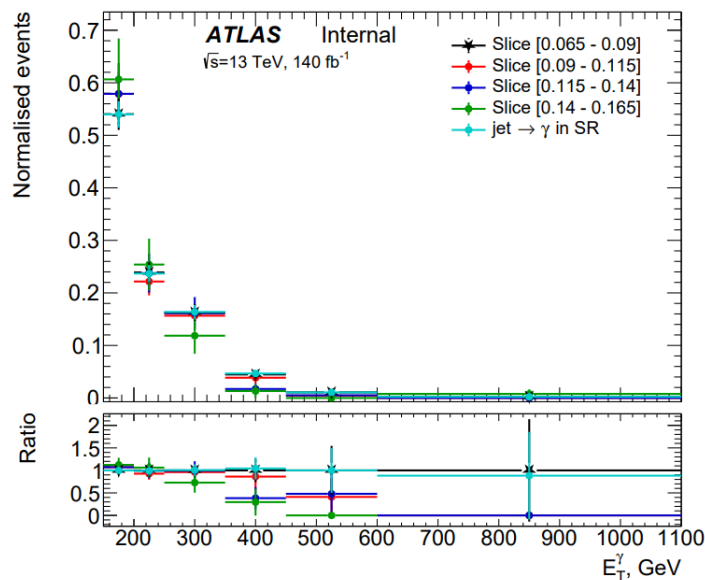
$$H_{jet \rightarrow \gamma}^{[0.A,0.B]} = H_{data}^{[0.A,0.B]}[X] - H_{sig}^{[0.A,0.B]}[X] - H_{bkg}^{[0.A,0.B]}[X],$$

$$\Delta^{CR2}[X] = \left(\frac{H_{jet \rightarrow \gamma}^{[0.065,0.09]}[X] - H_{jet \rightarrow \gamma}^{[0.115,0.14]}[X]}{2} + \frac{H_{jet \rightarrow \gamma}^{[0.09,0.115]}[X] - H_{jet \rightarrow \gamma}^{[0.14,0.165]}[X]}{2} \right)$$

$$H_{jet \rightarrow \gamma}^{SR} = H_{jet \rightarrow \gamma}^{[0.A_1,0.B_1]}[X] + 2 \cdot \Delta^{CR}[X]$$

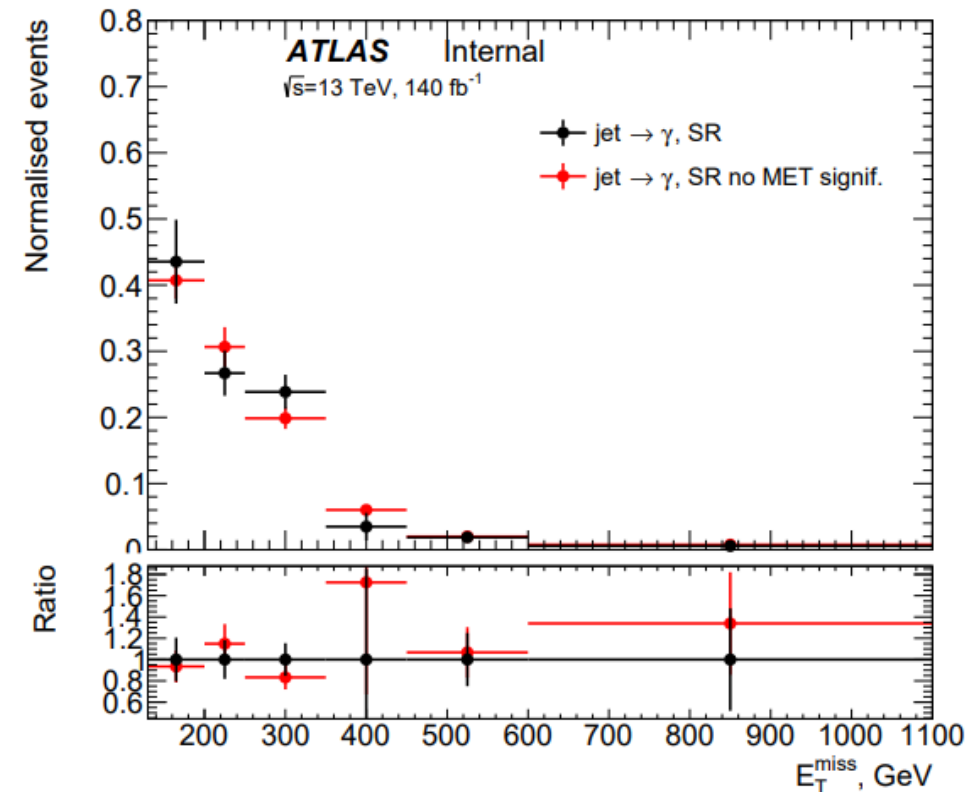
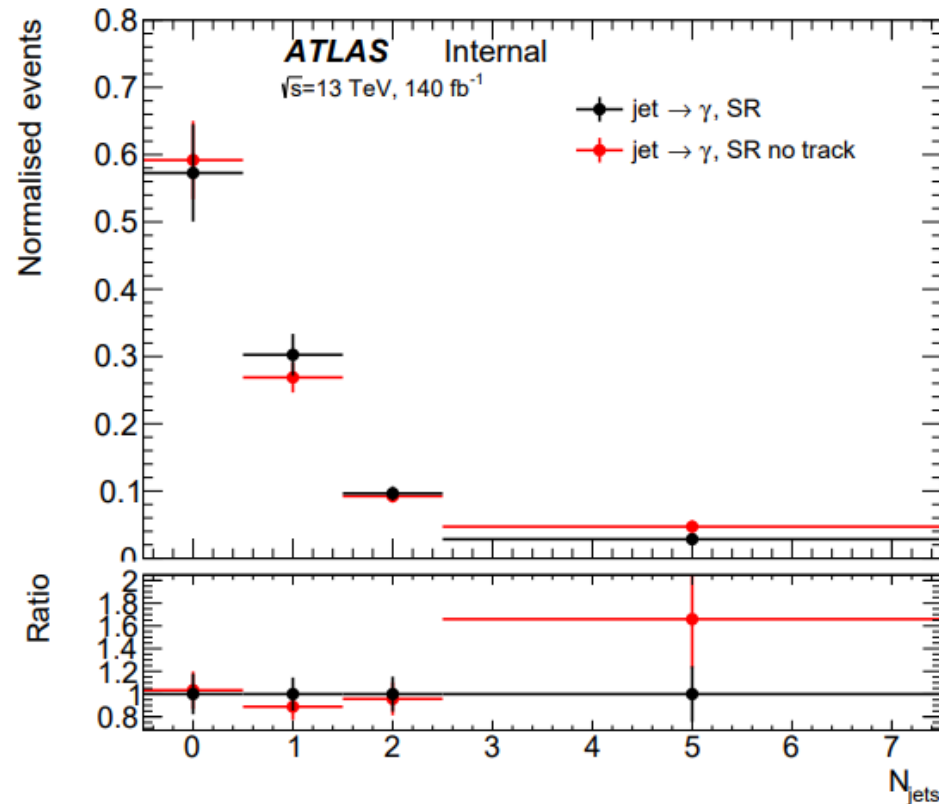


jet \rightarrow γ misID background: slice method



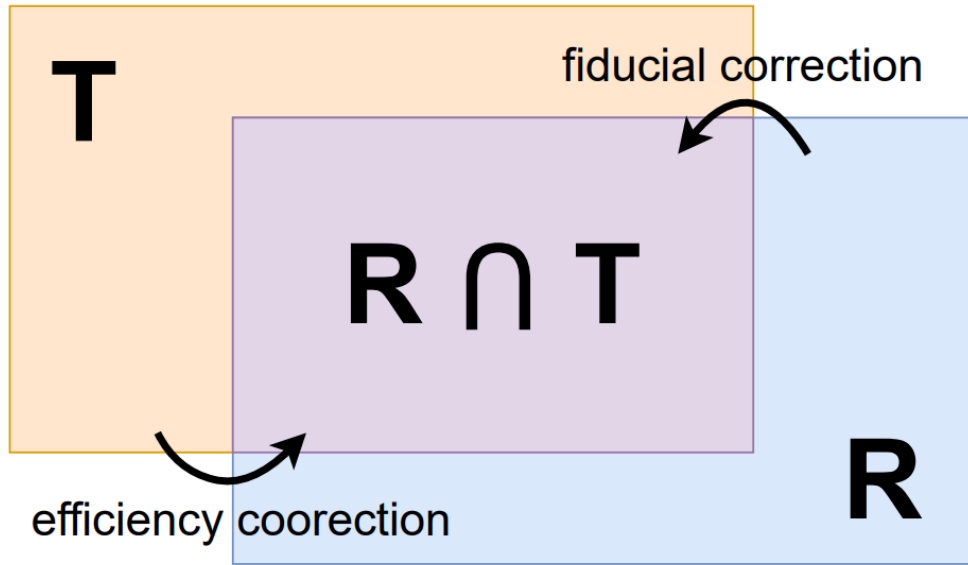
jet \rightarrow γ misID background: slice method

The detailed procedure of $jet \rightarrow \gamma$ background shape estimation is presented in Section 5.2.2. To increase the statistics in the anti-isolated slices, the cut on track isolation is relaxed. Figure 51 shows that the shape of the $jet \rightarrow \gamma$ distribution in the SR does not change when relaxing track isolated in the CR2. Figure 52 shows that the shape of the $jet \rightarrow \gamma$ distribution for E_T^{miss} in the SR does not change when relaxing cut on E_T^{miss} significance in the CR2.



Unfolding procedure

$$R_{ij} = \frac{1}{\alpha_i} \varepsilon_j M_{ij}, \quad M_{ij} = \frac{N_{ij}^{\text{det.} \cap \text{fid.}}}{N_j^{\text{det.} \cap \text{fid.}}}, \quad \alpha_i = \frac{N_i^{\text{det.} \cap \text{fid.}}}{N_i^{\text{det.}}}, \quad \varepsilon_j = \frac{N_j^{\text{det.} \cap \text{fid.}}}{N_j^{\text{fid.}}}, \quad \frac{\sigma_j}{\Delta x_j} = \frac{N_j^{\text{unfold}}}{(\int \mathcal{L} dt) \cdot \Delta x_j},$$



Correction factor	Value
$A_{Z\gamma}$	0.9049 ± 0.0008
$C_{Z\gamma}$	0.7487 ± 0.0007

The unfolding procedure by folding can be performed with following steps:

- Multiplying the response matrix \hat{R} and the particle-level distribution:

$$F_{ij} = R_{ij} \cdot T_j = \begin{pmatrix} \vec{r}_1 \\ \vec{r}_1 \\ \vdots \\ \vec{r}_n \end{pmatrix} \cdot \begin{pmatrix} t_1 \\ t_1 \\ \vdots \\ t_n \end{pmatrix} = \begin{pmatrix} \vec{f}_1 \\ \vec{f}_1 \\ \vdots \\ \vec{f}_n \end{pmatrix},$$

- Multiplying each of the n histograms by the NFs $\mu_j = (\mu_1, \mu_2, \dots, \mu_n)$:

$$G_{ij} = F_{ij} \cdot \mu_j = \begin{pmatrix} \vec{f}_1 \\ \vec{f}_1 \\ \vdots \\ \vec{f}_n \end{pmatrix} \cdot \begin{pmatrix} \mu_1 \\ \mu_1 \\ \vdots \\ \mu_n \end{pmatrix} = \begin{pmatrix} \vec{g}_1 \\ \vec{g}_1 \\ \vdots \\ \vec{g}_n \end{pmatrix}.$$

The next step is to add all vectors \vec{g}_j . As a result we get one histogram with m bins.

- Fit the folded distribution by tuning NFs μ_j . As a result one gets the fitted parameters $\mu'_j = (\mu'_1, \mu'_2, \dots, \mu'_n)$.
- Dot multiply normalised NFs and truth histogram.

Unfolding procedure

Fiducial region:

Category	Cut
Photons	Isolated, $E_T^\gamma > 150$ GeV $ \eta < 2.37$ excluding $1.37 < \eta < 1.52$
Jets	$ \eta < 4.5$ $p_T > 50$ GeV $\Delta R(jet, \gamma) > 0.3$
Lepton	$N_l = 0$
Neutrino	$p_T^{\nu\bar{\nu}} > 130$ GeV
Events	$ \Delta\phi(\vec{p}_T^{\text{miss}}, \gamma) > 0.7$ $ \Delta\phi(\vec{p}_T^{\text{miss}}, j_1) > 0.4$ $p_T^{\nu\bar{\nu}}$ significance > 11

$$\mathcal{L}(\sigma, \theta, \lambda) = \prod_i P \left(N_i | \mathcal{L}_{\text{int}} \sum_j \mathcal{R}_{ij}(\vec{\theta}) \sigma_j(\vec{\theta}) + \mathcal{B}_i(\vec{\theta}, \lambda) \right) \times \prod_k G(\theta_k)$$

$$N_j = \mathcal{L}_{\text{int}} \sigma_j \text{ with } \sigma_j = \mu_j \sigma_j^{\text{MC}}$$

$$\mathcal{L}(\sigma, \theta, \lambda) = \mathcal{L}(\sigma, \theta, \lambda)_{\text{noreg.}} \times \left(-\frac{\tau^2}{2} \sum_{i=2}^{i+2 < N_{\text{bins}}} ((\mu_i - \mu_{i-1}) - (\mu_{i+1} - \mu_i))^2 \right)$$

$$\frac{\sigma_j}{\Delta x_j} = \frac{N_j^{\text{unfold}}}{(\int \mathcal{L} dt) \cdot \Delta x_j}$$

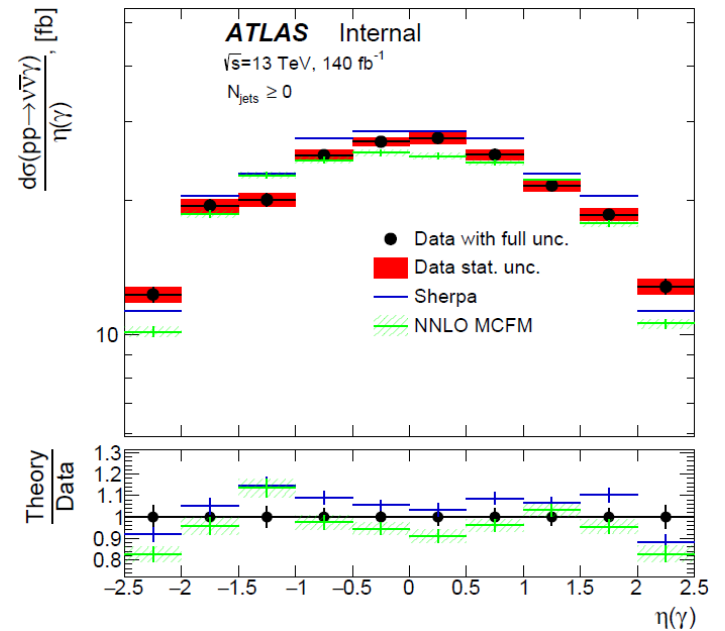
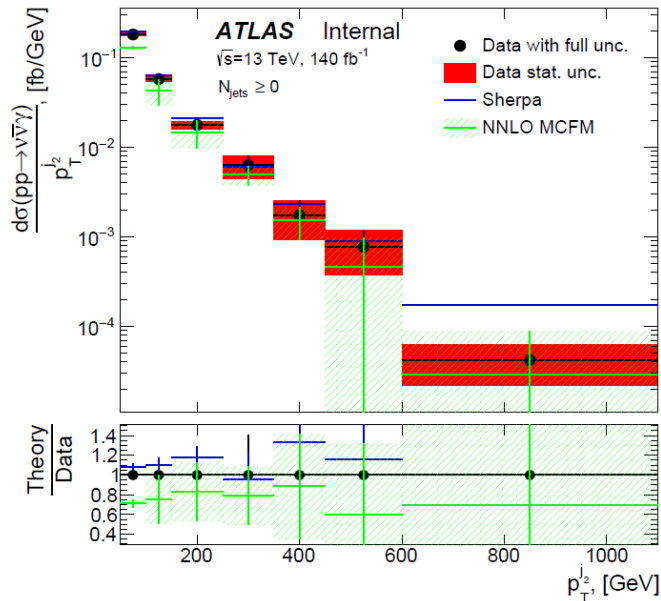
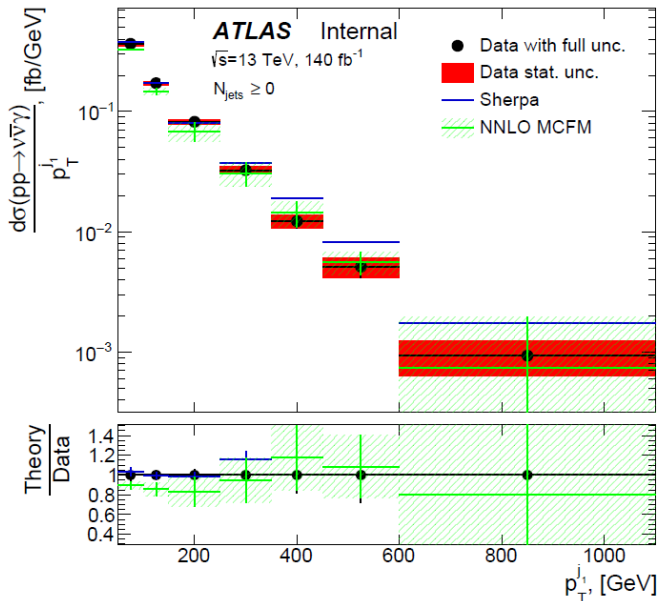
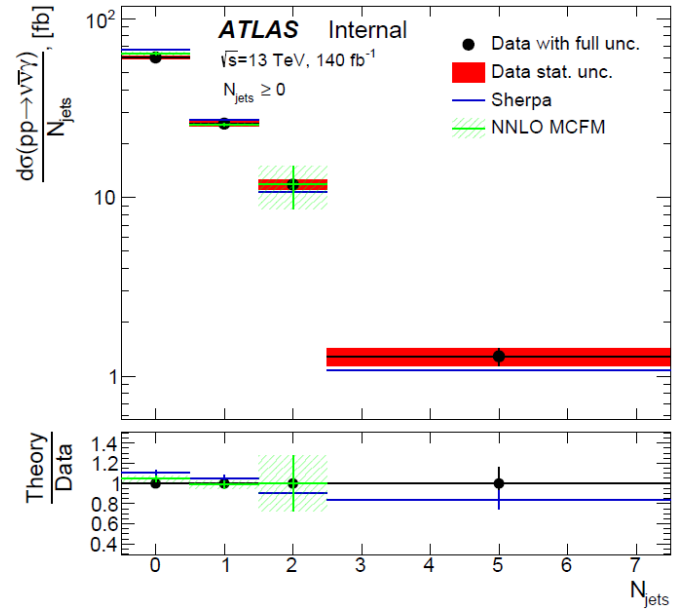
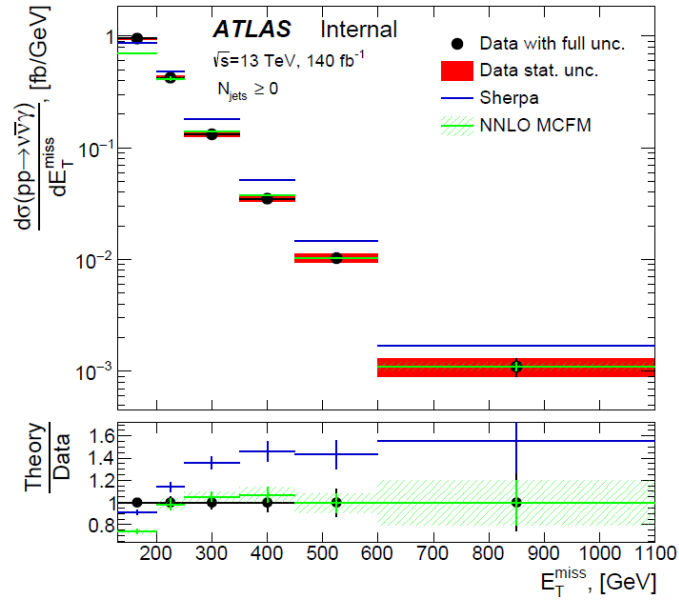
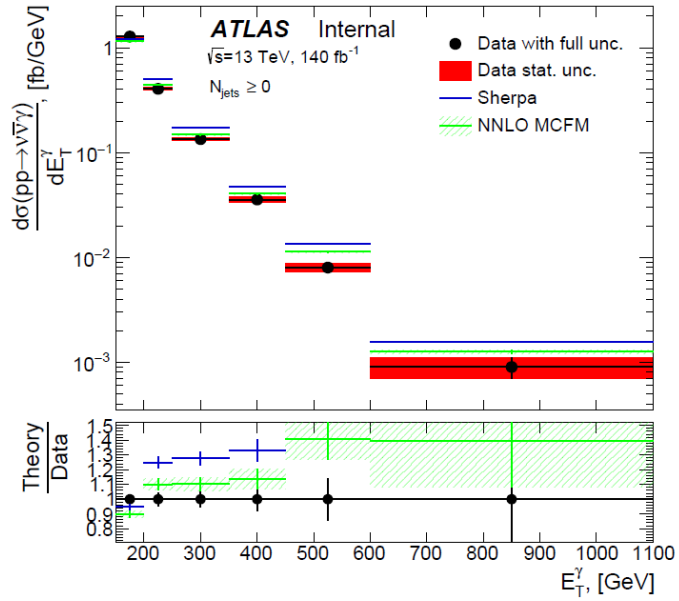
Observable	Binning
p_T^γ	[150, 200], [200, 250], [250, 350], [350, 450], [450, 600], [600, 1100]
E_T^{miss}	[130, 200], [200, 250], [250, 350], [350, 450], [450, 600], [600, 1100]
N_{jets}	[-0.5, 0.5], [0.5, 1.5], [1.5, 2.5], [2.5, 7.5]
η_γ	[-3, -2, -1, 0, 1, 2, 3]
$p_T^{j_1}$	[50, 100, 150, 250, 350, 450, 600, 1100]
$p_T^{j_2}$	[50, 100, 150, 250, 350, 450, 600, 1100]
$ \Delta\phi(j, j) $	[0.0 - 3.2], 16 bins
$ \Delta\phi(p_T^{\text{miss}}, j) $	[0.4 - 3.2], 14 bins

Table 29: Summary of the differential measurements in the analysis

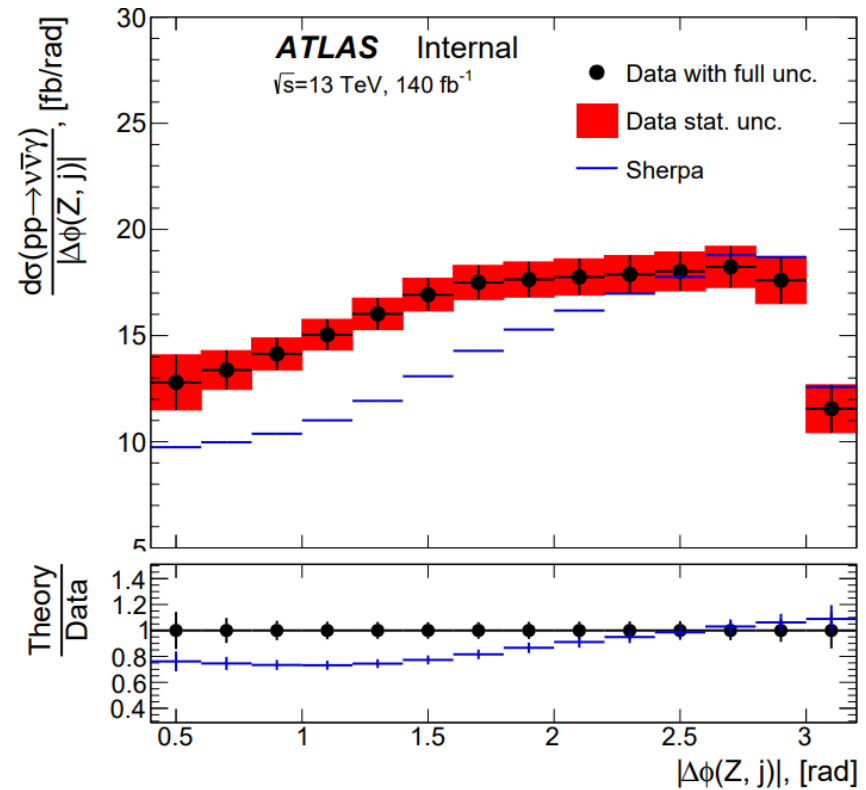
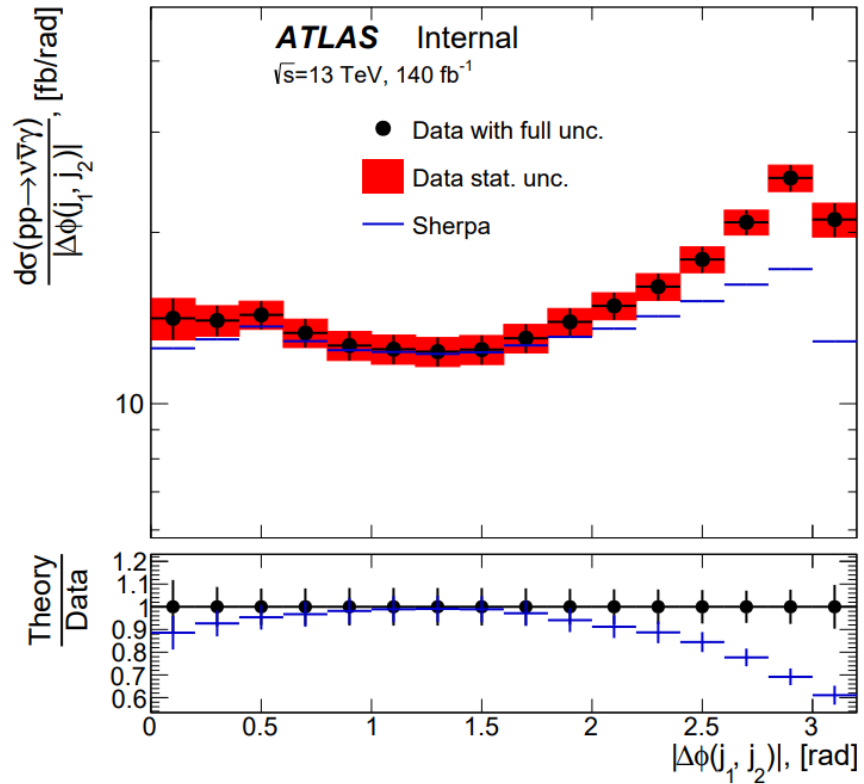
Extended fiducial region:

Category	Cut
Photons	Isolated, $E_T^\gamma > 150$ GeV $ \eta < 2.37$
Jets	$ \eta < 4.5$ $p_T > 50$ GeV $\Delta R(jet, \gamma) > 0.3$
Neutrino	$p_T^{\nu\bar{\nu}} > 130$ GeV

Unfolding procedure



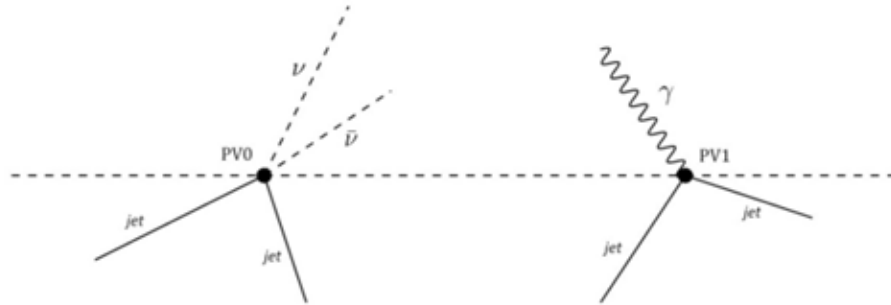
Unfolding procedure



OMC method

Overlay Monte-Carlo (OMC) Method

Strategy:



1. To estimate the number of pile-up events (referred to as **A+B**) in the diboson production (referred to as **AB**) the overlay Monte-Carlo (OMC) method uses **separate A and B samples** at the particle-level.

2. **The overlay** of B over A is performed by adding objects (photons, jets, etc.) from B into A;

3. The variables that define the **AB** final state are calculated in order to form a valid combined **A+B** event (referred to as OMC event). These variables are used to be **checked against analysis selections**;

4. The weight of the combined **A+B** event is determined as:

$$w_{A+B} = \frac{w_A w_B}{\langle w_A \rangle \langle w_B \rangle} \frac{L \sigma_{A+B}}{N_{\text{OMC}}}$$

$$\sigma_{A+B} = \langle \mu \rangle \frac{\sigma_A \sigma_B}{\sigma_{\text{inel}}}$$

5. The number of **A+B** events at the **particle-level** is defined as the sum of OMC sample weights:


$$N_{A+B}^{\text{gen}} = \sum w_{A+B}$$

6. The predicted number of pile-up events at the **detector-level** in the SR is estimated as follows:

$$N_{A+B}^{\text{rec}} = N_{A+B}^{\text{gen}} C$$

***Correction factor (C)** is defined as the reconstructed MC signal **AB** events passing all selections divided by the number of MC signal **AB** events at the particle-level within the fiducial region.

OMC method

- The **Z boson** (taken as **A**) and the **photon** (taken as **B**) components of Z+ γ OMC events are taken from Zj and γ +j MC samples, respectively;
- The particle-level photon from γ +j process is being overlaid over random particle-level Z boson from Zj process until it becomes a part of Z+ γ OMC event, that passes [the fiducial region requirements](#); 
- The procedure for such a combination of events is performed for every γ +j sample with a certain Zj sample **in each of the MC simulation campaigns** (MC16a, MC16d, MC16e);
- Iterating through all γ +j events requires significant computing resources, therefore **only 100k events** of every statistically large γ +j sample [are used to form](#) OMC sample;
- The total number of pile-up events at the particle-level is obtained by combining **each γ +j** sample sequentially **with each Zj** sample.

Definition of the fiducial region:

Category	Cut
Photons	Isolated, $E_T^\gamma > 150$ GeV $ \eta < 2.37$ excl. $1.37 < \eta < 1.52$
Jets	$ \eta < 4.5$ $p_T > 50$ GeV $\Delta R(jet, \gamma) > 0.3$
Lepton	$N_l = 0$
Neutrino	$p_T^{\nu\bar{\nu}} > 130$ GeV
Events	Significance $E_T^{\text{miss}} > 11$ $ \Delta\phi(\vec{p}_T^{\text{miss}}, \gamma) > 0.6$ $ \Delta\phi(\vec{p}_T^{\text{miss}}, j_1) > 0.3$

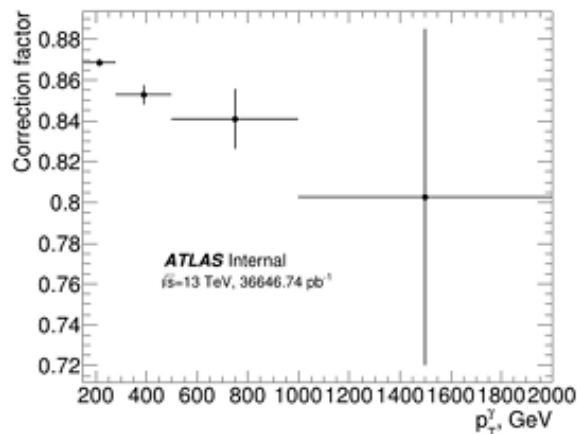
The weight and the cross section of [the combined Z+ \$\gamma\$ event](#):

$$w_{Z+\gamma} = \frac{w_Z w_\gamma L \sigma_{Z+\gamma}}{\langle w_Z \rangle \langle w_\gamma \rangle N_{\text{OMC}}}$$

$$\sigma_{Z+\gamma} = \langle \mu \rangle \frac{\sigma_Z \cdot SF_Z \cdot \sigma_\gamma \cdot SF_\gamma}{\sigma_{\text{inel}}}$$

OMC method

- The C-factor is parameterized by the transverse momentum of the photon, since the total number of pile-up events at the particle-level is summed from the number of pile-up events calculated for each $\gamma+j$ sample.



The estimates of correction factor obtained with $Z(\nu\nu)\gamma$ MC signal for 4 intervals of the transverse momentum of the photon [150; 280; 500; 1000; 2000] GeV:

$p_T^\gamma, \Gamma \rightarrow B$	MC16a	MC16d	MC16e
150-280	0.8685 ± 0.0018	0.8155 ± 0.0017	0.8246 ± 0.0014
280-500	0.853 ± 0.005	0.818 ± 0.004	0.822 ± 0.004
500-1000	0.841 ± 0.015	0.803 ± 0.014	0.829 ± 0.012
1000-2000	0.80 ± 0.08	0.84 ± 0.11	0.73 ± 0.06

$$C = \frac{N_{Z\gamma}^{\text{rec}}}{N_{Z\gamma}^{\text{gen}}}$$

$$N_{Z+\gamma}^{SR} = N_{Z+\gamma}^{FR} C$$

- The final estimate* of background events due to multiple pp collisions: $N_{Z+\gamma}^{SR} = 2.938 \pm 0.018(\text{stat.})$ events; *(more in back-up)

The statistical uncertainties come from:

- The uncertainty of the weights w_γ and w_Z of events used in the combination of $\gamma+j$ samples with Z_j samples;
- The uncertainty of C-factor;
- The uncertainty of SF-factors;

The fraction of pile-up events in relation to the data obtained using the OMC method is $(0.01257 \pm 0.00011)\%$.